THE ROLE OF MEF2 TRANSCRIPTION FACTORS IN NEOCORTICAL CIRCUIT AND SYNAPSE DEVELOPMENT *IN VIVO*

APPROVED BY SUPERVISORY COMMITTEE

(14 spaces down)

Kimberly Huber, Ph.D. (Supervisor)

Jay Gibson, Ph.D.

Genevieve Konopka, Ph.D.

Craig Powell, M.D., Ph.D.

Todd Roberts, Ph.D.

DEDICATION

I dedicate this work to those who have provided inspiration, unwavering support, personal and scientific discussion, and a new perspective for thinking, living, and loving.

I would like to especially thank the following:

Drs. Kimberly Huber, PhD and Jay R. Gibson, PhD for a stable and nurturing foundation in scientific thought and practice. My scientific training would not have been the same without your support, patience, and guidance. Through your example I have acquired a greater appreciation for things that I do not understand and the struggles – both internal and external – that pave the way for discovery. You have taught me patience and have forever changed the manner in which I approach a problem.

Drs. Saïd Kourrich, PhD, Gemma Molinaro, PhD, Rachel Penrod-Martin, PhD, Jakub Jedynak, PhD, Carly F. Hale, PhD, Carolyn Fairbanks, PhD, Lorene Lanier, PhD, Christopher Cowan, PhD, and Ege Kavalali, PhD for inspiration, advice, courage, guidance, console, optimism, and motivation to pursue a career in academic science.

Dr. Kristina Y. Aguilera, PhD, Egemen Agi, Jacob A. Zahm, Katie D. London, Joel R. Hodge, II, Jacob M. Whitehouse, Joseph W. Carpenter, Alyxandre J. Caceres, Christopher D. Clayborn, Dr. Ankur B. Patel, PhD, Yasemin Onder, Sally M. Hughes-Perrin, Joseph Hughes, Dr. Jaswinder Kumar, MD/PhD, Guy LeTourneau, II, Trent C. Braden, M. Neset Ozel, Damien Martin, and Scott Ward for their cherished friendship and tremendous personal and professional inspiration. You make my life beautiful from anywhere in the world, and all of you bring me happiness and make me a better person.

My mother, Patricia J. Rajkovich: Your sacrifice throughout the years and your unconditional love have been the basis for my confidence, accomplishment, and development. I have no words to fully convey the gratitude for the love that you have provided throughout my life. My gratitude for your patience, understanding, and selflessness is undying.

My father, Richard A. Rajkovich: My interest in science blossomed from your self-acquired enthusiasm for physics and chemistry. You provided the basis for my cynicism, skepticism, and intuition, which ultimately has provided me with determination and motivation to finish whatever I start whether in company or in solitude. Even in death, your contribution to my personal development is never forgotten.

THE ROLE OF MEF2 TRANSCRIPTION FACTORS IN NEOCORTICAL CIRCUIT AND SYNAPSE DEVELOPMENT *IN VIVO*

by

KACEY ELISE RAJKOVICH

DISSERTATION

Presented to the Faculty of the Graduate School of Biomedical Sciences

The University of Texas Southwestern Medical Center at Dallas

In Partial Fulfillment of the Requirements

For the Degree of

DOCTOR OF PHILOSOPHY

The University of Texas Southwestern Medical Center at Dallas

Dallas, Texas

August 2016

THE ROLE FOR MEF2 TRANSCRIPTION FACTORS IN NEOCORTICAL CIRCUIT AND SYNAPSE DEVELOPMENT *IN VIVO*

Kacey Elise Rajkovich, Ph.D.

The University of Texas Southwestern Medical Center at Dallas, 2016

Kimberly M. Huber, Ph.D. & Jay R. Gibson, Ph.D.

Proper neocortical circuit development requires postnatal experience and transcription. Neocortical neurons migrate to their proper layers and then undergo robust synapse proliferation to maximize contacts with presynaptic partners. Synapses are dynamic structures subjected to an equilibrium of formation and elimination rates to preserve meaningful and prune superfluous synapses, respectively. A neuron receives heterogeneous inputs and must tightly regulate connectivity with distinct presynaptic entities. Dysregulated connectivity causes aberrant circuit function and ultimately abnormal behavior linked with neurodevelopmental disorders such as autism. Therefore, a neuron must contain cellular machinery to regulate synaptic connectivity. The activity-dependent Myocyte Enhancer Factor-2 (MEF2) transcription factors – MEF2A-D - have distinct but overlapping expression profiles throughout the brain and typically suppress synapse number. The cell-autonomous role for specific MEF2 genes in neocortical circuit development has never been explored. Furthermore, a link between MEF2 and experience has never been identified within the neocortex. Lastly, whether MEF2 transcription factors regulate specific synaptic pathways is unknown.

I report that MEF2A, MEF2C, and MEF2D non-redundantly regulate synapse development onto individual pyramidal neurons within layers 2 and 3 (L2/3) of the postnatal mouse primary somatosensory "barrel" cortex *in vivo*. Simultaneous deletion of *Mef2a* and *Mef2d* modestly decreases spontaneous glutamatergic synaptic transmission in comparison to neighboring control L2/3 neurons. MEF2C, however, cell-autonomously mediates several unique aspects of L2/3 circuit development at a postsynaptic locus. Sparse *Mef2c* deletion decreases excitatory synapse number onto basal dendrites of L2/3 neurons targeted by local inputs. Therefore, *Mef2c* promotes excitatory synapse formation and/or maintenance in neocortex. Additionally, MEF2C and sensory experience interact to promote strength of local L2/3 inputs. *Mef2c* deletion depresses these local inputs in spared barrel cortices comparably to the depression induced by sensory deprivation via whisker trimming onto wildtype (WT) L2/3 neurons; hence MEF2C is required for experience-dependent development of L2/3 circuitry. Lastly, MEF2C differentially suppresses long-range intercortical while promoting connectivity at local L2/3 synaptic input pathways. These data represent novel mechanisms through which MEF2C regulates neocortical synapse development *in vivo* and provides insight into how activity-dependent transcription within the nucleus interacts with experience to alter specific synapse populations at the neural plasma membrane.

PRIOR PUBLICATIONS

1. D.J. Araujo, A.G. Anderson, S. Berto, W. Runnels, M. Harper, S. Ammanuel, M.A. Rieger, H.C. Huang, K. Rajkovich, K.W. Loerwald, J.D. Dekker, H.O. Tucker, J.D. Dougherty, J.R. Gibson, and Genevieve Konopka. FoxP1 orchestration of ASD-relevant signaling pathways in the striatum. Genes and Development. DOI: 10.1101/gad.267989.115. 2015 Oct 15;29(20):2081-96.

LIST OF FIGURES

LIST OF TABLES

LIST OF DEFINITIONS

AAV – Adeno-associated virus

AChR – acetylcholine receptor

AMPAR – α-aino-3-hydroxy-5-methylisoxazole-4-propionic acid sensitive glutamate receptor

Arc – Activity-regulated cytoskeleton-associated protein

BDNF – brain-derived neurotrophic factor

BMI – Bicuculline methiodide, $GABA_A$ receptor antagonist

CaMK – calcium/calmodulin-mediated kinase

cAMP – cyclic adenosine monophosphate

Cdk5 – cyclin-dependent protein kinase 5

CDKL5 – Cyclin-dependent kinase-like-5

ChR2 – Channelrhodopsin-2

cKO – conditional knockout

CNS – Central nervous system

CREB – cyclic adenosine monophosphate response element-binding protein

cS1 – contralateral primary somatosensory sortex

DG – Dentate granule neurons

DIV – Day *in vitro*

DNA – deoxyribonucleic acid

DREAM – dimerization partner, RB-like, E2F and multi-vulval class B

E – embryonic day, age during gestation

E/I – Excitation-to-inhibition

EF1a – elongation factor 1a

EPSC/P – Excitatory postsynaptic current/potential

FACS – Fluorescence activated cell sorting

Flox – flanked by *LoxP* sites

Fmr1 – Fragile X mental retardation gene/mRNA

FMRP – Fragile X mental retardation protein

FXS – Fragile X syndrome

GABA – gamma-aminobutyric acid

GABAR - Gamma-aminobutyric acid receptor GABAR

GFP – green fluorescent protein

HET – Heterozygous

HAT – histone acetyltransferase

HDAC – histone deacetlyase

I → E – Inhibitory-to-excitatory, Inhibitory input onto an excitatory neuron

IPSC/P – Inhibitory postsynaptic current/potential

IR-DIC – Infrared differential interference contrast

KO – Knockout

L-VGCC – L-type voltage-gated calcium channel

L2/3 – Cortical layer 2/3

$L2/3_{adj}$ – Trancolumnar, horizontal inputs from L2/3 of adjacent barrel column

L4 – Cortical layer 4

$L4_{adj}$ – Transcolumnar inputs from L4 of adjacent barrel column

L5 – Cortical layer 5

$L5_{adj}$ – Transcolumnar inputs from L5A of adjacent barrel column

LSPS – Laser Scanning Photostimulation

LTD – Long-term depression

LTP – Long-term potentiation

M1 – Primary motor cortex

M2 – Secondary motor cortex

MADS domain - MCM1, Agamous, Deficiens, and Serum response factor

MECP2 – methyl-CpG-binding protein 2

MEF – Myocyte enhancement factor

MEF2C cKO – MEF2C conditional knockout

mEPSC – Miniature excitatory postsynaptic current

MERFISH – Multiplexed error-robust fluorescence in situ hybridization

mGluR – Metabotropic glutamate receptor

mGluR-LTD – metabotropic glutmate receptor-dependent long-term depression

mIPSC – Miniature inhibitory postsynaptic current

miRNA – micro-RNA

MNI – 4-Methoxy-7-nitroindolinyl-caged-L-glutamate

MRE – MEF2 response element

MRI – Magnetic resonance imaging

mRNA – Messenger ribonucleic acid

NFAT – nuclear factor of activated T-cells

NGF – nerve growth factor

NL-1 – Neuroligin-1

NLS – nuclear localization signal

NMDAR – N-methyl-D-aspartate sensitive glutamate receptor

NPAS4 – Neuronal Per-Arnt-Sim domain protein-4

NR1/2 – NMDAR subunit 1/2

P – postnatal day, age from birth

p38 MAPK - p38 mitogen-activated protein kinase

POM - Posterior medial thalamic nucleus

PP1α – Protein phosphatase-1 alpha, catalytic subunit

PCDH10 – Protocadherin-10

PSD – Postsynaptic density

PSD-95 – post-synaptic density protein of 95 kDa

PV - Parvalbumin

RNA – ribonucleic acid

S1 – primary somatosensory cortex

S1BF – Barrel field of the primary somatosensory cortex

S2 – Secondary somatosensory cortex

sCRACM – Subcellular Channelrhodopsin-assisted Circuit Mapping

SCZ – schizophrenia

SD – standard deviation

SEM – standard error of the mean

shRNA – Short-hairpin RNA

SLTP – Spike-timing long-term depression

SLTP – Spike-timing long-term potentiation

SRF – Serum response factor

SST - Somatostatin

SUMO – small ubiquitin-like modifier

TBS – theta burst stimulation

tLTD – Timing-dependent LTD

tLTP – Timing-dependent LTP

V_m – Membrane potential

VPM - Ventral posterior medial thalamic nucleus

VP16 – Herpes simplex viral protein 16

WT – wild-type

TABLE OF CONTENTS

CHAPTER ONE

NEOCORTICAL SYNAPSE DEVELOPMENT AND CIRCUIT FORMATION

The Neocortex: Overview and Development

The human neocortex is a complex sheet of neural tissue folded into gyri and sulci that holds the very essence of human thought, memory, learning, personality, guilt, regret, and sensation. Within this structure resides ~20 billion neurons interconnected into a labyrinth of circuits that mediate our consciousness and survival (Pelvig et al 2008). The neocortex is the latest evolutionary addition to the nervous system having developed into a six-layered structure within organisms belonging to several taxonomic classes within the animal kingdom including primate, rodent, amphibian, and avian species. Although the evolutionary development of the human neocortex has branched off from that of *mus musculus* approximately 90-100 million years ago and that of the masque monkey within the last 25 million years, the basic principles of its organization and development are remarkably similar to those of "lower-order" organisms (Rakic 2009). Hence, throughout the last century much insight into the physiology and development of the human neocortex has been acquired via experimentation in several animal species, namely *mus musculus* for advances in genetic manipulations. Therefore, whether considering the neocortex of either mouse or man, the functional unit of the neural circuit is the synapse: a specialized structure allowing apposition of the postsynapse with the presynaptic axon terminal for exchange of electrical and chemical information. The establishment and regulation of neocortical synapse and circuit development is essential for normal brain function and behavior, but many key developmental events must occur for a neuron to integrate itself into a functional circuit, synapsing with tens of thousands of presynaptic axon terminals.

The mammalian neocortex is a six-layered structure that develops in an "inside-out" fashion during embryogenesis whereby development of Layer 6 (L6) precedes that of Layer 5 (L5) and then of Layer 4 (L4), and so on until Layer 1 (L1) is positioned as the most superficial cortical layer underneath the pia mater. Neural progenitor cells dividing on the periphery of ventricular zones differentiate into neurons that undergo distant migration along the processes of radial glial cells. Neurons en route to comprise the neocortex migrate for tens to several thousands of micrometers to their destined cortical region. In the developing mouse brain, neurons comprising Layer 6 (L6) are the first to migrate at embryonic day (E) 12. L2/3 is then established at E15-16, and finally, neocortical migration completes with formation of L1 at ~E17 (Sauvageot & Stiles 2002). Neurogenesis also coincides with the migration stage of development; commencing at E12, peaking at E14, and subsiding at ~E17 (Sauvageot & Stiles 2002). Hence, the neocortical circuit framework is established before birth.

Considering the heterogeneity of presynaptic inputs onto an individual neocortical neuron, this neuron must accurately reach its intended destination within the cortex while abiding by the organizational rules of neocortical development. Thus, the question at hand is: Does a migrating neuron have a distinct molecular identity conferring its position or does the synaptic and cellular environment determine the position of the neuron? There are hypotheses for both scenarios. The "protomap hypothesis" states that neocortical neurons are molecularly distinct from one another and that this molecular identity is what determines the cortical destination for a given neuron, and therefore synaptic connectivity will be dictated by the cellular position (Rakic 1988). In contrast, the "protocortex hypothesis" assumes that all neocortical neurons have equipotential and therefore achieve

molecular distinction based upon cellular position and external factors such as available synaptic inputs (De Haan & Johnson 2005). The cortical "arealization" or segregation into specialized cortical regions is initially dictated by cell-autonomous genetic factors and molecular gradients during initial cortical development during embryogenesis (McConnell & Kaznowski 1991, Rash & Grove 2006). Subsequently, spontaneous and experience-driven neural activity promotes functional integration of a neuron into the developing circuit. Excitatory GABAergic and glutamatergic synaptic transmission as well as electrical synaptic coupling synchronize neural networks during corticogenesis in early postnatal development (Feldmeyer et al 2013). Into the second postnatal week of development, synaptic activity in the cortex becomes more desynchronized, resembling activity of the more mature, adult cortex. This developmental stage also marks the transition of GABAergic synaptic transmission from an excitatory to an inhibitory signal. At this time, L4 neurons within sensory cortices undergo prominent activity- and experience-dependent plasticity to refine relevant circuits via a multitude of physiological mechanisms until closure of the critical period (Ben-Ari et al 2012, Feldmeyer et al 2013, Fox 2002).

In this work I discuss the anatomy and physiology of neural circuits within the barrel fields of the developing rodent primary somatosensory "barrel" cortex. The canonical circuitry and experience-dependent plasticity occurring within the barrel cortex makes this brain region an exception model system for studying neural circuit development. Lastly, I focus on the influence exerted by neural activity on the development of neural circuits and synapse dynamics with special emphasis on activity-dependent transcriptional regulation.

Organization of the Barrel cortex

The barrel cortex is a subregion of the primary somatosensory cortex that processes whisker-mediated sensation as the whiskers are mechanically displaced by external stimuli. This sensory cortex is somatotopically organized and dedicates cortical area to each individual whisker in a pattern strikingly similar to that of whiskers on the contralateral facial pad. Cortical columns referred to as "barrel columns" are the functional and anatomical units of the barrel cortex, whereby each barrel column represents a single whisker on the contralateral facial pad and spans all six cortical layers, which are distinguishable molecularly and by neuron density. The borders of a barrel column are visibly identified at edges of the barrel-like structures representing L4, specifically. During the first 3 weeks of postnatal development in mice, the circuitry of the barrel cortex readily undergoes varies modes of experience-dependent synaptic plasticity until closure of the critical period: a developmental timeframe during which the long-term framework of neural circuits is acquired and stabilized.

Here I first discuss the circuitry within the barrel cortex as well as its synaptic interaction with other brain areas. Afterward I highlight how experience induces plasticity and sculpts neural circuits within the barrel cortex throughout development.

From the whisker to the cortex

Whisker deflection activates mechanogated ion channels which depolarize and cause action potential firing in sensory neurons within the infraorbital branch of the trigeminal nerve. A single sensory neuron will only fire action potentials in response to

deflection of one specific whisker. These sensory neurons within the trigeminal nerve provide strong, high-fidelity excitatory synaptic input onto neurons residing within the ipsilateral principal trigeminal nucleus of the brain stem. Trigeminothalamic neurons are somatotopically organized into structures called "barrelettes". These neurons synapse onto thalamocortical neurons within the contralateral ventral posterior medial thalamic nucleus (VPM) that are somatotopically organized into structures called "barreloids". Trigeminothalamic neurons provide strong excitatory drive onto excitatory spiny stellate neurons within L4 "barrel" structures. This neuroanatomical pathway is commonly known as the mono-whisker "lemniscal" pathway. Whisker-mediated, tactile sensation is completely segregated and confined to circuitry representing a single whisker upstream of and into the barrel cortex (Feldmeyer 2012b, Petersen 2007, Schubert et al 2007).

The synaptic pathways through which ascending whisker sensation is processed diverges within the brain stem and eventually target different thalamic nuclei and cortical layers. For example, whisker-mediated synaptic activity travels from trigeminal sensory neurons onto neurons within the spinal trigeminal nuclei as well as to both rostral and caudal regions of the trigeminal spinal interpolaris nucleus which form the beginning of the "paralemniscal" and "extralemniscal" pathways, respectively. The "extralemnsical" pathway consists of neurons within the caudal interpolaris nucleus that project to the ventrolateral VPM, which in turn, synapses onto neurons residing within barrel septa: regions between barrel columns. The "paralemniscal" pathway is demarcated by rostral interpolaris nuclei neurons projecting onto the thalamic posterior medial (POM) nucleus, and then POM neurons innervate L1 and L5A cortical neurons of S1BF. The extralemniscal and paralemniscal pathways integrate inputs associated with multiple

whiskers and relay whisker-mediated feed-forward excitation to multiple cortical regions including the primary somatosensory (S1), secondary somatosensory (S2), and primary motor (M1) cortices. Although the extralemniscal and paralemniscal neuroanatomical pathways mediate critical facets of whisker sensation, this work primarily studies the development of the mono-whisker lemniscal pathway. Additionally, septa within the mouse barrel cortex are extremely small as barrel columns are tightly apposed (Petersen 2007). Hence I will no longer discuss circuit and physiological processes involving the extralemniscal and paralemniscal pathways.

Local intracolumnar and transcolumnar excitatory circuitry of the barrel cortex

Once strong, thalamocortical feed-forward excitation reaches excitatory spiny stellate neurons within L4 of S1, excitatory drive spread laterally within a barrel and vertically into L2 and L3. Local L4 neurons have high recurrent excitation and connection probability, and spiny stellate neurons have highly compact dendritic and axonal arbors that are confined within the barrel column. Thus, L4 may function to amplify ascending thalamocortical input (Feldmeyer et al 1999). L4 axons provide strong, converging synaptic input onto the basal dendrites of excitatory pyramidal neurons within L2 and L3 of the same barrel column, forming ~4-5 synaptic connections onto each L2/3 pyramidal neuron (Feldmeyer et al 2002), but form relatively weak transcolumnar L4 → L2/3 inputs (Bureau et al 2008, Shepherd et al 2003). Interestingly, L2/3 → L4 inputs are not reciprocal and extremely rare (Feldmeyer et al 2002, Lefort et al 2009, Petreanu et al 2007b).

Although L2 and L3 are generally recognized as a single, functionally uniform layer, recent studies have elucidated heterogeneity and distinction of pyramidal neurons

among these layers in terms of morphology and inputs. L2 pyramidal neurons have short apical dendrites with large, widespread apical tufts within L1 extending throughout multiple barrel columns and are thus poised to receive and integrate cross-column inputs from multiple whiskers (Feldmeyer 2012a, Larsen & Callaway 2006, Schubert et al 2007). L3 pyramidal neurons tend to have longer apical dendrites and more slender apical tufts to maintain isolation of ascending whisker-mediated activity (Feldmeyer 2012a, Schubert et al 2007). In general, L2/3 pyramidal neurons have axonal arbors extending mostly into L5 and L2/3 and expand laterally throughout multiple barrel columns (Adesnik & Scanziani 2010, Feldmeyer 2012a), thus "multi-whisker" crosstalk occurs within L2/3 of the barrel cortex. L2/3 neurons not only integrate synaptic input of multiple barrel columns but also relay input locally onto neighboring L2/3 neurons with high release probability and connectivity, similar to that of L4 → L2/3 innervation (Feldmeyer 2012a, Feldmeyer et al 2006). High-fidelity excitatory transmission of L2/3 microcircuits may also have an amplification purpose for relaying whisker-mediated neural activity to higher-order cortical regions.

L2/3 pyramidal neurons have axon arbors that also heavily innervate basal dendrites of pyramidal neurons within L5A and L5B within and across barrel columns. L2/3 → L5 input is relatively weak with low connection probability and release probability (Feldmeyer 2012a, Lefort et al 2009, Petreanu et al 2009). Interestingly, synaptically uncoupled L2/3 pyramidal neurons tend to more strongly innervate synaptically coupled L5 pyramidal neurons within the same barrel column, suggesting that L2/3 neurons exist in small subnetworks and preferentially synapse onto specific subnetworks of L5 pyramidal

neurons that integrate some currently unidentified aspects of neural activity associated with whisker sensation (Kampa et al 2006).

In general, L5 is considered the "output" cortical layer, integrating sensory information from multiple whiskers and having heterogeneous pyramidal neuron subtypes possessing elaborate, extensive axonal arbors. Slender-tufted pyramidal neurons constitute the majority of L5A pyramidal neurons, while thick-tufted and non-tufted pyramidal neurons are found mostly within L5B (Feldmeyer 2012b, Larsen & Callaway 2006, Schubert et al 2006). L5 pyramidal neurons innervate local L5 neurons and L2/3 neurons within and across barrel columns, consistent with the location and span of their axonal arbors. Slender-tufted L5A pyramidal neurons synapse onto L2/3 pyramidal neurons with a ~2-fold connection ratio in comparison to thick-tufted L5B pyramidal neurons (Lefort et al 2009). Furthermore, a subset of L5 neurons projects to distal cortical regions including ipsilateral M1 as well as L2/3 and L5 of the contralateral S1 (Larsen & Callaway 2006, Larsen et al 2007, Le Bé et al 2007, Mao et al 2011). L5B neurons also participate in thalamo-corticothalamic feedback loops to POM excitatory neurons, and these loops are thought to serve "synaptic relay" roles through the thalamus and into more divergent high-order cortical areas including S2, M1, etc. (Theyel et al 2010) Hence L5 is a site of lemniscal, extralemniscal, and paralemniscal integration and can transmit outgoing cortical activity from essentially all cortical layers directly to and through the same thalamic nuclei for high-order cortical processing.

Layer 6 is primarily considered to be the source of corticothalamic projections from S1, and is divided into two specialized layers: L6A derived from the cortical plate, and L6B having orginated predominantly from the cortical subplate (Marin-Padilla 1978).

The cell-type heterogeneity among these layers gives rise to a plethora of network regulation and has thus far been largely understudied. L6A pyramidal neurons are classified into two main groups based upon their axonal projections to either intracortical layers 3-5A or thalamocortical inputs to VPM and POM (Feldmeyer 2012b). The corticocortical-projecting L6A pyramidal neurons have axonal arbors largely confined to L5/6 of S1 with occasional long-range projections into S2 and M1, and importantly, do not establish subcortical synapses. The corticothalamic L6A neurons receive relatively strong input from L4 neurons within the same barrel column, and furthermore, the L4 spiny stellate and star pyramidal neurons target largely non-overlapping dendritic compartments of the L6A pyramidal neurons which suggests further circuit specificity in mediating whisker sensation (Tanaka et al 2011). To date, only few studies have assessed axonal projections of L6B pyramidal neurons of any subtype. Essentially, L6B neurons can project to POM and into L1 (Feldmeyer 2012b). Additional studies must be performed to scratch the surface of how L6 pyramidal neurons contribute to neocortical circuit function.

The spread of excitation throughout barrel cortical circuits is of great relevance to sensation and perception of whisking behavior, and thus, identifying the modes of structural and functional synaptic plasticity utilized at each pathway can help to elucidate pathway-specific significance resultant of postnatal experience.

Circuitry of inhibition within the barrel cortex

Exploration of the role for cortical inhibition has only recently begun. There are multiple cellular subtypes of GABAergic interneurons found throughout all six layers of a barrel column, and they are distinctly classified by molecular markers, action potential

firing patterns, and innveration distribution onto excitatory neurons. The variety of interneurons allows for phase-locking and fine-tuning of excitation onto excitatory neurons. Parvalbumin (PV)-expressing, fast-spiking interneurons are non-adapting and tend to innervate the perisomatic region of neocortical pyramidal neurons. These interneurons are generally considered to control the gain of synaptic input integrated throughout the dendritic tree as it spreads into the soma. Furthermore, PV interneurons are thought to facilitate firing synchrony across populations of L2/3 pyramidal neurons through disynaptic inhibition caused by simultaneous excitatory L4 inputs onto both L2/3 pyramidal neurons and PV interneurons. The somatostatin (SST)-expressing interneurons have rapidly adapting action potential bursting and are primarily located in supragranular layers, especially within L1. SST interneurons tend to synapse onto distal apical dendrites of pyramidal neurons at dendritic regions surrounding excitatory synapses and serve to filter and finely tune excitatory input. Similar to SST interneurons, a third class of interneurons expressing 5-HT_{3A} serotonin receptor also functions to finely tune excitatory inputs onto distal apical dendrites of cortical pyramidal neurons and have axon arbors ramifying L1. SST and 5-HT_{3A} interneurons receive excitatory inputs from long-range excitatory projections and can modulate the penetration of back-propagating action potentials into the distal apical tufts of L2/3 and L5 pyramidal neurons within S1, hence regulating the window for plasticity at synapses onto those dendritic segments (Higley 2014, Lee et al 2013). Inhibitory neural networks are heterogeneously coupled synaptically and homogeneously coupled electrically within the barrel cortex (Gibson et al 1999), and thus can regulate each other on a smaller scale via synaptic transmission and can also

regulate excitation and action potential propagation throughout more expansive neural networks via gap junctions nearly instantaneously.

Although this work highlights development of excitatory circuitry onto L2/3 pyramidal neurons in the rodent barrel cortex, it is important to consider the role of inhibition in sculpting synaptic input onto L2/3 pyramidal neurons as L2/3 circuit plasticity is mediated, in part, via GABAergic synaptic signaling. Furthermore, the manipulations I employ and discuss throughout subsequent chapters leave cortical inhibitory networks intact.

Long-range, intercortical inputs onto S1 neurons: Focus on L2/3

S1 also receives inputs from long-range, distal cortical regions through reciprocal synaptic connections with contralateral S1 (cS1), S2, M1, insular cortex, and perirhinal cortex. Trans-callosal projections emanating from L2/3, L5, and L6 of cS1 target L2/3, L5, and L6 of S1 in a column-like fashion (Ivy et al 1979). Additionally, trans-callosal projections from L2/3 of cS1 never synapse onto L4 neurons of S1(Petreanu et al 2007b). Mostly cS1 L3 and L5 pyramidal neuron axons comprise the majority of trans-collosal projections to S1 (Wise & Jones 1976). Interestingly, trans-callosal projections from L2/3 mirror ipsilateral connection patterns in terms of laminar specificity, connection probability, and synaptic strength; this suggests that L2/3 pyramidal neurons may function to coordinate and synchronize bilateral activity of barrel cortices across hemispheres (Petreanu et al 2007b).

Reciprocal synaptic connections between S1 and ipsilateral M1 form the basis of strong cortical feedback loops. L2/3 pyramidal neurons in S1 project onto neurons within

L1 and L2/3 of the ipsilateral M1, and importantly, somatotopic organization is preserved across these synapses to facilitate motor and sensory integration for a single whisker (Bosman et al 2011, Feldmeyer 2012b, Petreanu et al 2009). Conversely, projection axons emanating from ipsilateral M1 travel through the L1 axon tract and synapse onto the apical tufts of both L2/3 and L5 pyramidal neurons within S1 (Petreanu et al 2009, Veinante & Deschênes 2003, White & DeAmicis 1977).

Inputs from ipsilateral S2 onto S1 occurs via two distinct routes: 1) directly through the L1 axon tract and supragranular layers (Aronoff et al 2010), and 2) indirectly through corticothalamocortical feedback loops (Bosman et al 2011, Feldmeyer 2012b). Therefore, S2 and S1 are reciprocally connected, although S1 → S2 connections are more abundant than projections from S2 → S1 (Aronoff et al 2010). The extent to which S2 → S1 inputs are involved in experience-dependent circuit plasticity and perception is unclear and understudied, but likely integration of neural activity associated with multiple whiskers through convergence of lemniscal, extralemniscal, and paralemniscal pathways are involved.

L2/3 pyramidal neurons as postsynaptic entities

The L2/3 pyramidal neurons are the targets of the first corticocortical synaptic activity in the ascending lemniscal "mono-whisker" circuit. These neurons receive heterogeneous local, intracolumnar, transcolumnar, and long-range presynaptic inputs. In viewing the L2/3 pyramidal neuron as a postsynaptic recipient of activity in a functional neocortical circuit, this neuron must be able to distinguish physiologically salient information among the populations of excitatory and inhibitory inputs. L2/3 pyramidal

neurons have asymmetrical dendritic arbors in that they have short basal dendrites and a primary apical dendrite that bifurcates into an apical tuft of extensively branched distal dendrites that extend into L1. Distinct inputs target dendritic segments within each of these subcellular compartments, but untangling the web of tens of thousands of synapses onto a L2/3 neuron has proven difficult. For example, L2/3 pyramidal neurons have basal and apical dendrites that are much thinner than those of L5 pyramidal neurons, making the L2/3 pyramidal neuron very electrically compact (Larkum et al 2007). Hence, only recently have morphological, tracing, and functional studies been used to compartmentalize the pyramidal neuron into more specific segments and to evaluate the source and physiological consequences of presynaptic inputs targeting such segments, especially with regard to experience-dependent circuit plasticity *in vivo*.

Basal dendrites are the targets of local synaptic inputs emanating from vertical L4, horizontal transcolumnar L2/3, and neighboring L2/3 pyramidal neurons, for example. L2/3 neurons synapsing locally onto neighboring L2/3 neurons form 2-4 synapses onto basal and proximal apical oblique dendrites within ~90 µm of the soma (Feldmeyer et al 2006), and L4 axons tend to form ~4-5 synapses onto L2/3 basal dendrites (Feldmeyer et al 2002). For example, synapses formed by a single L4 axon onto a L2/3 pyramidal neuron have an average geometric distance of ~70 µm from the soma, suggesting that L2/3 neurons require simultaneous activation of L4 inputs in order to reach the threshold for firing an action potential for relaying whisker-driven neural activity (Feldmeyer et al 2002). Therefore, L2/3 pyramidal neurons likely establish, in part, the threshold for sensation of relevant and salient experience for deflection of a single whisker. L2/3 and L5A pyramidal neurons residing in ipsilateral M1 synapse onto both basal and apical dendrites of L2/3

pyramidal neurons in S1 (Mao et al 2011), which integrate synaptic input emanating from both local and distal cortical regions. Additionally, imaging of trans-callosal cS1 L2/3 projection axons reveals dense targeting in L5 and supragranular layers in S1, but these axons also traverse all cortical layers of S1 while ascending from the corpus callosum (Petreanu et al 2007b), hence identification of trans-callosal cS1 L2/3 axon terminals onto the S1 L2/3 dendritic tree seems diffuse, spanning both basal and apical dendritic compartments.

L2/3 apical dendrites are capable of generating calcium spikes at the apical dendritic bifurcation into the apical tuft. Additionally, back-propagating somatic action potentials can evoke only a single apical dendritic spike, demonstrating that L2/3 apical dendrites cannot "burst" as is the case with the large-diameter L5 apical dendrites (Larkum et al 2007). Thus, apical dendrites of L2/3 neurons establish a very limited window for coincidence detection in mediating spike-timing-dependent plasticity. The relatively low propensity for action potential generation within L2/3 pyramidal neurons, therefore, dampens sensory input and requires strong, synchronous, patterned whisker deflection to cause LTP- and LTD-like mechanisms at most apical dendritic synapses, especially for coordinating long-range cortical activity. Apical dendrites of L2/3 pyramidal neurons in S1 are considered to be the main targets of long-range cortical inputs (Bosman et al 2011, Feldmeyer 2012b), but they are targeted by a mixture of local and distal corticocortical inputs. More investigation is needed to identify patterns of subcellular synaptic targeting within the L2/3 apical dendritic compartment, especially within the apical tuft, as no studies – to my knowledge – have identified inputs specifically targeting this dendritic compartment.

Experience-dependent synapse development and dynamics in the barrel cortex: Focus on L2/3 pyramidal neurons

Following the completion of neural migration and the basic establishment of the circuit framework, neocortical neurons undergo several developmentally regulated temporal and dynamic phases for regulating the strength and number of synaptic contacts formed with presynaptic partners. In general, synapse number is low during embryogenesis as neurons extend their dendritic and axonal arbors. During early postnatal development, this number drastically increases as axons and dendrites of different neurons come within close proximity to one another, resulting in an excess of synaptic connections. Concurrently, small protrusions rapidly emerge on the dendrites of excitatory neurons, which are known as dendritic spines and considered to be the structural correlates of excitatory synapses (Harris & Kater 1994). An excess of highly dynamic synapses are formed at a fast rate as neuronal dendritic and axon arbors mature and gain complexity, which is thought to maximize the potential pathways for information processing among neural networks (Holtmaat & Svoboda 2009, Rakic et al 1986). In the mouse, synapse proliferation in the neocortex is most robust during the first 2-4 weeks of postnatal life (De Felipe et al 1997). However, eventually a threshold is surpassed in later postnatal development at approximately the onset of adolescence, triggering synapse elimination processes that result in an overall pruning or reduction of synapses number to as the circuit matures (De Felipe et al 1997, Huttenlocher 1979, Rakic et al 1986) (Chen & Regehr 2000, Patel et al 2014).

Synapses are dynamic structures and undergo turnover through the lifespan at different rates, even during adulthood when plasticity mechanism are less robust (Trachtenberg et al 2002). The fate of a synapse is subjected to an equilibrium of synapse formation and elimination processes, and thus, synapses are eliminated and formed throughout postnatal development (Holtmaat & Svoboda 2009). Importantly, evidence suggests that the erection of a dendritic spine precedes synapse formation, and hence, does not necessarily mark the site of synaptic transmission (Knott et al 2006). Additionally, some dendritic spines exist without presynaptic boutons (Harris & Kater 1994). Nonetheless, dendritic spine density is highly correlated with the developmental control of synapse formation, maintenance, and elimination (Holtmaat & Svoboda 2009).

L2/3 pyramidal neurons within the barrel cortex are subjected to experience-dependent plasticity through whisking. Sensory experience promotes the strength of L4 → L2/3 inputs until closure of the critical period – a time of robust synaptic plasticity – occurring after the second week of postnatal development in mice (Bender et al 2006a, Bureau et al 2008, Shepherd et al 2003); neither whisker stimulation nor trimming robustly affects synaptic plasticity and receptive fields of barrel columns beyond this age (Fox 1992, Lendvai et al 2000). An important initial consideration is that sensory experience does not drastically alter dendritic arborization of L2/3 neurons (Maravall et al 2004), suggesting that circuit plasticity occurring here is a synaptic phenomenon and relies on the interplay of specific synaptic inputs to shape the postsynaptic behavior of L2/3 pyramidal neurons.

Regulation of connectivity and synapse number

The robust experience-dependent plasticity within the barrel cortex allows for both functional and structural synaptic reorganization such that spared cortical regions out-compete deprived areas for synaptic resources (Feldman & Brecht 2005, Petersen 2007). Sensory experience causes changes in L2/3 synaptic connectivity and synapse number, and such regulation depends on the synaptic input pathway and dendritic compartment of focus. Sensory deprivation by trimming only a single row of whiskers (D-row trimming) induces a shift in local connectivity between synaptically coupled L2/3 pyramidal neurons specifically within barrel columns at the border between spared and deprived columns (Cheetham et al 2007b). Furthermore, D-row whisker trimming results depression of L4 → L2/3 and potentiation of L5A → L2/3 inputs within the same barrel column (Bureau et al 2008). Mice reared in an enriched environment displayed increased dendritic spine density on basal dendrites of neocortical L2/3 neurons is comparison to mice housed in solitude in "impoverished" environments without light and objects (Globus et al 1973). However, long-term *in vivo* imaging studies employing "sparse" whisker removal report increases in the motility but the not number of dendritic spines on L2/3 apical dendrites (Lendvai et al 2000). These studies may reflect a compartment-specific regulation of synapses by sensory experience. Consistent with this, experience-dependent synapse elimination of dendritic spines on L2/3 basal dendrites is blocked by whisker trimming, which prevents synaptic competition for β-catenin (Bian et al 2015). However, inconsistent with this thought, cofilin-1 – a regulator of actin filament turnover – is required for shifting the barrel cortical map representation; it promotes the number of synapses formed between spared horizontal axons and dendritic spines on distal apical dendrites of deprived L2/3 neurons (Tsubota et al 2015). Thus, experience-dependent regulation of

synapses within the apical dendritic compartment may play a more significant role in circuit plasticity at the edges between spared and deprived cortical areas.

Regulation of input strength by synaptic plasticity mechanisms

Neocortical L2/3 pyramidal neurons adjust the strength of synaptic inputs via both synapse-specific and global plasticity mechanisms in response to sensory experience and deprivation.

Short-term plasticity at L4 → L2/3 inputs is altered by sensory deprivation, which has been proposed to reflect *in vivo* LTD-like plasticity occurring at the presynaptic boutons (Bender et al 2006a, Cheetham & Fox 2010). Weakening of presynaptic L4 → L2/3 inputs likely does not affect the maturation of L2/3 synapses but instead allows for competition between L4 axons and horizontal inputs to make the L2/3 neurons more versatile in facilitating a shift in their cortical representation.

Spike-timing-dependent LTD (SLTD) and LTP (SLTP) are forms of homosynaptic plasticity that alter L2/3 synaptic function dependent on the timing between actional potential firing and subsequent glutamate release from L4 axons and L2/3 action potential firing. L2/3 synapses undergo SLTP when L4 firing closely precedes L2/3 action potential firing within approximately 20 milliseconds. SLTD causes L2/3 synaptic depression when the firing of L4 axons occurs after or is not correlated with L2/3 firing. Whisker stimulation mediates SLTP that requires activation of NMDARs, while sensory deprivation induces SLTD by drastically decorrelating L4 and L2/3 action potential firing through NMDAR- and endocannabinoid-dependent mechanisms (Bender et al 2006c, Celikel et al 2004, Feldman 2012).

Interestingly, neocortical L2/3 pyramidal neurons undergo more complex types of synaptic plasticity that involve multiple synapses and/or multiple means of synaptic regulation that occur seemingly simultaneously. For example, whisker stimulation causes two modes of experience-dependent plasticity L2/3 neurons *in vivo*: a LTP-like potentiation of nearby or "clustered" GluA1-containing synapses and concomitant homeostatic synaptic scaling of evenly distributed GluA2-containing synapses (Makino & Malinow 2011). Furthermore, neighboring excitatory synapses within a small dendritic segment are activated in close temporal and spatial proximity *in vivo* (Harvey & Svoboda 2007, Takahashi et al 2012) after experience onto basal dendrites of neocortical L2/3 neurons (Makino & Malinow 2011). Additionally, competition for synaptic resources occurs within L2/3 neurons such that local increases in synaptic activity onto specific L2/3 dendritic spines causes the stabilization of the stimulated spine and subsequent elimination of neighboring spines (Bian et al 2015). Therefore, it is likely that sensory experience can induce heterosynaptic plasticity within and around these synaptic "clusters".

It is becoming more apparent that the interplay between specific synapses is critical for experience-dependent circuit development in neocortical neurons for regulating input-specific changes in connectivity and synaptic strength. These plasticity mechanisms allow L2/3 pyramidal neurons to rapidly adapt to sensory stimuli as well as to amplify and/or dampen activation of synapses that are either primarily or secondarily involved with salient experience.

ACTIVITY-DEPENDENT REGULATION OF GENE TRANSCRIPTION MODULATES SYNAPSE DYNAMICS AND CIRCUIT DEVELOPMENT

Activity-dependent plasticity allows the brain to respond to environmental stimuli, regulating synapse formation and maturation, refinement, and dynamics throughout the lifespan of an organism. Hence, a strong interaction between genetic and environmental factors facilitates proper neural circuit development. Sensory experience and neural activity induce transcriptional mechanisms that are temporally regulated and heavily intertwined with changes in synaptic plasticity (West & Greenberg 2011b). Here I highlight important mechanisms and physiological consequences associated with communication between the synapse and nucleus.

Role for Calcium in synapse-to-nucleus signaling

Plasticity mechanisms including long-term potentiation (LTP) and long-term depression (LTD) require postsynaptic calcium influx for induction, which in turn, causes signaling cascades to drive transcription that is critical for the maintenance of both LTD and LTP as well as other long-lasting changing in synaptic physiology (Lynch et al 1983, Madison et al 1991, Malenka & Bear 2004, Mulkey & Malenka 1992). Calcium influx through L-type voltage-gated calcium channels (L-VGCCs) and NMDARs induces transcription of immediate early genes (IEGs) and is required for experience-dependent synapse and circuit refinement (Morgan et al 1987, Zuo et al 2005). Calcium binding proteins such as CaMK, calcineurin, and MAPK are activated by activity-induced calcium influx (West & Greenberg 2011b). Interestingly, the route through which calcium enters a neuron results in activation of different transcriptional programs as, for example, activation of either NMDARs or L-VGCCs stimulates different CaMK signaling pathways resulting in activation of different cis-acting regulatory elements of the c-fos promoter (Bading et al

1993). Additionally, different means of calcium influx and localization of calcium binding proteins are likely to modulate transcription differently resulting from synaptic input and/or widespread depolarization due to backpropagating action potentials (West & Greenberg 2011b). Further adding to the variety and complexity of calcium signaling is that calcium can in some cases directly bind transcription factors such as the dimerization partner, RB-like, E2F and multi-vulval class B (DREAM) to rapidly regulate transcription (Carrion et al 1999).

Role in synapse formation and maturation

Calcium is critical for regulating and balancing synaptogenesis and synapse stabilization by activation activity-dependent transcription factors such as NFAT and CREB. Calcium promotes the association of calcineurin with NFAT in the cytoplasm, which causes a shuttling of NFAT into the nucleus where transcription of its target genes eventually suppresses synaptogenesis (Schwartz et al 2009).

Calcium-dependent activation of CaMKIV in response to sensory experience induces the transcriptional activity of CREB, which triggers experience-dependent dendritic spine formation and enlargement (Cohen & Greenberg 2008, Pignataro et al 2015, West & Greenberg 2011b). Additionally, phosphorylation of several serine residues is required for maximal calcium responsiveness of CREB, and point mutations preventing phosphorylation of these serine residues impairs synaptic plasticity typically induced by visual experience, demonstrating that CREB is critical for experience-dependent synapse formation in early postnatal development (Cohen & Greenberg 2008, Gau et al 2002).

Neuronal activity also induces expression of and stimulates the transcription factor NPAS4, which positively regulates inhibitory GABAergic synapse number through BDNF signaling (Lin et al 2008). In CA1 pyramidal neurons of the hippocampus, NPAS4 differentially regulates the strength of specific dendritic compartments. Specifically, NPAS4 promoted inhibitory synapse number onto the somatic but not dendritic compartments within individual CA1 neurons in mice exposed to an enriched environment (Bloodgood et al 2013b). Given the somatic compartmentalization by NPAS4, the increased inhibitory synapses are likely established with axons of PV-expressing interneurons. This, however, has never been tested.

Role in synapse elimination

Calcium influx is also critical for the elimination of synaptic connections, especially during adolescence when neural circuits are being refined and stabilized (Holtmaat & Svoboda 2009, Zuo et al 2005). The Myocyte Enhancer Factor-2 (MEF2) family of activity-dependent transcription factors eliminates excitatory synapses within several brain areas. The activity-dependent transcriptional regulation by MEF2 will be discussed in great detail within the next section of this chapter as it is the primary focus of this work. But here I will discuss what is known regarding the mechanisms associated with MEF2-dependent synapse elimination.

The molecular mechanisms facilitating hippocampal MEF2-dependent synapse elimination has been primarily examined *in vitro* with the overexpression of constitutively active and/or dominant-negative regulators of "pan" MEF2-dependent transcription that are not specific for the individual *Mef2* genes. Hippocampal synapses are subjected to

MEF2-dependent synapse elimination, and this process requires upstream activation of the metabotropic glutamate receptor-5 (mGluR5) to eliminate structural and functional excitatory synapses on the dendrites – but not soma – of CA1 pyramidal neurons (Wilkerson et al 2014). Activation of MEF2 via mGluR5 signaling causes transcription of MEF2 target genes including Homer 1a, Arc, and BDNF. MEF2 requires Fragile X Mental Retardation Protein (FMRP) – a RNA binding protein and translational repressor – to eliminate synapses (Pfeiffer et al 2010a). This likely involves an interaction between MEF2 and FMRP such that MEF2 transcripts are bound my FMRP and transported to the synapses for local dendritic translation. This possibility has yet to be investigated. Further supporting the hypothesis that FMRP and MEF2 transcription factors interact in a common molecular pathway, FMRP also prunes excitatory synapses among microcircuits of L5A pyramidal neurons in the mouse barrel cortex and suggests that MEF2-dependent synapse elimination may occur in other brain areas through an FMRP-dependent mechanism (Patel et al 2014).

MEF2 target genes such as Arc and protocadherin-10 (PCDH10) mediate AMPA receptor endocytosis and degradation of the synaptic scaffolding protein postsynaptic density-95 (PDS-95), respectively (Chowdhury et al 2006, Colledge et al 2003). Indeed, Arc is required for hippocampal MEF2-dependent synapse elimination (Wilkerson et al 2014), demonstrating how MEF2, in the nucleus, drives transcription of IEGs directly involved in regulating glutamate receptors. PCDH10 is also necessary for MEF2-dependent synapse elimination by promoting proteosomal degradation of PSD-95 through interactions with the ubiquitin E3 ligase murine minute-2 (Tsai et al 2012).

Hence, the mechanisms through which activity-dependent regulation of synapses is complex and multifaceted, requiring extensive communication between the synapse and nucleus to regulate circuit development.

THE MEF2 FAMILY OF TRANSCRIPTION FACTORS

Named appropriately for their discovery in skeletal and cardiac tissues, MEF2 transcription factors are expressed throughout the body and are critical for development of muscular, cardiac, immune, and nervous systems (Potthoff & Olson 2007). In the brain, MEF2 mediates a plethora of important cellular processes including cell death regulation, maturation, neural migration, synaptic connectivity, and synaptic metaplasticity (references; Li et al., 2008; Akhtar et al., 2012; Barbosa et al., 2008; Flavell 2006, Flavell 2008, Chen et al., 2012). The MEF2 family transcription factors is comprised of four independent genes – *Mef2a, Mef2b, Mef2c,* and *Mef2d* – having distinct yet overlapping expression profiles throughout the brain that are developmentally regulated (Lyons 1995)(Lyons et al 2012b). *Mef2c* is the first of the MEF2 genes to be expressed in differentiated neurons at E11.5 within the telencephalon and is closely followed by *Mef2a*, *Mef2b*, and *Mef2d* in a brain-region-specific manner. In the hippocampus, *Mef2c* is highly expressed initially but then largely diminishes such that *Mef2c* expression is largely restricted to the dentate gyrus in the postnatal brain. In contrast, *Mef2a* and *Mef2d* expression levels are relatively low until birth and then become highly expressed throughout the hippocampus by the second postnatal week of development. Hippocampal *Mef2b* expression, however, remains low throughout the lifespan. MEF2 expression within the thalamus is stable throughout development; *Mef2a* is highly expressed embryonically

and postnatally, while *Mef2b*, *Mef2c*, and *Mef2d* remain at low levels. In the neocortex, *Mef2c* is the predominant MEF2 gene throughout development, comprising ~80% of total MEF2 expression in differentiated neurons (Lyons et al 1995a, Lyons et al 2012b). Neocortical *Mef2a* and *Mef2d* mRNA levels are relatively low prenatally and postnatally. Some debate surrounds the neocortical expression profile of *Mef2b* because measurement of mRNA levels *in vitro* (Lyons et al 2012b) reveal absence of *Mef2b*, whereas expression appears abundant *in vivo* (Lyons et al 1995a). Similar expression profiles exist in human fetal brain and skeletal muscle tissues (Leifer et al 1993). Therefore, the temporal and spatial regulation of specific MEF2 genes in facilitating brain circuit development is complex.

Despite the uniqueness across MEF2 genes, there are several hallmark features shared among all of them, linking their abilities to regulate activity-dependent transcription. Highly conserved among all of the MEF2 transcription factors are the N-terminal (MCM1 Agamous Deficiens Serum Response factor (MADS)) and MEF2 domains, which facilitate DNA binding and dimerization, respectively (McKinsey et al 2002). These domains are required and sufficient for MEF2-dependent transcription as deletion of these domains prevents DNA binding while overexpression of MADS/MEF domains fused to a viral activation domain drives MEF2-dependent transcription (Molkentin et al 1996). The MADS/MEF2 domains have been useful in generation of genetic mouse models for deleting transcriptional activity of specific MEF2 genes (Akhtar et al 2012, Arnold et al 2007a, Kim et al 2008, Vong et al 2005). DNA binding of MEF2 occurs at specific CTA(A/T)$_4$TAG nucleotide sequences called MEF2 response elements (MREs), which are located proximally to target gene promoters and also at distal enhancer

regions several kilobase pairs away from transcriptional start sites (Andrés et al 1995, Flavell et al 2008). Since the DNA binding site of MEF2 transcription factors is highly conserved, it is assumed that a large population of target genes are bound and regulated redundantly by these transcription factors, and in fact, transcriptome sequencing studies identifying libraries of putative MEF2 target genes are used to infer potential targets among all MEF2 proteins. This, however, does not reflect the phenotypic variability on behavior and synaptic physiology when specific MEF2 genes are deleted across different neuron populations, which will be further discussed later. The adjacent MEF2 domain facilitates dimerization as well as cofactor binding but the extent to which is could contribute to the distinctiveness of individual MEF2 proteins in regulating transcription is unknown because it, too, is a highly conserved protein domain. Furthermore, MEF2 proteins are bound to DNA as homo- and heterodimers (McKinsey et al 2002), and interestingly, the effects of different MEF2 dimer entities has never been studied. Perhaps this could add another facet to understanding the complexity of transcriptional regulation by specific MEF2 proteins across distinct neuron populations (i.e. neocortical pyramidal neurons versus hippocampal pyramidal neurons), especially given the region-specific spatial overlap among MEF2 genes.

The C-terminal transcription activation domains of MEF2 genes are less conserved and contain multiple transcriptional activation domains and a bipartite nuclear localization signal (McKinsey et al 2002). Additionally, many cofactor interactions occur within this region to regulate transcriptional activation and repression as well as nuclear retention. Regulation of MEF2 transcriptional activity is also achieved through post-translational

modification and alternative splicing mechanisms within the C-terminus, which primarily modulate calcium responsiveness in neurons (Lyons et al 2012b, Zhu & Gulick 2004).

To study general MEF2-dependent transcription, mutant forms of MEF2 have been developed. The herpes simplex viral protein (VP16) is a strong transcriptional activator that has been fused to the MADS and MEF2 domains of MEF2C, thus creating a constitutively active MEF2 that binds to all MEF2 DNA binding sites (Molkentin et al 1996). Additionally, mutations replacing hydrophobic amino acid residues located within the MADS-box and MEF2 domain prevent cofactor interactions, dimerization, and DNA binding. Deletion of the MEF2 domain – immediately adjacent to the MADS-box – also is sufficient to block dimerization of MEF2C monomers (Molkentin et al 1996). Fusion of Engrailed – a strong transcriptional repressor – to the MEF2 C-terminus functions as a dominant-negative and robustly inhibits MEF2-dependent transcription (Arnold et al 2007a).

Early MEF2 studies were carried out in cardiac and skeletal muscle tissues and discovered to be critically involved with myocyte differentiation (Potthoff & Olson 2007). However, over the last two decades the role of MEF2 in brain development has been more extensively scrutinized. In neurons, MEF2 mediates activity-dependent transcription via calcium sensitivity, which is required for neuronal cell survival (Mao et al 1999, Mao & Wiedmann 1999). The calcium responsiveness of MEF2 is also critical for induction of immediate early genes and critical signaling factors mediating synaptic plasticity (Flavell et al 2008, Lyons et al 2012b). Thus, MEF2 transcription factors are vital factors for regulating the development and maintenance of neural circuits.

Mechanisms of MEF2 regulation

The calcium responsiveness of MEF2 transcription factors has been a hallmark feature in their ability to regulate gene transcription in response to cellular activity in electrically excitable cell types including skeletal myocytes, cardiac myocytes, and neurons. In neurons, synaptic transmission can cause calcium influx to trigger a wave of depolarization that propagates to the soma, where in the nucleus MEF2 proteins are activated and initiate activity-dependent transcription of target genes through transcriptional activation. The mechanisms through which calcium regulates MEF2 is diverse.

All MEF2 transcription factors undergo alternative splicing with the exon exclusion occurring within the transcriptional activation domains (Zhu & Gulick 2004). Additionally, accessory domains are also exchanged post-transcriptionally, giving rise to the diversity among MEF2 genes, their tissue localization, and their ability to regulate gene expression through transcriptional activation or repression. In neurons, all MEF2 splice variants contain the α_1 exon; α_2-containing splice variants are localized to muscle tissue (Janson et al 2001, Zhu & Gulick 2004). The β exon may be included or excluded in *Mef2c* mRNA expressed in neurons (Janson et al 2001). A third C-terminal accessory gamma (γ) domain, however, is specific to *Mef2c* pre-mRNA and is included in 50% of mature *Mef2c* mRNA within the neocortex, and when present, greatly reduces calcium sensitivity of the MEF2C protein (Lyons et al 2012b, Zhu & Gulick 2004). Additionally, the γ-domain of MEF2C contains several key residues at which sumoylation and phosphorylation occur and interact to decrease calcium sensitivity (Kang et al 2006).

In addition to alternative splicing, MEF2 proteins are also regulated by cofactor interactions and post-translational modifications dependent on calcium signaling in neurons and non-neuronal cell types. The calcium/calmodulin-dependent protein kinase (CaMK) family is critical for regulating calcium-dependent cellular processes in neurons, including synaptic plasticity and other activity-dependent mechanisms (Wayman et al 2008). MEF2 activation is positively regulated by CaMK in the nucleus (McKinsey et al 2000b). CaMKIV can directly phosphorylate MEF2D but not MEF2A, MEF2B, or MEF2C (Blaeser et al 2000), and thus CaMKIV-dependent regulation of MEF2-dependent transcription is via indirection interactions.

A likely mechanism through which CaMK regulates MEF2 is indirectly through CaMK binding to specific subtypes of histone deacetylases (HDACs), which disrupts the repressive interaction between HDACs and MEF2 (McKinsey et al 2000b). HDACs generally repress the activity of transcription factors by promoting chromatin condensation (Yang & Seto 2007). Additionally, CaMK facilitates nuclear export of HDAC4 and HDAC5, but this is reportedly not required for activation of MEF2 (McKinsey et al 2000a, McKinsey et al 2000b).

Like CaMK, the calcium-responsive phosphatase, calcineurin, also promotes MEF2 activation. The affinity of MEF2 for MREs is increased upon direct phosphorylation by calcineurin (Mao & Wiedmann 1999).

MEF2 activation is required for pro-survival cellular mechanisms in neurons (Mao et al 1999, Mao & Wiedmann 1999, Perry et al 2009). The catalytic subunit of protein phosphatase-1α (PP1α) directly binds and dephosphorylates serine and threonine residues at both N- and C-termini of MEF2A, MEF2C, and MEF2D, which ultimately causes

repression of MEF2 via recruitment of HDACs and interference with the calcineurin binding. PP1α binds directly to class I HDACs, is sufficient to block CaMKIV-mediated activation of MEF2A, and competes directly with calcineurin for dephosphorylation of Serine 408 (Perry et al 2009, Pulipparacharuvil et al 2008a). Ultimately, this induces apoptosis.

Similarly, MEF2 is phosphorylated by cyclin-dependent kinase 5 (CdK5), which is activated following chronic exposure to psychostimulants such as cocaine (Bibb et al 2001, Pulipparacharuvil et al 2008a). CdK5 phosphorylation at Ser 408 and Ser 444 of MEF2 causes repression of MEF2-dependent transcription via suppression of calcineurin-mediated dephosphorylation of MEF2 (Pulipparacharuvil et al 2008a). CdK5-mediated repression of MEF2 can also initiate caspase-mediated degradation of MEF2 (Tang et al 2005).

In addition to CaMK and calcineurin, other cofactor interactions are critical for regulating MEF2-dependent cell survival. For example, the p38 mitogen-activated protein kinase (p38 MAPK) phosphorylates MEF2C at Serine 387 in response to calcium-influx to promote calcium-mediated neuron survival in cerebellar neurons (Mao et al 1999).

Sumoylation of MEF2 proteins near the C-terminus represses MEF2-dependent transcription, and furthermore, the lysine residue is sumoylated depending upon the phosphorylated state of a nearby serine (Kang et al 2006, Zhu & Gulick 2004). Thus, MEF2 function can be modulated through a multitude of post-translational modifications. For example, the C-terminus of MEF2A is sumoylated in cerebellar granule neurons and acts as a transcriptional repressor until calcineurin can dephosphorylate a nearby serine

residue to allow cleavage of the SUMO group and revert MEF2A back into a transcriptional activator (Shalizi et al 2006).

MEF2 transcription factors are targets of caspase-3 – a traditional apoptotic factor – in neurons only during activity conditions that promote synaptic plasticity but not apoptosis (Chen et al 2012). This caspase-mediated degradation allows the cleavage product to bind uncleaved MEF2, thus acting as a dominant-negative regulator (Okamoto et al 2002). Mitochondrial activation of has been linked to activity-induced calcium influx associated with experience-dependent metaplasticity, which results in degradation of MEF2 to shift the plasticity threshold (Brusco & Haas 2015).

The mechanisms through which MEF2 is regulated is diverse, including both pre- and post-translational control. The influence of each splice variant and cofactor interaction on MEF2-dependent regulation of target genes is unknown. Furthermore, the salient physiological conditions under which specific MEF2 transcription factors preferentially transcribe subsets of target genes is also unknown. Understanding the subcellular and molecular players involved in the regulation of MEF2-dependent transcription is critical for understanding the consequences of MEF2 transcription factors in brain circuit development and behavior.

MEF2 transcription factors and synapse function

MEF2 transcription factors are traditionally implicated in regulation of synapse number on excitatory neurons in several brain and brain-associated areas including hippocampal CA1, dentate gyrus, nucleus accumbens, amygdala, cochlea, and optic tectum of the tadpole (Adachi et al 2015, Barbosa et al 2008, Chen et al 2012, Cole et al

2012, Flavell et al 2006, Li et al 2016, Pfeiffer et al 2010a, Pulipparacharuvil et al 2008a, Shalizi et al 2006, Tsai et al 2012, Wilkerson et al 2014, Zhang et al 2016). Depending on the MEF2 gene and the brain region of interest, whether or not MEF2 genes function to positively or negatively regulate synapse number is controversial in the field, thus highlighting the complexity of unraveling the distinct role of specific MEF2 genes in brain circuit development.

The first characterization of MEF2 genes in synapse development were carried out in hippocampal and cerebellar neurons *in vitro* with seemingly contradictory findings. In hippocampal cultures, *Mef2a* and *Mef2d* are involved in the suppression or elimination of structural and functional synapse number, whereas non-sumoylated MEF2A promoted maturation of the dendritic claw in cerebellar granule neurons (Flavell et al 2006, Shalizi et al 2006). Interestingly, both of these studies report that their phenotypes are mediated through a calcineurin-dependent mechanism at Ser 408. Were these discrepancies due to brain region specificity, MEF2 gene specificity, the developmental stage at which experiments were conducted, or the type of genetic mutation employed to study MEF2 function? From the beginning, the function of specific MEF2 genes was complex and difficult to distinguish.

In general, MEF2 transcription factors are considered to be suppressors of excitatory synapse number. In hippocampal organotypic slice cultures, overexpression of a constitutively active MEF2, MEF2-VP16, in CA1 pyramidal neurons reveals decreases in structural and function synapse number (Pfeiffer et al 2010a). Similarly, deletion of *Mef2c* increases structural and functional synapse number within excitatory granule neurons in dentate gyrus of the hippocampus *in vivo* (Adachi et al 2015, Barbosa et al

2008). In contrast to what is observed in dissociated hippocampal cultures, deletion of *Mef2a* and *Mef2d* does not affect dendritic spine density *in vivo* (Akhtar et al 2012). Interestingly, spatial memory formation is blocked by acute overexpression of MEF2C-VP16 in the dentate gyrus and positively correlated with increased phosphorylation of MEF2A at Ser 408, which represses MEF2 function through CdK5-dependent phosphorylation (Cole et al 2012). Therefore, *Mef2a* suppresses dendritic spine proliferation required for spatial memory formation. Similarly, MEF2 activation via overexpression of MEF2-VP16 in the anterior cingulate cortex prevents consolidation of fear memory when injected after training; MEF2 activation within one week of training prevents spine growth induced by fear learning and memory (Vetere et al 2011). Consistent with the idea that MEF2 prevents memory formation, *Mef2a* and *Mef2d* within the nucleus accumbens drive structural synapse elimination that antagonizes the ability of cocaine to induce psychomotor sensitization, which is arguably a form of experience-dependent learning and memory (Pulipparacharuvil et al 2008a). However, cocaine is able to override MEF2-dependent synapse elimination by elevating CdK5 levels which, in turn, decreases calcineurin activity to ultimately repress MEF2-dependent transcription (Pulipparacharuvil et al 2008a). However, these findings differ from the reported role for *Mef2c* in promoting hippocampal-dependent learning and memory (Barbosa et al 2008). Thus, it is possible that specific MEF2 genes differentially regulate learning and memory in the postnatal brain. Interestingly, postnatal *Mef2c* is dispensable for learning and memory (Adachi et al 2015). It is also possible that repression of *Mef2c* could promote learning and memory when acting as a transcriptional repressor bound to DNA because the Barbosa et al., 2008 study deleted

only exon 2, which does not include the CdK5 and calcineurin binding sites and prevents DNA binding.

Interestingly, MEF2 transcription factors appear to also regulation presynaptic function. For example, deletion of both *Mef2a* and *Mef2d* increases paired-pulse ratios, which is consistent with decreased presynaptic release probability (Akhtar et al 2012). Additionally, sumoylated MEF2A, specifically, eliminates synapses in cerebellar granule neurons by acting as a direct transcriptional repressor of the presynaptically localized calcium sensor: Synaptotagmin-1, suggesting that MEF2A suppresses formation of "orphaned" presynaptic boutons not apposed to a postsynaptic entity (Yamada et al 2013). Although most studies have focused upon postsynaptic mechanisms of MEF2-dependent regulation of synapse development, understanding modes of presynaptic regulation is critical for further delineating the roles of specific MEF2 genes in neural circuit development.

MEF2 transcription factors have also been implicated in positive regulation of structural and functional synapse development. *Mef2c* promotes hippocampal and cortical excitatory synaptic transmission, but however, the synaptic locus at which this regulation occurs is unclear (Li et al 2008). Embryonic deletion of *Mef2c* decreases anxiety and novel object exploration and causes impairment of both hippocampal- and amgydala-dependent learning and memory in mice (Li et al 2008), thus yielding the same behavioral phenotype but via a different mode of *Mef2c*-dependent regulation of synapse development as reported previously in this chapter (Barbosa et al 2008). Additionally, *Mef2a* and *Mef2d* stabilize synapses within neurons of the optic tectum in developing tadpoles following visual experience; this is described in more detail below (Chen et al 2012).

MEF2A has been implicated in activity-dependent synaptic maturation and morphogenesis of the dendritic claw: a specialized synaptic structure in cerebellar granule neurons (Shalizi et al 2006). Knockdown of MEF2A expression decreased the density of dendritic claws *in vitro*, and furthermore, expression of MEF2-Engrailed increased the number of dendritic claws, suggesting that MEF2A promotes dendritic claw maturation when acting as a transcriptional repressor. A calcineurin-dependent dephosphorylation of Ser 408 – a repressive MEF2A modification – caused desumoylation of MEF2A in response to calcium-induced depolarization. This ultimately resulted in the acetylation and subsequent activation of MEF2A, which in turn, decreased the density of dendritic claws. This study highlights differential roles for a single MFE2 transcription factor in regulating synapse development that is dependent upon the phosphorylated and sumoylated states of the protein. Thus, determining the role for specific MEF2 genes should extend beyond simply modifying DNA binding and dimerization and should lend great consideration to identifying the cofactor interactions that alter the mode of MEF2 transcriptional regulation to modify synapse development.

Role of MEF2 in metaplasticity

A role for MEF2 in regulating experience-dependent synaptic metaplasticity – "the plasticity of plasticity" – has been recently identified *in vivo* within the optic tectum of an intact tadpole that is presented with various light stimulus patterns (Chen et al 2012). MEF2A and MEF2D shift the threshold for plasticity by favoring LTP-like modes of synaptic plasticity which promote formation and stabilization of dendritic filopodial protrusions that undergo functional NMDAR-dependent calcium influx. Patterned light

stimuli potentiate calcium responses and filopodial density, whereas removal of a light stimulus depresses calcium influx and decreases filopodial density in tectal neurons. If these visual stimuli are sufficiently temporally separated then the impact on synapse number and function are exerted independently. However, if exposure to variable, unpatterned visual stimuli closely precedes a patterned plasticity-inducing light stimulus, then plasticity is altered and oftentimes in the opposite direction. MEF2A and MEF2D expression levels are temporally decreased through a caspase-3-mediated mechanism following exposure to unpatterned visual stimuli, which collapses the molecular framework available for the neuron to utilize LTP- and LTD-like plasticity mechanisms. It is interesting to consider the consequences for MEF2 transcription factors in regulating different modes of sensory experience prior to closure of the critical period. Perhaps altering MEF2-dependent transcription is sufficient for extending the critical period by keeping the circuit in a more "immature" state. Conversely, it is possible that MEF2 overexpression could prematurely close the critical period by preserving experience-induced plasticity to a level that prevents metaplasticity or subsequent plasticity that would typically induce an opposing effect on synaptic strength. The role of MEF2 in modulating the critical period has yet to be examined.

MEF2 association with neurodevelopmental and psychiatric disorders

Complete loss of *Mef2c* and *Mef2a* function results in embryonic lethality due to developmental cardiac deficits (Potthoff & Olson 2007). Although *MEF2C* haploinsufficiency is sufficient for survival, it is accompanied by detrimental and severe neurological and systemic effects.

MEF2C, specifically, has been recently identified as an autism-linked gene as human patients with *MEF2C* haploinsufficiency exhibit pronounced autistic behaviors, severe intellectual disability, stereotypic movement, and syndromic symptoms associated with autism spectrum disorders (ASDs). These patients typically do not acquire language, and at best, can utter short words or babble throughout life (Le Meur et al 2010, Novara et al 2010). Furthermore, they display poor sociability, rarely make eye contact, and display decreased reactivity to environmental stimuli. Additionally, they tend to experience seizures that can become more frequent and more severe with age, which can result in admission of the child to epilepsy treatment facilities as early as 5 years of age (Novara et al 2010).

Magnetic resonance imaging (MRI) of 5q14.3 deletion patients reveal gross neuroanatomical abnormalities. The ventricles and extracerebral space tend to be enlarged, and white matter is diminished (Le Meur et al 2010, Zweier et al 2010). Abnormal gyration, periventricular heterotopia, and formation of the corpus callosum is also observed (Cardoso et al 2009, Le Meur et al 2010).

Karyotyping and microarray genome sequencing were used to characterize the *de novo* genetic mutations observed in these patients. Duplication or deletion mutations of various sizes (~216 kb – 8.8 Mb) were identified within the q14.3 position of chromosome 5, which corresponds to *MEF2C* as well as other genes depending on the size of the mutation (Le Meur et al 2010). The size of the deletion appears to be directly proportional to the severity of symptoms exhibited by the patient (Le Meur et al 2010). Some patients exhibited two chromosomal breaks at the q14.3 and q15 positions of chromosome 5 – referred to as 5q14.3q15 deletion syndrome – and displayed decreased expression of

methyl CpG binding protein-2 (MECP2) and cycline-dependent kinase-like-5 (*CDKL5*), which phenocopies the ASD, Rett Syndrome (Cardoso et al 2009, Zweier et al 2010). These studies provide evidence that *MEF2C* may interact with other genes that are critical for normal brain development.

Aside from neurological abnormalities, 5q14.3 deletion patients also have systemic complications. Because *MEF2C* is highly expressed in skeletal muscle, the haploinsufficiency causes muscle hypotonia that becomes noticeable to parents as early as ~4 months of age. Patients are often wheelchair-bound and unable to crawl or walk independently. Posture is often slouched, and often the ability to sit upright is delayed into the toddler stage (Le Meur et al 2010). Gross anatomical malformations typically include microcephaly, wide forehead, anteverted nostrils, down-turned corners of the mouth, and pronounced eyebrows (Cardoso et al 2009, Le Meur et al 2010, Novara et al 2010, Zweier et al 2010). These studies have provided clear clinical relevance for MEF2C in human development.

MEF2C has also been recently implicated in schizophrenia (SCZ) and is located within one of the identified 108 genomic loci contributing to SCZ (Ripke et al 2014). Using the database derived from the DNA samples of over 38,000 schizophrenia patients obtained through the Schizophrenia Working Group of the Psychiatric Genomics Consortium, a group has found *MEF2C* to be more highly enriched in the frontal cortex of schizophrenic patients compared to normal individuals during late fetal development and into adulthood (Ohi et al 2016). Specific *MEF2C* mutations linked to schizophrenia have yet to be identified.

Motivation for Studies and Summary of Research

MEF2 transcription factors are critical for brain development and are involved in processes including cell survival, neural differentiation and maturation, synaptic physiology, and neural migration. Mutations in MEF2 genes are associated with autism and intellectual disability. The link between MEF2 genetic mutations and neurodevelopmental disorders translates to mouse models in which specific MEF2 genes can be manipulated within specific neuron populations throughout development. Mice with loss-of-function MEF2 mutations display autistic-like behaviors among other neurological phenotypes associated with autism. Thus, there is clear clinical relevance to understanding the role of MEF2 transcription factors in regulating neocortical circuit development.

Before the experiments described in chapter 2 were performed, it was unknown how specific MEF2 genes regulate neocortical synapse development *in vivo* and from what synaptic locus such regulation occurred. *In vitro* studies have been able to resolve postsynaptic MEF2-dependent regulation of synaptic function in organotypic hippocampal slice cultures, but these studies employ overexpression of a constitutively active MEF2 called MEF2-VP16 which contains only the MADS/MEF2 domains fused to a strong Herpesvirus Protein-16 transcriptional activation domain and thus induces "pan-MEF2" transcription and excludes the possibility to detect non-redundant synaptic regulation by the specific MEF2 transcription factors potentially occurring *in vivo*. These studies are also confounded by massive overexpression whereby MEF2-dependent transcription is non-physiologically upregulated. All previous *in vivo* studies probing synaptic regulation by specific MEF2 genes employ network deletion, hence is it unclear whether the reported

phenotypes are due to postsynaptic or presynaptic mechanisms or secondary, MEF2-independent effects. Additionally, MEF2 gene deletion has always occurred at various times in various neuron populations during embryonic development, which is likely confounded by non-synaptic MEF2 functions. Such experimental differences likely underlie the discrepancies in interpreting MEF2-dependent synaptic regulation, and thus, the question of how specific MEF2 transcription factors regulate synapse development within a single neuron remains unanswered.

Activity-dependent transcription regulates evoked synaptic transmission *in vivo*, which can induce circuit plasticity at specific synaptic input pathways (Bloodgood et al 2013b, West & Greenberg 2011b). Direct measurements of how MEF2 regulates evoked transmission are typically not utilized, and when performed, they are also confounded by network-wide alterations with global deletion. Therefore, it remains unclear if specific MEF2 genes differentially regulate different pools of synapses on dendrites targeted by specific synaptic input pathways onto a given neuron. No previous studies have directly assessed how MEF2 genes regulate evoked synaptic transmission *in vivo*, which is arguably the most relevant type of neural activity mediating MEF2 activation and experience-dependent circuit plasticity within the intact organism. To this end, few studies have linked MEF2 transcription to experience-dependent regulation of synapse development. For example, deletion of *Mef2a* and *Mef2d in vivo* reveals alterations in expression of a subset of activity-regulated target genes in response to novel experience. Additionally, changes in dendritic spine density in response to cocaine exposure have been reported. However, whether or not these effects have physiological consequences on neural circuit function remains to be elucidated.

Given the importance for understanding the unique mechanisms mediated by individual MEF2 genes and the underpinnings of neocortical processing of sensory experience and cognition, I sought to determine the cell-autonomous and postsynaptic roles of specific MEF2 transcription factors in regulating neocortical circuit and synapse development *in vivo*. More specifically, I wanted to understand how specific MEF2 transcription factors cell-autonomously regulate specific synaptic inputs onto a single neocortical neuron. Lastly, I sought to decipher if MEF2 transcription factors could regulate experience-dependent development of neocortical circuit function *in vivo* given that MEF2 mediates activity-dependent transcription. Here, I directly measure how both evoked and spontaneous glutamatergic transmission is regulated by specific MEF2 genes at the postsynapse and utilize a "sparse" deletion approach to examine the cell-autonomous effects of these genes on neocortical synapse and circuit development in more mature neurons within the postnatal mouse brain. Importantly, neocortical neurons have already migrated to their appropriate cortical layer prior to deletion of MEF2 genes, hence this postnatal deletion strategy allows me to circumvent the developmental and secondary effects occurring during embryonic development affecting neural migration to cortical layers. Additionally, this sparse deletion strategy affords the ability to determine the direct, cell-autonomous and postsynaptic effects of MEF2 gene deletion on neocortical synaptic function by performing side-by-side whole-cell electrophysiological and imaging experiments in MEF2-deleted (*Mef2*$^{fl/fl}$*; Cre-GFP+, MEF2 KO*) and neighboring uninfected WT (*Mef2*$^{fl/fl}$*; Cre-GFP-*) neocortical neurons in a circuit context where presynaptic input is largely normal and the neural network is minimally perturbed. All of my electrophysiological and imaging experiments are performed *ex vivo* in acutely

prepared brain slices containing the barrel cortex, and therefore all measurements closely reflect physiological changes occurring within the intact animal. I chose to study MEF2-dependent circuit development of L2/3 pyramidal neurons within the mouse barrel cortex as these neurons receive canonical corticocortical inputs and are malleable to experience-dependent plasticity in early postnatal development. Based on the prevalent evidence in the field linking MEF2 genes to suppression of excitatory synapse number and/or synapse elimination, I initially hypothesized that sparse postnatal deletion of MEF2 genes would increase excitatory synapse number onto neocortical L2/3 pyramidal neurons and that this effect would be regulated by whisker-mediated experience *in vivo*.

I observed that both *Mef2a* and *Mef2d* only modestly affect synaptic function of neocortical L2/3 neurons, whereas *Mef2c* differentially and oppositely regulates specific input pathways onto individual L2/3 neurons. Therefore, MEF2 transcription factors do not redundantly regulate L2/3 circuitry *in vivo*, and postsynaptic *Mef2c* is critical for proper neocortical synapse development. Additionally, this is the first report of an input-pathway-specific regulation of excitation by an activity-dependent transcription factor. I discovered that postsynaptic *Mef2c* cell-autonomously promotes synaptic connectivity without affecting synaptic strength at local L2/3 input pathways confined to local barrel columns, while long-range corticocortical inputs are potentiated. Additionally, *Mef2c* interacts with and functions downstream of whisker-mediated sensory experience to increase strength of local input pathways, suggesting a converging molecular mechanism between *Mef2c* and experience and also that *Mef2c* is required for and permits experience-dependent synapse proliferation and/or stabilization. These findings lend insight into the fine experience-

dependent circuit plasticity occurring within a single L2/3 pyramidal neuron and have identified *Mef2c* as a molecular regulator of sensory experience.

MEF2 genes are autosomal, and thus, MEF2 genetic mutations are expressed in neuron populations. Given that *Mef2c* is an autism-linked gene expressed in many neuron cell types, I sought to determine how late embryonic *Mef2c* deletion in excitatory cortical networks affected synaptic transmission onto L2/3 neurons within the barrel cortex. I also saw this as an opportunity to compare synaptic physiological changes observed when *Mef2c* is absent in sparse versus large cortical neuron populations, which could elucidate compensatory mechanisms resulting from pre- and postsynaptic loss of *Mef2c* in expansive neural networks. My experiments revealed an overall decrease in excitatory synaptic transmission but unexpectedly enhanced inhibitory transmission, suggesting that MEF2C is a negative regulator of inhibitory synapse development. Inhibition was unaffected with sparse *Mef2c* deletion. Although the potential underlying biological processes for these results are explained in detail within chapter 4, these findings demonstrate physiological differences that could underlie the discrepancies in the field surrounding the direct role of MEF2C in regulating brain circuit development. This also highlights the importance of cell-autonomous studies.

Taken together, the data I present detail novel effects of MEF2 transcription factors in regulating neuronal function and development within the mammalian neocortex in the context of how a postsynaptic neuron receives and adapts to heterogeneous presynaptic inputs. These findings also provide useful information regarding the physiological etiology associated with intellectual disability and autism spectrum disorders, namely 5q14.3-5 deletion syndrome.

CHAPTER TWO

Postsynaptic MEF2C differentially regulates local and long-range excitatory neocortical circuits in response to experience

Summary

Development of proper cortical circuits requires an interaction of sensory experience and genetic programs. Little is known of how experience and specific transcription factors interact to determine the development of specific synaptic connections *in vivo*. Here I demonstrate that the activity-dependent transcription factor, Myocyte enhancer factor-2C (*Mef2c*), postsynaptically and cell-autonomously promotes the development of excitatory synaptic connections from local input pathways onto individual layer (L) 2/3 neurons in the somatosensory, barrel cortex *in vivo*. Sensory deprivation by whisker trimming weakens local excitatory synaptic inputs onto wildtype, but not *Mef2c*-deleted, L2/3 neurons implicating *Mef2c* as a downstream effector of experience in the development of local excitatory circuits. In contrast to local inputs, *Mef2c* deletion strengthens excitatory long-range inputs originating from contralateral neocortex, revealing an input-specific regulation of synaptic connectivity by a postsynaptic transcription factor.

Introduction

Sensory experience and experience-driven patterns of neuronal activity are required for development of proper synaptic connectivity of neocortical circuits (Fox, 2002; Katz and Shatz, 1996). Activity-regulated transcription factors and their transcripts

are hypothesized to contribute to the experience-dependent development and refinement of synaptic connections (West & Greenberg 2011a). In support of this idea, the activity-regulated transcription factors, NPAS4 or Myocyte Enhancer Factor-2 (MEF2) regulate inhibitory and excitatory synapse number onto developing hippocampal neurons, respectively (West & Greenberg 2011a). In response to environmental enrichment, NPAS4 differentially regulates inhibitory synapses arising from distinct input pathways onto postsynaptic hippocampal CA1 neurons (Bloodgood et al 2013a). Whether a transcription factor regulates experience-dependent and input-specific development excitatory circuits is unknown.

Of the family of MEF2 transcription factors (MEF2A-D), MEF2C is the most highly expressed in the neocortex, and MEF2A/D are present at lower levels (Potthoff & Olson 2007) (Lyons et al 2012b). Expression of a constitutively active MEF2C eliminates functional and structural excitatory synapses both in cultured neurons and *in vivo* (Cole et al 2012, Flavell et al 2006, Pfeiffer et al 2010a). Consistent with this finding, embryonic or postnatal deletion of *Mef2c* in forebrain results in increased excitatory synapse function and dendritic spines *in vivo* in the granule cells of the hippocampal dentate gyrus (Adachi et al 2015, Barbosa et al 2008) and is necessary for synapse elimination in response to extracellular signals (Elmer et al 2013). The contribution of MEF2 genes to experience-dependent development and refinement of synaptic connectivity and its cell-autonomous role in such processes *in vivo* are unknown. Furthermore, nothing is known of any input-specific roles of MEF2 genes. Here I demonstrate that MEF2C in postsynaptic layer (L) 2/3 pyramidal neurons of somatosensory barrel cortex is necessary for experience-dependent development of excitatory synaptic connections specifically from local input

pathways. In contrast, MEF2C suppresses function of long-range excitatory inputs arising from contralateral neocortical regions. Lastly, MEF2A and MEF2D do not robustly affect synaptic transmission in neocortex Our results reveal new, unexpected, and non-redundant roles for MEF2 genes in regulation of specific synaptic circuits and provide key molecular insight into experience-dependent development of neocortical circuits.

Materials and Methods

Animals:

The conditional *Mef2c* (*Mef2c*$^{fl/fl}$), *Mef2a* (*Mef2a*$^{fl/fl}$) and *Mef2d* (*Mef2d*$^{fl/fl}$) have been previously described (Akhtar et al 2012, Arnold et al 2007b, Zang et al 2013) and were maintained on a mixed C57/B6J and 129/SvEv strain. Animals were given *ad libitum* access to food and water and were reared on a 12-hour light-dark cycle. All animal experiments were conducted in accordance with the Institutional Animal Care and Use Committee at University of Texas Southwestern Medical Center.

Adeno-associated virus:

AAV2.9-Cre-GFP (Adesnik et al 2008) and AAV2.9 ChR2-mCherry (Mao et al 2011) were obtained from the University of Pennsylvania Vector Core, Gene Therapy Program.

Dissociated cortical cultures

Cortical neurons were cultured from postnatal day 0 (P0) *Mef2c*$^{fl/fl}$ mice as described (Niere et al., 2012). Neurons were plated in Neurobasal A medium supplemented with B27 (Life Technologies), 0.5 µM glutamine and 1% fetal bovine serum onto poly-D-lysine (Sigma)-coated plates. One hour after plating, media was replaced with glial conditioned medium

(GCM) as described (Viviani 2006). At 1-2 *days in vitro* (DIV), cultures were infected with 10^{10} genome copies AAV-Cre-GFP. Cultures were fed at 5-6 DIV by replacing 50% of the medium with GCM. RNA was isolated at 4, 7, or 14 days following addition of virus.

RNA isolation, reverse transcription, and quantitative real-time PCR

RNA was extracted from dissociated neuron cultures using the RNeasy Micro kit (Qiagen) following manufacturer's instructions. The RNA concentration of each sample was determined using a NanoDrop spectrophotometer and was reverse transcribed using the Superscript III First-Strand Synthesis System for RT-PCR (Invitrogen). Quantitative analysis was performed using the StepOnePlus Real-Time PCR System (Life Technologies) with TaqMan primers (Applied Biosystems). These TaqMan probes (Life Technologies) were used: Mef2c – Mm01344728_m1, and Gapdh – Mm99999915_g1.

Neonatal stereotaxic virus injections:

Neonatal stereotaxic injections were performed as described (Adesnik et al 2008) with some modifications. Prior to surgery, AAV-Cre-GFP and AAV-ChR2-mCherry were diluted to 10^{12} titer in sterile saline and 2.5 mg/mL Fast Green FCF dye (Sigma) to assess injection quality and bilateral spread throughout the lateral ventricles. P1 *Mef2c*$^{fl/fl}$ or *Mef2a*$^{fl/fl}$ /*Mef2d*$^{fl/fl}$ mice were anesthetized on ice until immobilized and then fastened in a custom head mold prior to a single unilateral stereotaxic injection of AAV2.9-Cre-GFP (275-550 nL) targeting the lateral ventricle at a depth of approximately 1.1 mm into the brain with a beveled virus-filled pipette fastened to a Nanoject™ injector (Drummond Scientific, Inc.). AAV-ChR2-mCherry (400 nL) was injected into the somatosensory

cortex at a depth of ~500 µm within the contralateral hemisphere to the intraventricular AAV-Cre-GFP injection for labeling trans-colossal axons. Mice quickly recovered on a heating pad until regaining mobility and were then returned to the home cage until of age for experiments.

Brain slice preparation:

Male and female mice were used for acute-slice electrophysiological and imaging experiments. All experiments were performed in AAV-Cre-GFP-injected *Mef2c*$^{fl/fl}$ and *Mef2a*$^{fl/fl}$/*d*$^{fl/fl}$ *mice* at ages P18-P25, and the genotype of each animal was confirmed *post hoc* with a tail DNA sample following the slicing procedure. Prior to brain extraction, mice underwent acute transcardial perfusion with ice cold, aerated dissection solution. Acute coronal slices (300-µm thickness) containing barrel cortex were prepared in a semi-frozen 300 mOsM dissection solution containing in mM: 110 choline chloride, 2.5 KCl, 1.25 $Na_2H_2PO_4$, 25 $NaHCO_3$, 25 D-glucose, 3.1 Na pyruvate, 11.6 Na ascorbate, 7 $MgCl_2$, and 0.5 $CaCl_2$, and was continually perfused with 95% O_2 and 5% CO_2 prior to and during the slicing procedure. Slices were then transferred to a 300 mOsM normal artificial cerebrospinal fluid (ACSF) solution containing in mM: 125 NaCl, 2.5 KCl, 1.25 $Na_2H_2PO_4$, 25 $NaHCO_3$, 10 D-glucose, 1 kynurenate, 2 $MgCl_2$, and 2 $CaCl_2$, to recover at 37°C for 30 minutes, and then transferred to room temperature for an additional 30 minutes prior to recording.

Electrophysiology:

Layer 2/3 (L2/3) pyramidal neurons (depth 30-100 µm into the slice) were visualized with infrared differential interference contrast (IR-DIC) optics and patched using borosilicate pipettes (4-6 MΩ). Whole-cell recordings were performed using a Multiclamp 700A amplifier (Molecular Devices), and L2/3 pyramidal neurons were identified by their laminar location, apical dendrites, and burst spiking patterns in response to depolarizing current injection. Only L2/3 neurons located directly above L4 barrels (i.e. within the home column) were included for analysis; neurons located within barrel septa were discarded. Recordings were conducted in brain slices with < 10% local virus infection efficiency to maintain sparse AAV-Cre-GFP infection. Extracellular normal ACSF solution (described above) was continually aerated with 95% O_2 and 5% CO_2 and recycled. Unless stated otherwise, all imaging and electrophysiological experiments were performed in voltage clamp at -70mV using an internal solution containing in mM: 120 K-Gluconate, 5 NaCl, 10 HEPES, 1.1 EGTA, 4 MgATP, 0.4 Na_2GTP, 15 phosphocreatine, 2 $MgCl_2$, and 0.1 $CaCl_2$. All data was acquired and analyzed using custom Labview software (Labview 8.6, National Instruments Inc.).

Miniature postsynaptic currents:

Minature (m) PSCs were recorded from L2/3 pyramidal neurons in voltage clamp at -70 mV. For mEPSCs, the extracellular bath solution contained normal ACSF, 1 µM tetrodotoxin (TTX, Sigma Aldrich), and 100 µM pictrotoxin (Sigma Aldrich). mIPSCs were recorded using a high-chloride internal solution with a reversal potential at E_{Cl-} = -25 mV for chloride containing in mM: 79 K-gluconate, 44 KCl, 6 NaCl, 10 HEPES, 0.2 EGTA, 4 MgATP, 0.4 Na_2GTP, 15 phosphocreatine, 2 $MgCl_2$, and 0.1 $CaCl_2$,. The

extracellular bath solution contained normal ACSF, 1 μM TTX, 5 μM CPP (NMDA-receptor antagonist, Sigma-Aldrich), and 20 μM DNQX (AMPA-receptor antagonist, Sigma-Aldrich). Because action potential firing was blocked by TTX application, the mPSC kinetics and membrane time constant in response to hyperpolarizing current injection were used to distinguish excitatory from inhibitory L2/3 neurons. Inhibitory interneurons are identified by the following criteria: mPSC width at half-height < 2 ms, rise and decay of hyperpolarization < 50 ms (Povysheva et al 2006).

Laser-scanning photostimulation (LSPS) with glutamate uncaging:

All procedures closely resemble those described in (Shepherd et al 2003). For all LSPS experiments, only brain slices with L2/3 apical dendrites parallel to the slice surface were used to ensure preservation of the planar barrel cortical geometry of long-range synaptic pathways spanning at least 3 barrel columns. Usually 2-4 brain slices per animal met such criteria. ACSF was modified to include high-divalents (4 mM $MgCl_2$, 4 mM $CaCl_2$) to reduce spontaneous firing, (±)-3-(2-carboxypiperazin-4-yl)propyl-1-phosphonic acid (CPP, 5 μM,), and 4-Methoxy-7-nitroindolinyl-caged-L-glutamate, MNI glutamate (MNI, 0.4 mM, R&D Systems, Inc.). Water was periodically added to maintain bath osmolarity at ~300 mOsM to counteract evaporation. A 100 kHz ultraviolet laser (λ = 355nm, DPSS Lasers, Inc.) and mechanical shutter (Uniblitz) were commanded by custom Labview Software. Laser power was harnessed and calibrated daily by manual positioning of a gradient neutral density filter. During synaptic LSPS, a 30mW laser pulse was applied for 1 ms at a rate of 2 Hz in a serial pseudorandom order along a 16 × 16 stimulation grid (50μm × 60μm x-y spacing) during dual intracellular patch recordings of MEF2C-WT and

MEF2C-KO L2/3 pyramidal neurons. Direct LSPS utilized 5 mW laser pulses of 1-ms duration at a rate of 2 Hz along an 8 × 8 stimulation grid (50µm × 50µm x-y spacing in serial pseudorandom order) in the presence of 0.4 mM MNI and 1 µM TTX. 2-4 maps were acquired for each neuron included in all datasets.

Sensory deprivation:

At P9, AAV-Cre-GFP injected *Mef2c*$^{flx/flx}$ mice were subjected to daily unilateral whisker trimming until the day of experiments (P18-P20) such that all whiskers on the right facial pad were maintained at a length < 2 mm using a miniature electric shaver (BikiniTouch™).

Synaptic LSPS Analysis:

For each neuron, a single average map was calculated from acquired LSPS maps, where at each stimulation point the averaged light-evoked EPSC area was calculated within a time window of 5-80 ms following the laser pulse. If a response was observed within 5 ms of LSPS and displayed kinetics visibly distinguishable from the longer-latency EPSC then it was considered to be a non-synaptic, direct current that contaminated the LSPS synaptic response. These contaminating "direct" components were fitted with a double-exponential decay equation and subtracted from the trace obtained at all stimulation points at which they were observed. An IR-DIC image of the slice with dual patch pipettes in place and stimulation grid was acquired prior to LSPS for marking soma location and anatomical features of the slice (i.e. barrels, etc.). Finally, a color map for each neuron was created. All individual color maps within genotype were then overlaid upon spatial alignment with respect to the center of the "home" barrel directly beneath the pair of recorded L2/3

neurons. Superimposition of the average maps was achieved by 1) transposing each map such that the home barrel center was located at the origin of alignment grid, 2) preserving the medial-lateral orientation of the brain slice, and 3) stretching the home barrel in x and y dimensions to normalize barrel size. To provide better spatial resolution for the aligned maps, pixels represent half of the stimulation spacing distance (25 × 30 µm). Black pixels within an averaged color map indicate the deleted direct responses or pixels that did not meet the minimum sampling threshold (minimum of n = 8 neurons per stimulation point). These were typically at distances far away from the soma and were determined *post hoc*. Vertical distance synaptic input profiles were plotted by averaging all pixels within each horizontal row of pixels and plotted along vertical distance. Horizontal distance synaptic input profiles were plotted by averaging all pixels within each vertical column comprising the map and plotted along horizontal distance (line graphs). No statistics were performed on distance synaptic profiles. For region-specific analyses, all pixels within an anatomical region of interest for each neuron represented in the averaged color maps were averaged and compared by genotype (bar graphs). Statistical test for sensory deprivation LSPS region-specific analyses: 2-way ANOVA with repeated measures for genotype (Fig. 3E-G).

Direct LSPS analysis:

As described above, the average EPSC amplitude was calculated between 0-75 ms after the laser pulse at each stimulation point across all LSPS maps for each recorded L2/3 neuron. Color maps for individual neurons were superimposed within genotype after alignment with respect to soma location. To quantify direct responses, response amplitudes

at all pixels were summed for each neuron and compared between WT and MEF2C KO L2/3 neurons. No responses were deleted from the averaged direct LSPS color maps.

Evoked EPSCs:

AMPA-receptor-mediated excitatory postsynaptic currents (EPSCs) were recorded simultaneously from neighboring WT and MEF2C KO L2/3 neurons in response to extracellular electrical stimulation of excitatory L4 afferents (L4 → L2/3) or horizontal intercortical afferents onto the recorded L2/3 pyramidal neurons. A two-conductor cluster stimulating electrode (FHC, Inc.) was positioned in L4 directly underneath the recorded cell pair or in L2/3 of the adjacent barrel column. Disynaptic inhibition was blocked by positioning a third pipette near the recording electrodes to locally perfuse bicuculline methiodide (BMI, 5 mM, $GABA_A$ receptor antagonist) as previously described (Bender et al 2006b, Loerwald et al 2015b). A train of 4 biphasic pulses (200 µs, 0.5 - 10 µA, 50 ms inter-stimulus interval) were applied every 4 seconds in each sweep to measure L4 → L2/3 AMPA-mediated EPSC amplitude and short-term plasticity. A minimum of 8 sweeps per recorded cell pair was required for inclusion. All recordings were performed at a holding potential of -45 mV in the presence of high-divalent ACSF (see above, 4 mM $CaCl_2$, 4 mM $MgCl_2$) and 5 µM CPP. A similar recording configuration was used to record NMDA-mediated EPSCs from neighboring MEF2C-WT and MEF2C KO L2/3 neurons, except neurons were voltage clamped at +40 mV. A single EPSC was elicited every 15 sec and no BMI-containing pipette was used. High-divalent ACSF containing 20 µM DNQX, and 100 µM picrotoxin was used. Prior to analysis, traces were filtered with a 15-point box average.

Evoked GABA-mediated IPSCs:

Inhibitory postsynaptic currents (IPSCs) were simultaneously recorded from neighboring WT and MEF2C KO L2/3 neurons (intersomal distance ≤ 50 µm) upon extracellular stimulation of local inhibitory afferents with a 2-conductor cluster stimulating electrode (FHC, Inc.) positioned ~150 µm from the recorded cell pair, usually in L3 near the border of L4. Two biphasic pulses (200 µs, 5-90 µA, 100 ms inter-stimulus interval) were applied during each recording sweep where a minimum of 10 sweeps per recorded cell pair was required for inclusion. IPSCs were recorded at a holding potential of -45mV in normal ACSF containing 20 µM DNQX and 5 µM CPP.

Minimal stimulation for synaptic failures & Coefficient of Variance analysis:

In a similar set of experiments, AMPAR-mediated EPSCs were recorded in WT and MEF2C KO neuron pairs in response to a single minimal stimulation, defined as the stimulation intensity which evoked a mixture of synaptic response successes and failures in at least one cell in the cell pair. A synaptic failure was defined as a peak EPSC amplitude < 4 pA. Following this minimum stimulation protocol, EPSCs evoked by higher stimulation intensities (1.1 - 2.5 X minimal stimulation) were recorded and used to calculate the coefficient of variation (CV), defined as the square root of (VAR_{EPSC} - $VAR_{baseline}$) divided by the $Mean_{EPSC}$ where VAR_{EPSC} and $VAR_{baseline}$ are the variance of the EPSC and baseline noise respectively, and $Mean_{EPSC}$ is the mean of the EPSC (Faber & Korn 1991, Markram et al 1997).

Evoked EPSCs in strontium:

Quantal event frequency and amplitude of asynchronous EPSCs were measured as described (Bender et al 2006b) with some modifications. EPSCs were recorded simultaneously from WT and MEF2C KO L2/3 neurons in response to electrical stimulation of L4 in high-divalent ACSF containing 5 µM CPP with local BMI perfusion. Stimulation intensity was adjusted to evoke an EPSC of ~100 pA in WT neurons. ACSF containing 4 mM $SrCl_2$, no $CaCl_2$, was then applied. After 30 min, L4 → L2/3 asynchronous EPSCs were evoked at a -45mV holding potential with the same stimulation intensity. Quantal event frequency and amplitude were measured 40-190 ms after stimulation. Spontaneous event frequency was measured 40-190 ms before stimulation onset to differentiate effects of MEF2C on spontaneous vs. evoked quantal events.

Analysis of mPSC and evoked EPSCs in Sr2+:

Miniature EPSCs and mIPSCs and evoked EPSCs in Sr2+ were analyzed using MiniAnalysis (Synaptosoft) with a constant amplitude (6-7pA) and area (10 pC) threshold Events were initially detected by the automated software, and then non-events were manually deleted upon visual inspection of the traces.

Optogenetic stimulation of trans-colossal axons:

Acute coronal slices were prepared from *Mef2c*$^{fl/fl}$ mice that were injected with AAV-Cre-GFP and AAV-ChR2-mCherry at P1 as described above. Only slices within the barrel cortex exhibiting sparse nuclear AAV-Cre-GFP and axonal AAV-ChR2-mCherry expression were used for experiments; slices containing somatic AAV-ChR2-mCherry

were discarded to isolate light-evoked, ChR2-mediated synaptic currents at trans-callosal-projecting axons emanating from cS1. A shutter-controlled epifluorescence light source (λ = 470 nm) was used to administer 2-msec light pulses once every 30 seconds during simultaneous intracellular whole-cell recordings of WT and MEF2C KO L2/3 pyramidal neurons that were voltage clamped at -70 mV. The power of light stimulation was adjusted to elicit light-evoked EPSCs in the WT neuron with an amplitude of ~100 pA. Prior to recording, local AAV-ChR2-mCherry expression was visualized using a confocal laser (λ = 594 nm) and microscope to ensure dense trans-callosal innervation of the recorded cell pairs. The bath solution contained normal ACSF, 100 µM picrotoxin, 100 µM 4-aminopyridine (Sigma, potassium channel antagonist), 5 µM CPP, and 1 µM TTX. The amplitudes of light-evoked, ChR2-mediated EPSCs were analyzed using custom Labview software. Neurons pairs in which one neuron exhibited light-evoked EPSCs > 400 pA were excluded from analysis. A minimum of 10 stimulation sweeps per neuron were required for inclusion of each cell pair. All cell pairs were located directed above the barrel.

Cell filling & imaging of live neurons:

Acute slices were prepared from *Mef2c*$^{fl/fl}$ mice that were injected with AAV-Cre-GFP at P1 as described above. Same criteria as LSPS experiments apply (L2/3 apical dendrites are parallel to the slice surface, 2-4 slices per animal). Individual L2/3 pyramidal neurons were patched with a pipette containing 100 µM AlexaFluor488 dye (Life Technologies, Inc.) in K-gluconate internal solution (7 mM [Cl^-]). The dye perfused throughout the dendritic arbor for 20 minutes prior to imaging with a Zeiss LSM 510 two-photon laser

scanning microscope equipped with a Chameleon-Ti: sapphire standard laser at an excitation wavelength of 920 nm.

Dendritic arbor imaging:

To image the entire dendritic arbor for each filled neuron, several z-stacks (1 µm z-steps) were acquired using a 40x water-immersion objective at a 1024 x 1024 pixel resolution. Each z-stack was then collapsed and batched in Adobe Photoshop to create a montage for each neuron. Dendritic arbors were manually traced in Adobe Photoshop. Montages were processed in ImageJ2 using the Sholl Analysis and ImageJ plug-ins for performing Sholl analysis and calculating total dendritic length, respectively. Statistics: A 2-way ANOVA with repeated measures for Sholl distance was performed for Sholl analyses of basal and apical dendritic compartments separately. A 2-way ANOVA with repeated measures for dendritic compartment was used to analyze summed dendritic length. Only AlexaFluor488-filled L2/3 pyramidal neurons with an apical tuft extending > 240 µm to the pia were included for analysis.

Dendritic spine imaging:

Z-stacks of secondary and tertiary basal dendrites of filled L2/3 pyramidal neurons were acquired using a 63x water immersion objective at a 2048 × 2048 pixel resolution. 1-3 regions of interest were acquired per neuron on different dendrites. No more than 4 neurons were imaged from one animal. Z-stacks were processed in ImageJ2, and then dendritic spine density was quantified using NeuronStudio (Rodriguez et al 2008, Rodriguez et al

2006). Spines were automatically detected by the NeuronStudio and then artifacts were manually deleted upon visual inspection. Statistical analysis: unpaired t-test.

Dendritic spine imaging in multiple dendritic compartments:

L2/3 pyramidal neurons were intracellularly filled individually as described above with some modifications. The internal solution contained the standard K-gluconate solution with 100 µM AlexaFluor488 dye and 2 mg/mL biocytin (Life Technologies, Inc.). The AlexaFluor488 dye was included to ensure that dendrites of all filled L2/3 pyramidal neurons extended to the pia. Neurons were filled for 20 minutes, and then the pipette was retracted to obtain an outside-out patch to reseal the cell membrane. Slices recovered in normal ACSF for at least 1-4 hours after filling and then fixed in 4% sucrose/2.5% paraformaldehyde. Fixed slices were stained with Alexa488-conjugated steptavidin (Life Technologies, Inc.) and mounted on glass slides. 1-3 images of dendritic spines were acquired on secondary dendrites within basal, proximal apical, and distal apical compartments for every L2/3 pyramidal neuron included for analysis. Proximal apical dendrites were defined as branching off of the primary apical dendrite proximal to where the apical dendrite bifurcates to initiate the apical tuft. Distal apical dendrites were defined as apical tufts segments residing within L1. All images (1024 × 2048 pixel resolution, 2.5x digital zoom) were acquired using an oil-immersion 40x objective on a Zeiss LSM 780 microscope equipped with a Chameleon-Ti: sapphire standard laser at an excitation wavelength of 920 nm. Images were analyzed with Neuron Studio as described above. Statistical test: 2-way ANOVA with repeated measures for compartment.

Statistical analysis:

All electrophysiology data from pairs of WT and MEF2C KO neurons were analyzed with paired t-tests unless stated otherwise. Sr^{2+} EPSCs (Fig. $2B_3$) and sensory deprivation LSPS (Fig. 3E-G) were analyzed using a 2-way ANOVA with repeated measures for genotype. qRT-PCR data were analyzed with a repeated measures 2-way ANOVA for DIV and AAV-Cre-GFP treatment. A 2-way ANOVA with repeated measures for Sholl distance was performed for Sholl analyses of basal and apical dendritic compartments separately (Fig. 2F). A 2-way ANOVA with repeated measures for dendritic compartment was used to analyze summed dendritic length (Fig. $2F_4$). Dendritic spine density was analyzed by unpaired t-tests (live imaging) and 2-way repeated measures ANOVA for dendritic compartment only (biocytin imaging) because neurons were not imaged in a pairwise fashion. *$p < 0.05$, **$p < 0.01$, ***$p < 0.001$, ****$p < 0.0001$.

Results

MEF2C promotes development of local excitatory inputs onto L2/3 pyramidal neurons

To determine the cell-autonomous role of MEF2 genes in development of neocortical circuits, I deleted one or a combination of the major cortical *Mef2* genes in a sparse (1-5%) population of neocortical neurons by injecting AAV-Cre-GFP into the ventricles of mice floxed ($^{fl/fl}$) for either *Mef2c* or *Mef2a* and *Mef2d* at postnatal day 1 (P1). Cre recombination results in deletion of the MEF/MADS domains within the floxed alleles, leaving a truncated C-terminal fragment that is expressed in the infected neurons **(Fig. 2.1A).** A time course following AAV-Cre-GFP infection in dissociated neocortical cultures demonstrated complete knockdown of *Mef2c* mRNA after 7 days with qRT-PCR **(Figure 2.1B).** Furthermore, immunoblots performed on cortical lysates of AAV-Cre-

GFP-injected mice demonstrated that MEF2A and MEF2D protein were truncated by P14 **(Fig. 2.1C)** Because *Mef2c* is the most abundant *Mef2* gene expressed in neocortex, it was the initial focus of my study. Acute slices containing the barrel cortex were prepared at P20-25: a period of robust neocortical synapse proliferation (De Felipe et al 1997, Stern et al 2001). Simultaneous whole-cell voltage clamp recordings were performed in Cre-GFP(+) *MEF2c*$^{fl/fl}$ or "MEF2C KO" neurons and neighboring uninfected, GFP(-) *MEF2c*$^{fl/fl}$ or "WT" L2/3 pyramidal neurons **(Fig. 2.1D,G)**. MEF2C is required for proper neural migration and neocortical laminarization (Li et al 2008). Thus, postnatal deletion of *Mef2c* in a sparse number of L2/3 neurons allowed me to determine the cell-autonomous, postsynaptic role of MEF2C on synapse development in a primarily wildtype circuit.

In contrast to the predicted role of *Mef2c* in excitatory synapse elimination, postsynaptic deletion of *Mef2c* in L2/3 neurons resulted in a robust (>50%) decrease in the amplitude of AMPAR-mediated EPSCs evoked by electrical extracellular stimulation of L4 axons (L4 → L2/3) **(Fig 2.2A-B).** Short-term plasticity of L4→L2/3 evoked EPSCs was unaffected in MEF2C KO neurons **(Fig. 2.2C)**, suggesting the decrease in evoked AMPAR-mediated EPSCs is not due to reduced presynaptic release probability. Heterozygous deletion of *Mef2c* by expressing AAV-Cre-GFP in *Mef2c*$^{+/fl}$ mice had no effect on evoked L4→L2/3 EPSCs, revealing that one allele of *Mef2c* is sufficient to maintain L4→L2/3 synaptic transmission **(Fig 2.3)** and that AAV-Cre-GFP expression does not affect EPSCs. Additionally, AAV-Cre-GFP expression in WT mice does not affect miniature (m) EPSC amplitude or frequency, hence AAV-Cre-GFP does not alter ionotropic glutamatergic synaptic transmission **(Fig 2.4)**. Inhibitory synaptic transmission, as measured by evoked and spontaneous or mIPSCs, was unaffected in MEF2C KO

neurons **(Fig 2.5),** indicating that MEF2C cell-autonomously and selectively promotes excitatory synaptic transmission. In contrast to *Mef2c*, deletion of both *Mef2a* and *Mef2d,* by injecting AAV-Cre-GFP in *Mef2a*$^{fl/fl}$/*d*$^{fl/fl}$ mice did not affect evoked L4 → L2/3 EPSC amplitude or short-term plasticity **(Fig 2.6A)**. *Mef2a/d* deletion slightly decreased mEPSC frequency but not amplitude **(Fig 2.6B)**, consistent with previous reports of MEF2A- and MEF2D-dependent regulation of presynaptic function (Akhtar et al 2012, Yamada et al 2013). These data highlight the important and specific role of MEF2C in neocortical synapse development and demonstrate a non-redundant role for MEF2 transcription factors in regulating functional synaptic transmission. However, simultaneous deletion of *Mef2a*, *Mef2c*, and *Mef2d* by injection of AAV-Cre-GFP into P1 *Mef2a*$^{fl/fl}$*; Mef2c*$^{fl/fl}$*; Mef2d*$^{fl/fl}$ mice reduced the viability of L2/3 neurons as early as P8-P11, as assessed by cell appearance and the inability to obtain whole cell recordings from Cre-GFP(+) *Mef2a*$^{fl/fl}$*; Mef2c*$^{fl/fl}$ *Mef2d*$^{fl/fl}$ neurons **(Fig. 2.7).** This result is consistent with the reported redundant role of *Mef2a,c,d* genes in neuronal survival (Akhtar et al 2012). I was, however, able to delete most of MEF2 expression while maintaining neuronal viability with complete deletion of *Mef2c* and one allele for both *Mef2a* and *Mef2d* in *Mef2a*$^{fl/+}$*; Mef2c*$^{fl/fl}$*; Mef2d*$^{fl/+}$ mice. Neurons tended to have decreased mEPSC frequency and normal mEPSC amplitudes with a small sample size **(Fig. 2.8)**, which could suggest that MEF2A, MEF2C, and MEF2D must interact either directly or indirectly on target genes to regulate spontaneous synaptic transmission.

In the barrel cortex, L2/3 pyramidal neurons receive the strongest input from local synaptic pathways within and across adjacent barrel columns (Feldmeyer 2012a, Schubert et al 2007). To determine if *Mef2c* deletion similarly depresses synaptic function from

other neocortical input pathways, I performed laser scanning photostimulation (LSPS) by glutamate uncaging to map the source and strength of monosynaptic connections from local synaptic input pathways onto simultaneously recorded WT and MEF2C KO L2/3 neurons (Shepherd et al 2003). LSPS maps spanned three barrel columns allowing measurement of synaptic connectivity from different layers and columns onto WT and MEF2C KO L2/3 neurons. LSPS-evoked EPSCs onto both WT and MEF2C KO neurons were spatially preserved and transformed into a color map where the pixel color represents the mean synaptic strength at each stimulation location **(Fig. 2.9A-D).** Short-latency responses in which glutamate was directly uncaged onto the dendrites of the recorded neurons (i.e. direct responses) were excluded from analysis (black pixels; **Fig. 2.9B,D**). LSPS maps acquired from individual neurons were superimposed by genotype and aligned with respect to the barrels and pia mater. Finally, average maps representing all recorded WT and MEF2C KO L2/3 neurons were constructed **(Fig. 2.9D).** Vertical and horizontal profiles of synaptic input reveal a robust reduction of intracolumnar and transcolumnar excitatory input caused by *Mef2c* deletion **(Fig. 2.9E-F).** Region-specific analyses revealed that *Mef2c* deletion reduced LSPS-evoked EPSCs at all local pathways assayed: vertical L4→L2/3, adjacent L4→L2/3, adjacent L2/3→L2/3, vertical L5A→L2/3, and adjacent L5A→L2/3 **(Fig. 2.9G-K).** These data suggest that MEF2C promotes the development and function of multiple excitatory synaptic input pathways onto L2/3 neurons.

By measuring the amplitude of "direct responses" to LSPS, I determined whether MEF2C KO neurons have reduced postsynaptic sensitivity to glutamate, independent of presynaptic mechanisms. LSPS was performed on simultaneous recordings of WT and MEF2C KO L2/3 neurons in the presence of TTX to isolate postsynaptic currents evoked

by uncaging of glutamate directly onto the recorded neuron **(Fig 2.10A).** The average amplitude of summed direct responses onto MEF2C KO neurons was reduced by 34% in comparison to WT neurons indicating a robust decrease in postsynaptic sensitivity to glutamate **(Fig. 2.10B).** These maps were aligned by soma location and provide a readout of postsynaptic AMPA receptor content within the basal and proximal apical L2/3 dendritic compartments, but not within the distal apical tuft due to variability of distal dendritic arbor span among L2/3 neurons. Although direct responses are mediated by both synaptic and extrasynaptic AMPA receptors, these results suggest that the decreased evoked EPSCs in MEF2C KO neurons is mediated, in part, by a postsynaptic locus.

MEF2C promotes excitatory synapse number from L4 → L2/3 pyramidal neurons

A postsynaptic mechanism by which MEF2C may enhance synapse function is via a selective increase in AMPAR function or synapse number. To differentiate between these possibilities, I measured pharmacologically-isolated, evoked NMDAR-mediated EPSCs onto WT and MEF2C KO neurons in response to extracellular L4→L2/3 stimulation. Like AMPAR-EPSCs, NMDAR-EPSCs were reduced by 59% in MEF2C KO neurons **(Fig. 2.11),** suggesting that MEF2C stimulates glutamatergic synapse number. To further test this hypothesis, I measured L4-evoked AMPAR-mediated EPSCs from neighboring WT and MEF2C KO L2/3 neurons in the presence of Sr^{+2}. Sr^{+2} asynchronizes neurotransmitter release and allows the resolution of quantal synaptic events (Oliet et al 1996). Consistent with an effect on synapse number, *Mef2c* deletion decreased quantal event frequency by 40% but did not affect quantal amplitude, or strength of individual synapses, of L4→L2/3 EPSCs **(Fig. 2.12A)**. In a separate series of experiments in normal ACSF (in Ca^{2+}) I measured the coefficient of variance (C.V.) of L4 → L2/3 EPSCs onto pairs of WT and

MEF2C KO neurons. C.V. is inversely proportional to release probability and synapse number (Manabe et al 1993) and was increased by 93% in MEF2C KO neurons in comparison to WT neurons **(Fig. 2.12B)**. In these same neuron pairs, I minimally stimulated L4 → L2/3 and compared the relative number of functional synaptic connections made by one or a small number of axons onto both WT and MEF2C KO neurons. I observed both failures and successes of synaptic transmission which is a function of both functional synapse number and release probability. The synaptic failure rate was increased by 2.5-fold in MEF2C KO neurons in comparison to WT neurons **(Fig. 2.12C)**. Taken together, the changes in Sr^{+2} event frequency, C.V., and synaptic failure rates support a role for MEF2C in promoting functional synaptic number and/or presynaptic release probability. However, since short-term plasticity - a measure related primarily to release probability - is unchanged in MEF2C KO neurons, I argue that MEF2C promotes functional L4 → L2/3 synaptic connectivity.

To determine if MEF2C alters the number of structural synapses and/or the dendritic morphology, WT or MEF2C KO L2/3 neurons were filled with Alexa488 through the patch pipette, and dendrites were imaged live with 2-photon microscopy. Because L4 axons target basal dendrites of L2/3 neurons almost exclusively (Lübke et al 2003), I imaged dendritic spine density on basal dendrites and observed a 20% decrease in MEF2C KO neurons **(Fig. 2.12D-E)**. Dendritic complexity, measured with Sholl analysis, and dendritic length of MEF2C KO neurons was normal **(Fig. 2.13)**. Therefore, *Mef2c* deletion does not stunt growth or arborization of L2/3 pyramidal neuron dendrites but decreases excitatory synaptic connections from L4 and likely other local input pathways.

Although *Mef2c* deletion results in decreased excitatory synapse number onto L2/3 neurons, the intrinsic excitability of MEF2C KO neurons was increased, as measured by an increase in firing rates in response to a depolarizing current step (F/I curve), reduced spike latency, and a slightly (+2.6 mV) depolarized resting membrane potential. There were no changes in input resistance or threshold for an action potential, but the membrane capacitance was reduced in MEF2C KO neurons **(Fig 2.14, Table 1.1)**. These may be distinct effects of MEF2C or more likely a homeostatic response to reduced excitatory synaptic input (Lu et al 2013, Turrigiano 2011). Deletion of *Mef2a/d* did not affect input resistance and only minimally affected resting membrane potential **(Table 1.1)**.

MEF2C facilitates experience-dependent development of local input pathways onto L2/3 neurons

Sensory experience-driven patterned neuronal activity is necessary for the proper development of neocortical circuits (Fox 2002). MEF2 transcription factors are activated by neuronal depolarization, Ca^{+2} influx, and experience (Flavell et al 2008), and thus may be necessary for proper experience-dependent development of neocortical circuits. Sensory deprivation by whisker trimming in the second postnatal week depresses L4 → L2/3 strength (Bureau et al., 2008; Shepherd et al., 2003; Bender et al., 2006), similar to what I observe with *Mef2c* deletion **(Fig. 2.7)**. I hypothesized that MEF2C and sensory experience functioned in a common signaling pathway to promote synapse development onto L2/3 neurons. If so, then sensory deprivation may occlude or prevent effects of *Mef2c* deletion on L2/3 synaptic inputs. To test this possibility, AAV-Cre-GFP-injected *Mef2c*$^{fl/fl}$ mice were subjected to daily unilateral whisker trimming from P9-P18 which deprives the contralateral barrel cortex of sensory experience while the ipsilateral barrel cortex is

"spared" and provides a within-animal control **(Fig. 2.15A).** Synaptic LSPS maps were obtained simultaneously from WT and MEF2C KO L2/3 neuron pairs in either spared or deprived barrel cortices **(Fig. 2.15B).** In the spared barrel cortex, intracolumnar and transcolumnar L4 → L2/3 synaptic input strengths were reduced onto MEF2C KO neurons in comparison to neighboring WT neurons, as observed in non-deprived (i.e. non-trimmed) mice. However, in deprived cortex, L4 synaptic inputs onto MEF2C KO and WT L2/3 neurons were similar and weak like that observed onto MEF2C KO neurons in the spared cortex (Fig. 2.13C-E). In other words, *Mef2c* deletion weakened synaptic inputs onto L2/3 neurons in spared, but not deprived, cortex. Thus, a significant interaction between *Mef2c* deletion and sensory deprivation was observed for vertical L4 → L2/3 inputs ($p < 0.05$; **Fig. 2.15E**) which was not due to strengthening L4 → L2/3 inputs onto spared WT neurons because they were similar to L4 → L2/3 inputs onto WT neurons in non-deprived mice **(Fig. 2.16A)**. Furthermore, the interaction of *Mef2c* and experience persists when comparing vertical L4→L2/3 input onto WT and MEF2C KO neuron pairs between deprived and non-deprived barrel cortices **(Fig. 2.14B)**. Similar results were observed for horizontal L2/3→L2/3 inputs and vertical L5A→L2/3 **(Fig. 2.15F-G)** as these input pathways were reduced by *Mef2c* deletion in spared, but not in deprived cortex. These results suggest that MEF2C is required for and permits sensory experience to promote synapse function onto neocortical L2/3 pyramidal neurons.

Interestingly, an interaction between *Mef2c* deletion and sensory deprivation was not observed at all local input pathways as *Mef2c* deletion was still able to depress evoked synaptic transmission at the adjacent L4 → L2/3 and adjacent L5A → L2/3 pathways within the deprived barrel cortex **(Fig. 2.15H-I)**. Although adjacent L5A → L2/3 input was

not significantly depressed within deprived cortex, the variability of weak input strength makes interpreting the effects of *Mef2c* deletion on this input pathway difficult, and optimistically, *Mef2c* deletion and sensory deprivation appear to have additive effects in depressing inputs at this synaptic pathway **(Fig. 2.15I)**. These data suggest that there exists a role for MEF2C in regulating synaptic input strength independent of experience and/or that experience-dependent development of L2/3 circuits does not rely on inputs from granular and infragranular layers of surrounding barrel columns; this could be due to the whisker trimming paradigm used to conduct these experiments. Additionally, the strength of LSPS responses evoked in the vertical L4 → L2/3 pathway is normal within spared barrel cortex, suggesting that the observed interaction between *Mef2c* deletion and sensory deprivation is not simply due to a potentiation of spared WT neurons in comparison to non-deprived WT neurons **(Fig. 2.16)**. Lastly, it is possible that the interaction of MEF2C and sensory experience is confined to specific input pathways that are likely involved in specific computational modes of sensory-experience-dependent circuit plasticity. For example, experience-dependent changes in synaptic plasticity at $L4_{adj}$ → L2/3 only occurs when input onto L2/3 of a deprived barrel column originates from a spared barrel column to expand cortical representation of spared barrel columns (Tsubota et al., 2015). Hence, it is possible that trimming all whiskers on the facial pad prevents experience-dependent enlargement of spared barrel columns because contrast of juxtaposed spared and deprived cortical areas is lacking in this whisker trimming paradigm.

Lastly, I recorded mEPSCs in pairs of WT and MEF2C KO L2/3 neuron pairs in spared and deprived barrel cortices to determine the effects of *Mef2c* deletion and sensory deprivation on spontaneous glutamatergic transmission. Surprisingly, no prominent

changes in mEPSC frequency or amplitude were identified, suggesting that MEF2C and sensory experience interact to regulate evoked excitatory synaptic transmission. (**Figure 2.17**)

MEF2C differentially regulates local and distal intercortical excitatory synaptic inputs onto L2/3 pyramidal neurons

Our results suggest that MEF2C generally promotes excitatory synapses onto L2/3 neurons from all input pathways. To test this, I measured spontaneous or mEPSCs, in TTX, which reflects the total functional excitatory synaptic inputs onto a neuron. Surprisingly, *Mef2c* deletion resulted in robust increases in mEPSC frequency (65%) and amplitude (10%; **Fig. 2.18A**). Furthermore, mEPSC amplitudes in MEF2C KO neurons are increased by a factor of 1.2x that of WT neurons, suggesting that MEF2C KO neurons are undergoing homeostatic synaptic scaling *in vivo* (**Fig. 2.18B**). These results are difficult to reconcile with the 50% depression of EPSCs evoked by electrical stimulation of L4 or LSPS of many input pathways. LSPS maps only "local" synaptic inputs from neurons whose somata reside within the slice (Shepherd et al 2003) and originate from the same or adjacent barrel columns. L2/3 neurons also receive long-range inputs from distant cortical areas, including ipsilateral motor and secondary somatosensory cortices and from the contralateral somatosensory cortex (Bosman et al 2011, Feldmeyer 2012a). Contralateral S1 (cS1) inputs to L2/3 have similar strength and connectivity as local ipsilateral L2/3 → L2/3 synaptic inputs (Petreanu et al 2007a). Although neuron somata comprising these long-range intercortical pathways are not present in the slice, the severed axons remain and retain the ability to release glutamate, and thus, may contribute to mEPSCs measured in L2/3 neurons. Therefore, I hypothesized that long-range intercortical inputs onto L2/3 MEF2C

KO neurons may be strengthened and contribute to the enhanced mEPSCs. To test this possibility, I evoked EPSCs onto WT and MEF2C KO neuron pairs with extracellular electrical stimulation of adjacent L2/3 in which horizontally-projecting axons from both local and long-range pathways pass (Petreanu et al 2007a, Petrus et al 2015) (**Fig. 2.19A**). In contrast to stimulation of vertical L4 inputs, EPSCs evoked from adjacent L2/3 were unchanged in MEF2C KO neurons in comparison to neighboring WT neurons (**Fig. 2.19B**). This result revealed an input-specific effect of *Mef2c* deletion. LSPS maps indicate that local inputs from adjacent L2/3 onto MEF2C KO neurons are weak (**Fig. 2.9I**). Therefore, concurrent extracellular stimulation of weak local inputs may mask any potentiation of long-range inputs. To study effects of *Mef2c* deletion on a long-range intercortical inputs in isolation I expressed Channelrhodopsin-2 (ChR2) in axons projecting from cS1. At postnatal day 1, *Mef2c*$^{fl/fl}$ mice were injected in the lateral ventricle with AAV-Cre-GFP while AAV-ChR2-mCherry was stereotaxically injected into cS1 (**Fig. 2.20A**). Slices of barrel cortex contralateral to AAV-ChR2 injection were prepared at P20-25 and expressed mCherry-positive axons, and Cre-GFP (MEF2C KO) labeled cell bodies (**Fig. 2.20B**). EPSCs were evoked from the callosal ChR2-expressing axons onto pairs of WT and MEF2C KO L2/3 neurons with a brief (2 ms) pulse of blue light. To isolate monosynaptic EPSCs from ChR2-expressing axons, experiments were performed in TTX. Remarkably, the amplitude of EPSCs evoked from cS1 inputs was increased by 80% in MEF2C KO neurons compared to WT neurons (**Fig. 2.20C**), demonstrating potentiation of long-range inputs from cS1, which may contribute to the observed increase in mEPSC frequency and amplitude.

Given that connectivity with local inputs is decreased by approximately half while basal dendritic spine densities are decreased by merely ~20% in MEF2C KO in comparison to WT L2/3 neurons lends the possibility that *Mef2c* deletion causes a concomitant increase in connectivity with long-range intercortical inputs to offset the expected ~50% reduction in excitatory synapses targeted by local inputs. In other words, *Mef2c* deletion can increase long-range synapse number to make the ~50% decrease in local connectivity appear less, at least when counting structural synapse number along a dendrite where the source of presynaptic input for each dendritic spine is unknown. Inputs from cS1 synapse onto both apical and basal L2/3 dendritic compartments. Therefore, to determine if *Mef2c* deletion increased functional synapse number at long-range inputs, I measured the C.V. of the recorded light-evoked ChR2-mediated EPSCs and found no change (**Fig. 2.20D**). These data suggest that *Mef2c* deletion increases synaptic strength of long-range inputs without affecting functional synapse number.

My results indicate that MEF2C differentially regulates excitatory synaptic function from local and long-range input pathways. This differential regulation may be based on the dendritic compartments contacted by these inputs. For example, basal dendrites receive local inputs from L4 and L2/3 within barrel columns and from adjacent columns. Proximal apical dendrites also receive local inputs from L2/3. The distal apical "tufts" receive mostly long-range intercortical input from M1, M2, and S2 (Bosman et al 2011). To determine if MEF2C selectively regulates synapse number as a function of dendritic compartment, WT and MEF2C KO L2/3 neurons were filled with biocytin through the patch pipette and processed for immunofluorescence. Dendritic spines in three different dendritic compartments were imaged using 2-photon microscopy. Again,

dendritic spine density on basal dendrites was decreased by 14% on MEF2C KO L2/3 neurons, while densities were unchanged in proximal and distal apical dendrites (**Fig. 2.21**). These data suggest that MEF2C selectively promotes structural excitatory synapse number onto L2/3 basal dendrites: the site of synaptic inputs from local L4 and L2/3.

As a further attempt to delineate compartment- versus input-pathway-specific regulation by MEF2C, I used a laser-guided mapping technique to measure excitatory ChR2-evoked EPSCs onto small dendritic segments along the L2/3 dendritic arbors of WT and MEF2C KO (**Fig. 2.22A-D,H**). This technique is formally called subcellular ChR2-assisted circuit mapping (sCRACM) (Petreanu et al 2007a). Initial L2/3 sCRACM experiments were performed in mice that were injected with 400 nL of AAV-ChR2-mCherry, which although preliminary, revealed stronger EPSCs in MEF2C KO neurons in all dendritic compartments (**Fig. 2.22D-G**). This preliminarily suggests that MEF2C regulates specific pools of synapses among heterogeneous synaptic populations even on the same dendritic segment. However, additional sCRACM L2/3 responses were recorded from WT and MEF2C KO neurons in mice that were injected with only 250 nL of AAV-ChR2-mCherry, and ChR2-evoked EPSCs were normal in MEF2C KO neurons (**Fig. 2.22H-I**). These data are not conclusive because it is possible that the smaller volume of virus did not penetrate cortical tissues that were previously infected with 400 nL injection volume, thus other distal inputs emanating from cortical regions other than from cS1 could be differentially by MEF2C. A simple explanation for why ChR2-evoked EPSCs were not increased in MEF2C KO neurons focuses upon the technical sensitivity of sCRACM; ChR2-evoked EPSCs are extremely variable in amplitude, hence any differences could be lost during *post hoc* analyses. Additionally, I never performed sCRACM experiments with

intracellular dye filling. This poses a problem for interpreting my results because L2/3 pyramidal neurons have variable dendritic span and apical dendritic length. Thus, without directly linking the morphology of the recorded neuron with the sCRACM maps diminishes the average signal and sharply increases variability. The possibility that MEF2C regulates compartment or input specificity must be revisited.

Thus far, I have demonstrated that *Mef2c* deletion differentially and bidirectionally regulate long-range and local inputs, and thus the primary role for MEF2C in regulating neocortical synapse development could be to promote connectivity of local inputs or to strengthen long-range inputs onto neocortical L2/3 neurons, given the role of MEF2C in suppression of hippocampal synaptic function. To determine the primary role of MEF2C, I performed LSPS mapping in MEF2C KO and WT L2/3 neurons at P13-P17 which revealed a trend toward decreased L4 → L2/3 input strength onto MEF2C KO neurons (**Fig. 2.23A**). However, mEPSC recordings at this age were normal in MEF2C KO neurons (**Fig. 2.23B**). These data – although rather preliminary – suggest that MEF2C likely decreases connectivity of local inputs prior to potentiating long-range inputs. Obtaining a high sample number for LSPS experiments could more definitively resolve whether or not L4 → L2/3 inputs are, in fact, weakened at P13-P17. Additionally, mEPSCs are normal at P13-P17 with simultaneous deletion of *Mef2a* and *Mef2d* (**Fig. 2.23C**). Taken together, these data suggest that MEF2C likely functions primarily to promote connectivity at local inputs onto neocortical L2/3 neurons: the opposite of the tradition role for MEF2C in regulating synapse development in other brain regions. Furthermore, it is possible that MEF2 transcription factors become critical for excitatory synaptic function during the third week of postnatal development *in vivo*, or otherwise such MEF2-dependent synaptic

regulation is due to the postnatal deletion strategy and could be revealed at earlier developmental ages if the sparse deletion occurred during embryogenesis.

Discussion

Here I demonstrate that postsynaptic *Mef2c* bidirectionally regulates distinct excitatory synaptic input pathways onto L2/3 pyramidal neurons in the developing barrel cortex *in vivo*. Data indicate that MEF2C KO neurons have fewer functional and structural synaptic connections from all local input pathways (L4, L2/3 and L5A), and these effects require sensory experience. In stark contrast, long-range inputs onto MEF2C KO neurons from cS1 are potentiated. These data suggest that, in response to experience, postsynaptic MEF2C regulates transcripts that differentially affect synaptic connectivity from distinct input pathways. (See circuit model, **Fig. 2.24**)

MEF2C promotes excitatory synapse number onto neocortical L2/3 pyramidal neurons

Transcriptional activation of MEF2 family members has been primarily implicated in elimination of excitatory synapses. Embryonic or postnatal brain-wide deletion of *Mef2c* increases spine density and synaptic transmission onto dentate gyrus granule cells of the hippocampus (Adachi et al 2015, Barbosa et al 2008), while excitatory synaptic transmission is reduced in CA1 and onto L5 neurons (Li et al 2008). Because embryonic deletion of *Mef2c* also affects neuronal migration and gross laminarization of neocortex the cell-autonomous and synaptic effects of *Mef2c* were unknown (Li et al 2008). To assess the cell-autonomous function of *Mef2c* on postnatal circuit development, I deleted *Mef2c* in a sparse population of neurons within a wildtype circuit. Based on the evidence for MEF2C in synapse elimination, the increase in mEPSC frequency and potentiation of distal inputs in MEF2C KO neurons may be a direct effect of *Mef2c*

deletion, while the depressed local inputs may be a homeostatic response or competition for postsynaptic resources (Bian et al 2015). Alternatively, *Mef2c* may regulate transcripts that promote development or stabilization of synapses targeted by local inputs. Preliminary studies reveal that MEF2C may decrease evoked L4 → L2/3 synaptic transmission prior to increasing mEPSCs during the second week of postnatal development, which could suggest that local connectivity is decreased prior to potentiation of long-range inputs and hence that MEF2C primarily functions to promote synapse number onto neocortical L2/3 neurons. In support of this idea, a sumoylated, transcriptional repressor form of MEF2A promotes postsynaptic maturation of cerebellar granule neurons (Shalizi et al 2006).

MEF2C is a molecular correlate of sensory experience

My data suggest that sensory experience, via regulation of MEF2C, differentially modifies specific L2/3 inputs. Supporting this model, the multiple and diverse effects of sparse postnatal *Mef2c* deletion on L2/3 circuitry parallel that of sensory deprivation. Whisker trimming decreases the strength of local input pathways onto L2/3 neurons in barrel cortex (Bender et al 2006b, Bureau et al 2008, Shepherd et al 2003) and this prevents or occludes weakening by *Mef2c* deletion, suggesting that *Mef2c* functions downstream of experience to promote synapse development from local circuits onto L2/3 neurons. Whisker deprivation decreases connectivity between L2/3 neurons while also potentiating mEPSP amplitudes, suggesting differential changes in distinct input pathways (Cheetham et al 2007a). Furthermore, visual deprivation potentiates intercortical inputs onto L2/3 while depressing vertical L4 → L2/3 inputs (Petrus et al 2015). To my knowledge, the effects of sensory deprivation on the strength of interhemispheric excitatory inputs to L2/3 have not been examined. MEF2C KO neurons exhibit a selective decrease in structural

synapses onto basal dendrites: the primary target of vertical L4 inputs (Feldmeyer et al 2006). Similarly, sensory experience regulates dendritic spine density onto basal but not apical L2/3 dendrites (Bian et al 2015, Globus et al 1973, Holtmaat et al 2005, Ma et al 2016).

In contrast to the effects of *Mef2c* deletion, plucking a single whisker row results in decreased release probability of L4 → L2/3 inputs and no change in mEPSCs onto L2/3 neurons (Bender et al 2006b). Furthermore, this study reports no changes in AMPA/NMDA ratios and quantal amplitude and infers that there are no postsynaptic changes induced by sensory deprivation (Bender et al., 2006). Aside from changes in presynaptic release probability, the data in this study can support the hypothesis that sensory deprivation decreases activity-dependent synapse number at L4 → L2/3, which exactly mirrors my observations with cell-autonomous *Mef2c* deletion. Additionally, the synaptic plasticity mechanisms engaged may depend on the deprivation paradigm. Nonetheless, the striking similarities between the effects of cell-autonomous *Mef2c* deletion on excitatory synapse number, the interaction between sensory deprivation and *Mef2c* deletion, and the Bender et al., 2006 study make a strong argument that MEF2C is regulating synapse number promoted by sensory experience.

Interestingly, changes in mEPSCs observed in L2/3 neurons in response to either experience (Petrus et al 2015) or *Mef2c* deletion (Fig. 2.16) are correlated with changes in evoked synaptic transmission from horizontal inputs, and not vertical L4 →L2/3 inputs (Petrus et al 2015). These results suggest that mEPSCs mainly reflect long-range intercortical synapses despite L2/3 pyramidal neurons having the highest connection probability with L4 axons and other local synaptic pathways (Lefort et al 2009, Silver et al

2003). Remarkably, MEF2C KO neurons displayed increases in mEPSC frequency and amplitude, while evoked synaptic transmission from all measured local inputs was decreased. The 80% increase in synaptic strength from cS1 inputs likely contributes to the increased mEPSCs, and other distal intercortical pathways from ipsilateral M1 or S2 are also likely potentiated. However, I cannot rule out the possibility that MEF2C, and experience, differentially regulate evoked and spontaneous synaptic transmission from the same local inputs (Kavalali 2015).

Mef2c deletion also "scales" amplitudes of mEPSCs (Fig. 2.16B), suggesting that synapses onto MEF2C KO L2/3 pyramidal neurons are undergoing homeostatic synaptic scaling (Desai et al 2002, Turrigiano et al 1998). My data suggest that *Mef2c* is promoting experience-dependent circuit plasticity via a postsynaptic mechanism that differentially modulates specific synaptic inputs. Previous studies demonstrate that L2/3 pyramidal neurons within the mouse barrel cortex undergo seemingly simultaneously LTP-like potentiation of local clustered GluA1-contianing synapses and homeostatic scaling of evenly distributed GluA2-containing synapses (Makino & Malinow 2011). Furthermore, neighboring excitatory synapses within a small dendritic segment are activated in close temporal and spatial proximity *in vivo* (Harvey & Svoboda 2007, Takahashi et al 2012) after experience onto basal dendrites of neocortical L2/3 neurons (Makino & Malinow 2011). Furthermore, motor learning tasks induce formation of clustered dendritic spines *in vivo* (Fu et al 2012). Perhaps MEF2C drives expression of a target gene following whisker stimulation to facilitate formation or maintenance of synapse clusters targeted by local L4 axons but not at synaptic clusters receiving distal inputs from cS1, for example, which synapse onto both basal and apical L2/3 dendritic compartments. The diffuse

targeting of cS1 inputs onto the L2/3 dendritic arbor could resemble the "evenly distributed" synaptic population that undergoes homeostatic scaling when ascending local inputs are deprived of sensory input or of MEF2C-dependent transcription. This could allow for precise subcellular postsynaptic regulation of synapse number within small dendritic segments rather than tagging L2/3 basal dendritic synapses regardless of their presynaptic inputs. Whether or not clustered synapses receive inputs from the same neuron or neuron population is unknown (Larkum & Nevian 2008).

My findings alone and in the context of other studies support a clear role for MEF2C as a critical permissive transcriptional signal for driving experience-dependent development of evoked synaptic transmission at local neocortical L2/3 inputs. These results were obtained through utilization of a unilateral whisker trimming paradigm, which deprives the contralateral barrel cortex while sparing the ipsilateral barrel cortex within the same animal. Furthermore, the mapping of local LSPS-evoked EPSCs that I employed assayed only local inputs with preserved neurogeometry. In contrast, I did not observe the expected increase of mEPSC frequency and amplitude in MEF2C KO L2/3 neurons within spared barrel cortex, which accompanies sparse *Mef2c* deletion within barrel cortices of non-deprived (i.e. non-whisker trimmed) mice as well as sensory deprivation studies involving the removal of a small number of whiskers or comparisons across trimmed and non-trimmed animals (Bender et al 2006b, Cheetham et al 2007a, Makino & Malinow 2011). These results are not surprising because the increased mEPSCs in MEF2C KO L2/3 neurons or deprived L2/3 neurons are likely due to scaling or potentiation of inputs received from spared cortex. The unilateral whisker trimming results in spared L2/3 pyramidal neurons receiving inputs from deprived long-range intercortical inputs, which

are likely depressed due to sensory deprivation. I observed a small but significant increase in mEPSC amplitude in MEF2C KO neurons in comparison to WT neurons within deprived barrel cortex, which receive spared long-range corticocortical inputs, and are thus able to undergo potentiation or scaling. Additionally, no changes in mEPSC frequency were observed in spared and deprived barrel cortices with or without *Mef2c* deletion. Initially, one would expect that mEPSC frequency should be decreased in spared MEF2C KO neurons in comparison to spared WT neurons because MEF2C KO neurons have an approximate 50% decrease in local connectivity in addition to weakened long-range intercortical inputs. However, the fact that mEPSC frequency is unchanged may speak to the abundance of long-range intercortical inputs onto L2/3 pyramidal neurons such that the weakening of these inputs – common to both WT and MEF2C KO neurons – is sufficient to mask the decreased connectivity of local inputs, and thus WT and MEF2C KO neurons appear to have the same global number of synaptic connections. In parallel, mEPSC frequency between WT and MEF2C KO L2/3 neurons within deprived cortex is likely unchanged because local connectivity is decreased by ~50% onto both neurons.

Does MEF2C facilitate neocortical synapse development through input pathway or compartment specificity?

Transcription factors control development of axons and dendrites, as well as formation of layer-specific synaptic inputs in part through production of gradients of guidance cues (Santiago & Bashaw 2014). Here I demonstrate that a postsynaptic transcription factor differentially regulates distinct synaptic inputs onto an individual cortical neuron without affecting dendritic morphology. The activity-regulated transcription factor, NPAS4, differentially regulates strength of inhibitory synaptic inputs

impinging on different dendritic domains of CA1 pyramidal neurons in an experience-dependent manner (Bloodgood et al 2013a). Thus, experience and activity, through a coordinated regulation of NPAS4 and MEF2C, may determine the connectivity and strength of specific inhibitory and excitatory circuits, respectively. Dendritic spine densities were reduced on basal, but not apical, dendrites of MEF2C KO neurons suggesting that MEF2C may differentially regulate inputs based on dendritic compartment. Although L4 and local L2/3 inputs synapse onto basal dendrites of L2/3 neurons, local L2/3 inputs also contact proximal apical dendrites (Feldmeyer et al 2006), where I did not detect a change in spines. In this scenario, one would expect that inputs from cS1 to primarily contact apical dendrites of L2/3 neurons in barrel cortex, which to my knowledge, is unknown. Alternatively, the origin of the presynaptic input, local versus distal, may determine regulation by postsynaptic MEF2C. MEF2 transcription factors regulate cell adhesion molecules, such as protocadherins and semaphorins, which may stabilize or eliminate specific input pathways through trans-synaptic signaling pathways (Flavell et al 2008, Tsai et al 2012).

Differential regulation of neocortical inputs by MEF2C and implications for neurodevelopmental disorders

Mutations in *MEF2C* are associated with intellectual disability, epilepsy, autism and schizophrenia (Paciorkowski et al 2013b, Schizophrenia Working Group of the Psychiatric Genomics 2014). Interestingly, imbalances in local versus long-range functional connectivity among cortical and other regions are associated with autism and perhaps schizophrenia (Cao et al 2016, Ha et al 2015). Sparse heterozygous deletion of *Mef2c* does not weaken local inputs onto L2/3 pyramidal neurons **(Fig. 2.3)**, suggesting

that autistic-like phenotypes associated with *Mef2c* haploinsufficiency or 5q14.3-5 deletion syndrome are non-cell-autonomous and that network-level heterozygous loss of *Mef2c* is likely required for expression of autistic-like behaviors in mammals. This point is discussed in more detail in Chapter 4. Nonetheless, my demonstration that an autism- and schizophrenia-linked gene, *MEF2C*, differentially and cell-autonomously regulates local and long-range cortical connections provides a novel molecular link from the genetics of these disorders and the abnormal brain connectivity.

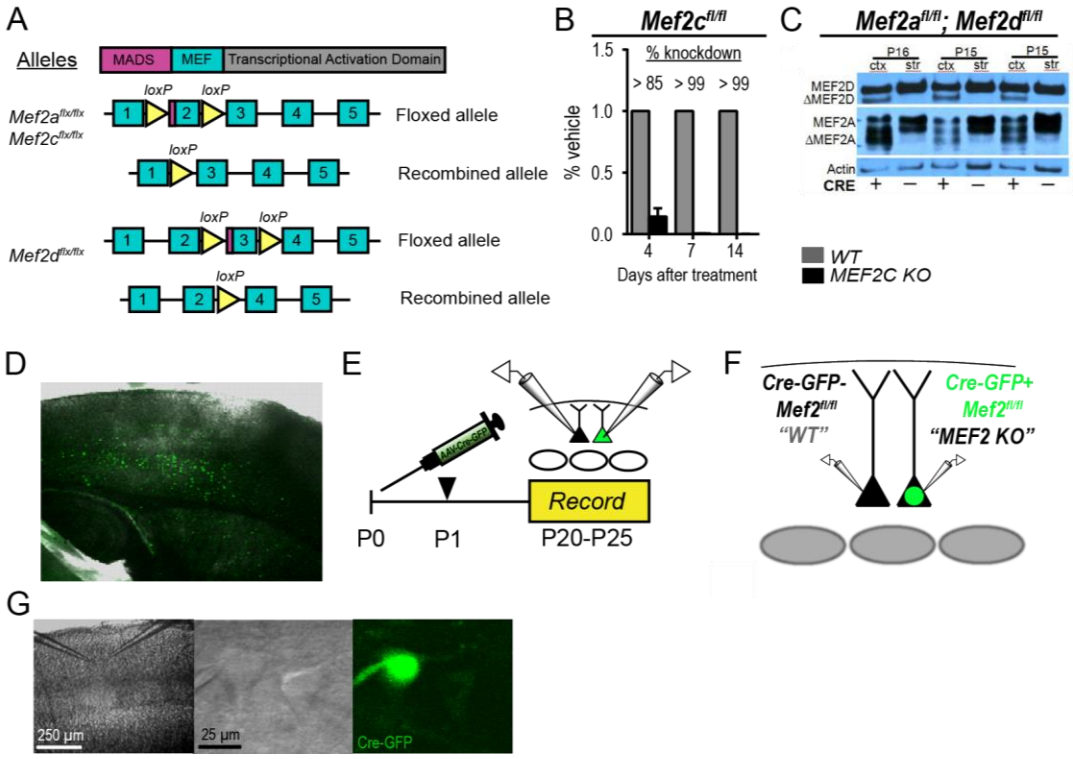

Figure 2.1: Sparse postnatal MEF2 gene deletion and schematic of electrophysiological recording paradigm. (A) Schematics of specific floxed MEF2 genes

and final gene products after Cre recombination. **(B**) *In vitro* time course of *Mef2c* deletion measured by depletion of *Mef2c* mRNA obtained from dissociated neocortical cultures. **(C)** Western blots demonstrating truncation of MEF2A and MEF2D were obtained from cortical and striatal lysates of AAV-Cre-GFP-injected *Mef2a*$^{fl/fl}$*; Mef2d*$^{fl/fl}$ mice at 2 weeks of age. Note lack of truncation in striatal lysates to where AAV-Cre-GFP should not diffuse. **(D**) Image of IR-DIC and 488-nm fluorescence overlay depicting sparse AAV-Cre-GFP expression in the barrel cortex of an acute brain slice (4x magnification). **(E)** Schematic of experimental timeline. **(F)** Cartoon of dual whole-cell recordings of WT and MEF2 KO L2/3 neurons within the barrel cortex. Gray ovals indicate barrels. **(G)** IR-DIC and 488-nm fluorescent images (40x magnification) of WT and MEF2 KO L2/3 neurons during dual whole-cell recordings.

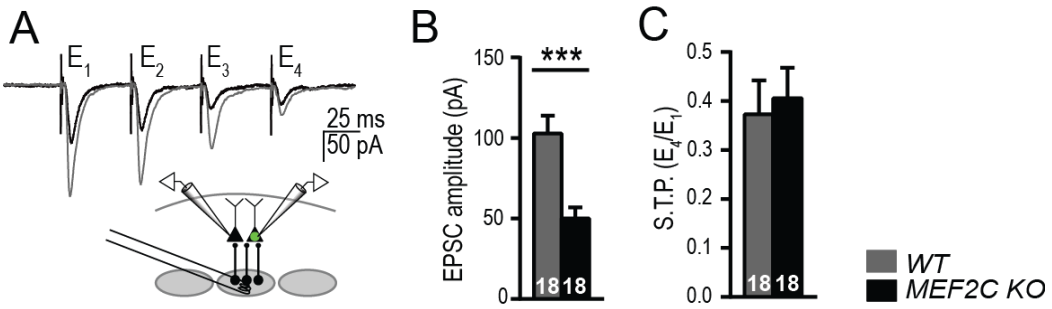

Figure 2.2: Sparse postnatal *Mef2c* deletion depresses evoked AMPAR-mediated glutamatergic input from L4 onto neocortical L2/3 pyramidal neurons. (A) Example traces of evoked EPSCs recorded from WT and MEF2C KO L2/3 neurons in response to electrical stimulation of L4. Inset: Recording paradigm. Average EPSC amplitude **(B)** and short-term plasticity (**C**, STP). For all figures, sample numbers or "n" is on bar graphs. p < 0.05*, 0.01**, 0.001***, 0.0001****

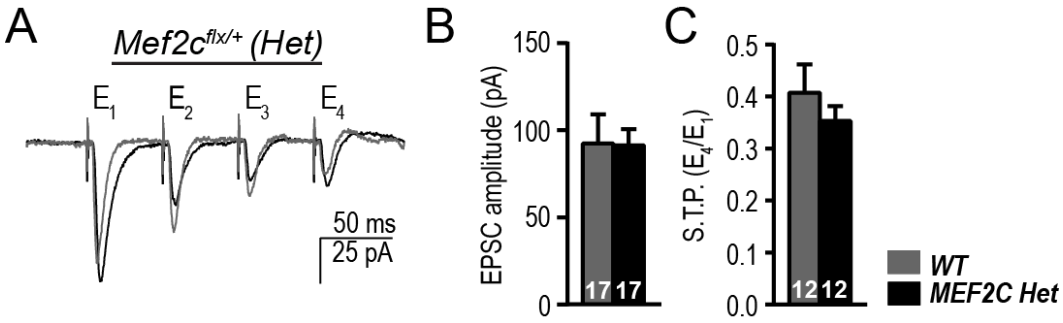

Figure 2.3: Heterozygous *Mef2c* deletion does not affect AMPAR-mediated evoked transmission from L4 inputs onto neocortical L2/3 neurons. (A) Example EPSCs recorded from WT and MEF2C HET neurons to electrical L4 stimulation. Average evoked EPSC amplitude **(B)** and short-term plasticity (**C).**

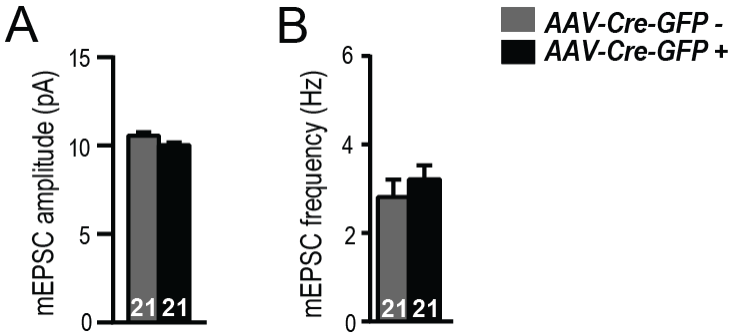

Figure 2.4: AAV-Cre-GFP does not affect spontaneous or miniature EPSCs onto neocortical L2/3 neurons in WT mice. Miniature EPSC amplitude **(A)** and frequency **(B).**

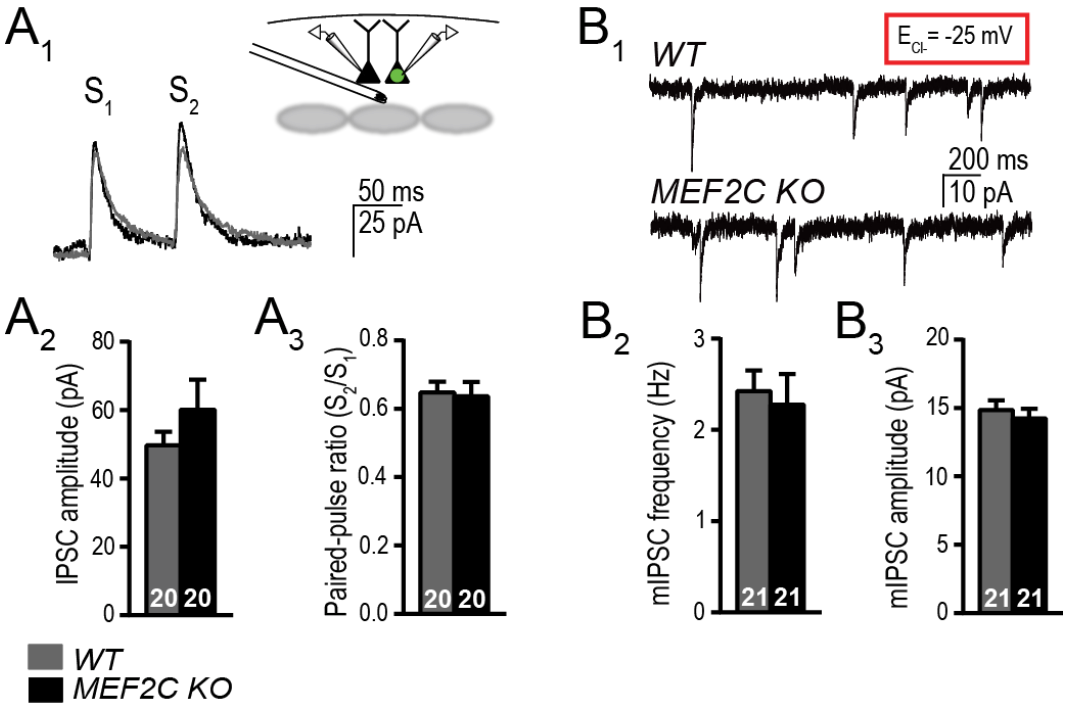

Figure 2.5: Postnatal sparse *Mef2c* deletion does not affect evoked or spontaneous GABAergic synaptic transmission. (A_1) Example evoked IPSCs recorded from WT and MEF2C KO L2/3 neuron pairs in response to local extracellular electrical stimulation. Average IPSC amplitude **(A_2)** and paired-pulse ratios **(A_3). (B_1)** Example traces of mIPSCs from WT and MEF2C KO neurons. Average mIPSC frequency **(B_2)** and amplitude **(B_3).**

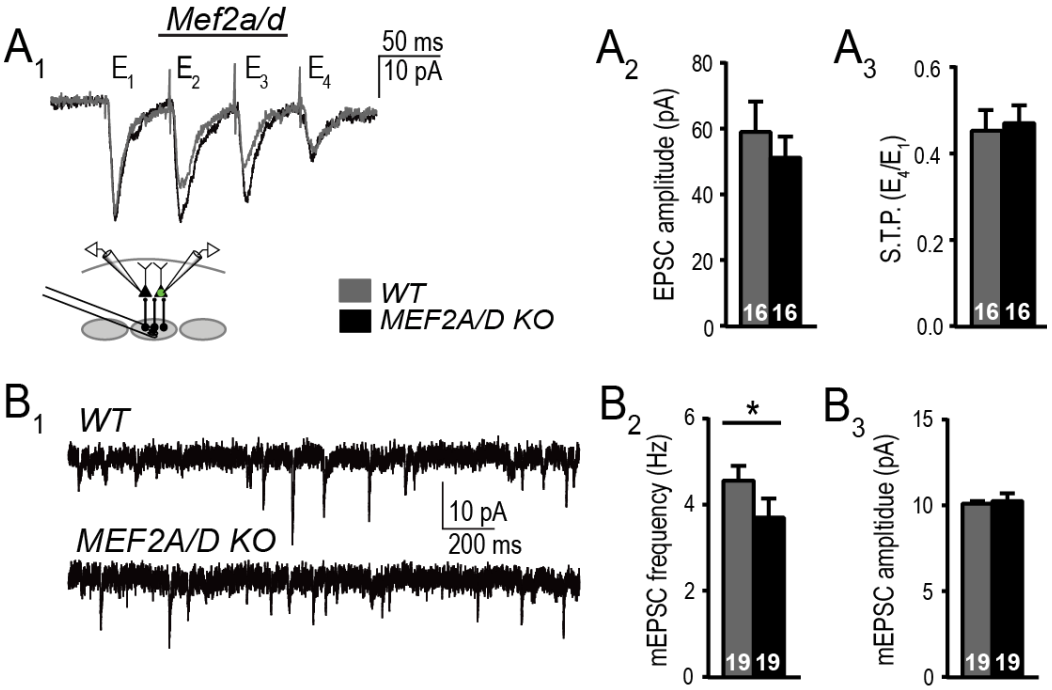

Figure 2.6: Simultaneous deletion of *Mef2a* and *Mef2d* modestly affects glutamatergic synaptic transmission. (A_1) Example EPSCs from WT and MEF2A/D KO neurons in response to L4 stimulation. Average EPSC amplitude **(A_2)** and short-term plasticity **(A_3)**. **(B_1)** Example traces of mEPSCs recorded from WT and MEF2A/D KO L2/3 neurons. Miniature EPSC frequency **(B_2)** and amplitude **(B_3)**.

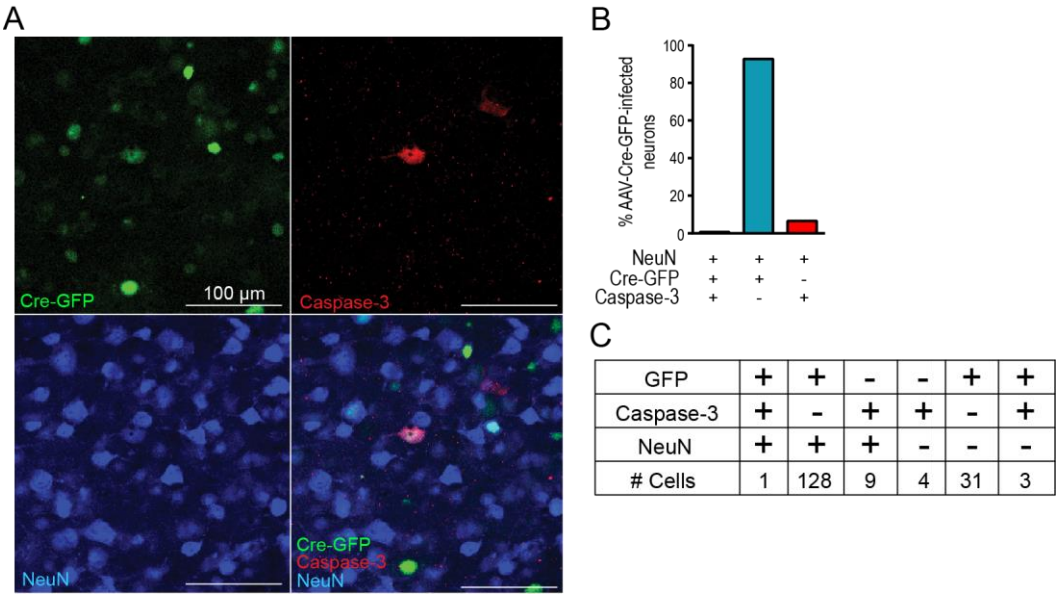

GFP	+	+	-	-	+	+
Caspase-3	+	-	+	+	-	+
NeuN	+	+	+	-	-	-
# Cells	1	128	9	4	31	3

Figure 2.7: Simultaneous deletion of *Mef2a, Mef2c,* and *Mef2d* does not cause cell death via apoptosis. (A) Confocal image of Cre-GFP, Caspase-3, and NeuN expression in barrel cortical L2/3 of fixed brain slices obtained from *Mef2a*$^{fl/fl}$*; Mef2c*$^{fl/fl}$*; Mef2d*$^{fl/fl}$ mice at P14 (40x magnification). **(B)** Quantification of L2/3 neurons expressing caspase-3 with and without AAV-Cre-GFP infection**. (C)** Table of raw data represented in B.

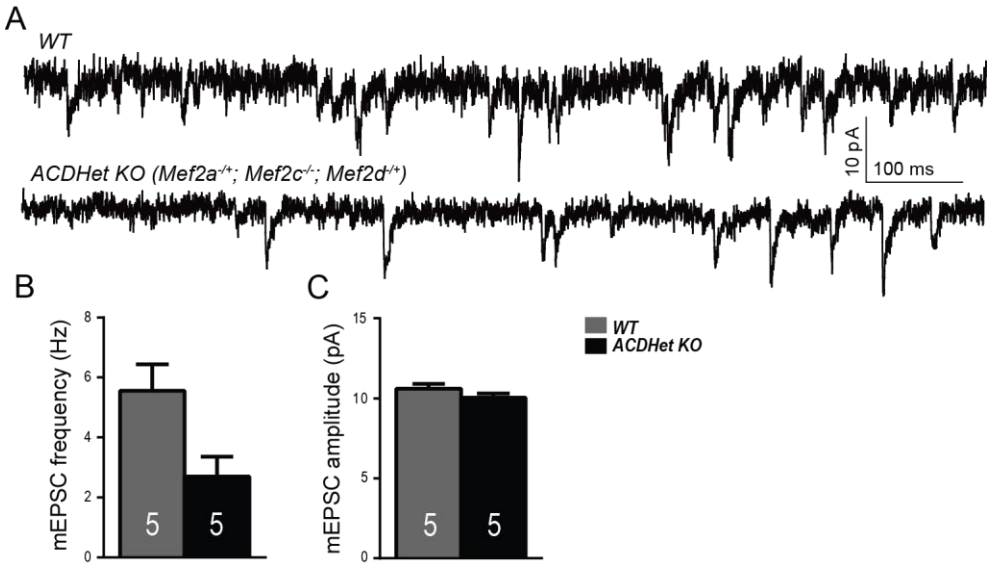

Figure 2.8: Preliminary effects of sparse AAV-Cre-GFP on spontaneous or miniature EPSCs onto neocortical L2/3 neurons in "ACDHet" or *Mef2a*$^{fl/+}$; *Mef2c*$^{fl/fl}$; *Mef2d*$^{fl/+}$ mice. (A) Example traces of mEPSCs recorded simultaneously from WT and ACDHet L2/3 pyramidal neurons. Miniature EPSC frequency **(B)** and amplitude **(C).**

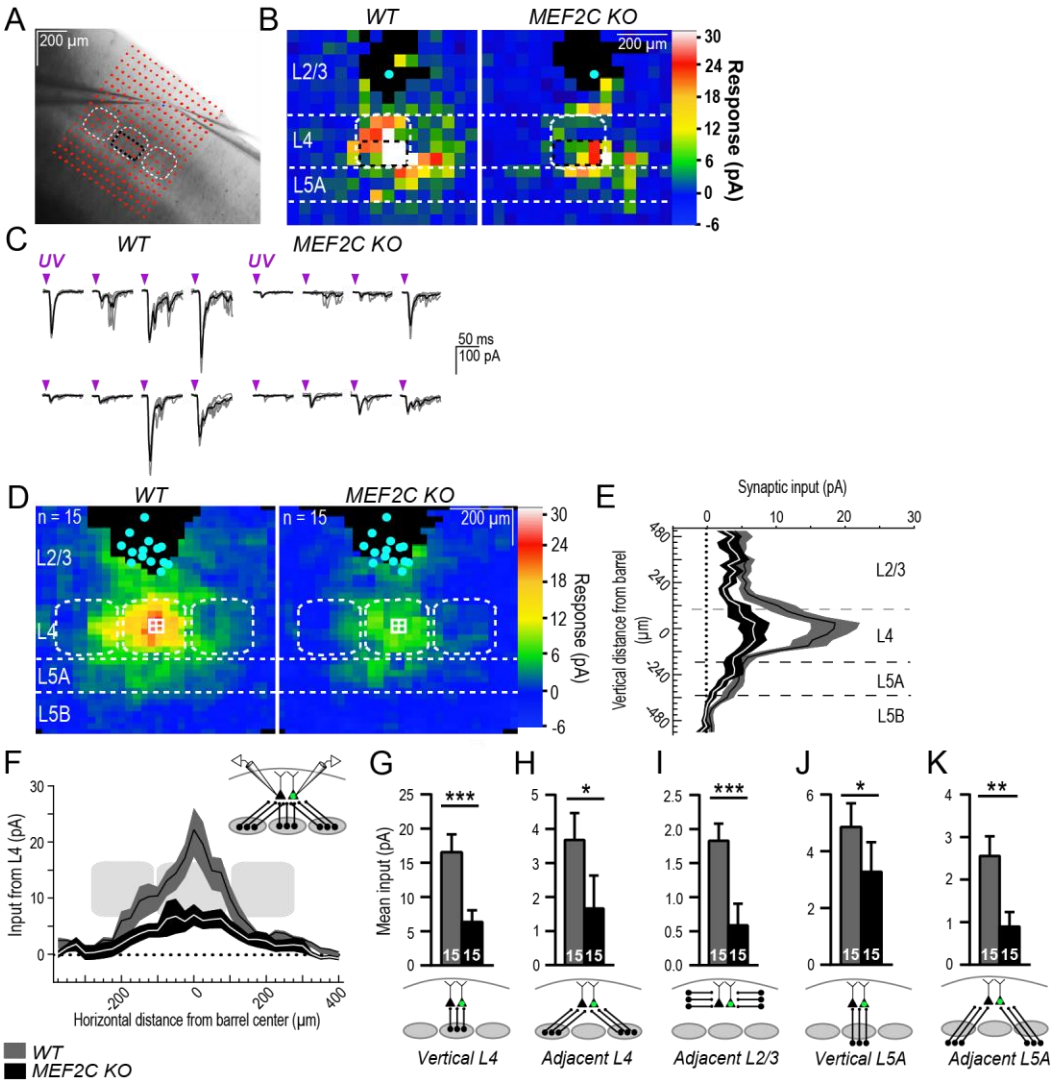

Figure 2.9: Postnatal *Mef2c* deletion weakens excitatory synaptic inputs from local neocortical circuits. (A) IR-DIC image of barrel cortex slice overlaid with the LSPS stimulation grid (red dots) during dual recordings of WT and MEF2C KO neurons. White dotted lines outline barrel columns. **(B)** Color coded, LSPS synaptic input maps of individual WT and MEF2C KO L2/3 neurons. For this and all maps, cyan dots indicate soma location, direct responses are blacked out, and dashed lines are barrels and columns. LSPS-evoked EPSC amplitudes are color coded according to scale. Pixels within dotted black line correspond to stimulation locations in **(A)**. **(C)** Representative LSPS-evoked

EPSCs recorded from WT and MEF2C KO neurons in **(A)** and **(B)** with preserved spatial orientation. Triangles mark UV laser pulses. Black: averaged EPSC. Gray: individual EPSCs. **(D)** Averaged LSPS maps of all WT and MEF2C KO pairs. Maps are aligned to the "home" barrel center (white crosshair) and averaged. **(E)** Vertical profile of mean synaptic inputs within the home barrel column of WT and MEF2C KO neurons. Shaded region represents ± S.E.M. **(F)** Horizontal profiles of mean synaptic L4 → L2/3 input across barrel columns (gray boxes). Inset: Represented L4 → L2/3 input pathways. Mean synaptic inputs onto WT and MEF2C KO neuron pairs in the **(G)** vertical L4 → L2/3, **(H)** adjacent L4 → L2/3, **(I)** adjacent L2/3 → L2/3, **(J)** vertical L5A → L2/3, and **(K)** adjacent L5A → L2/3 input pathways from averaged LSPS responses of neurons shown in **(D)**.

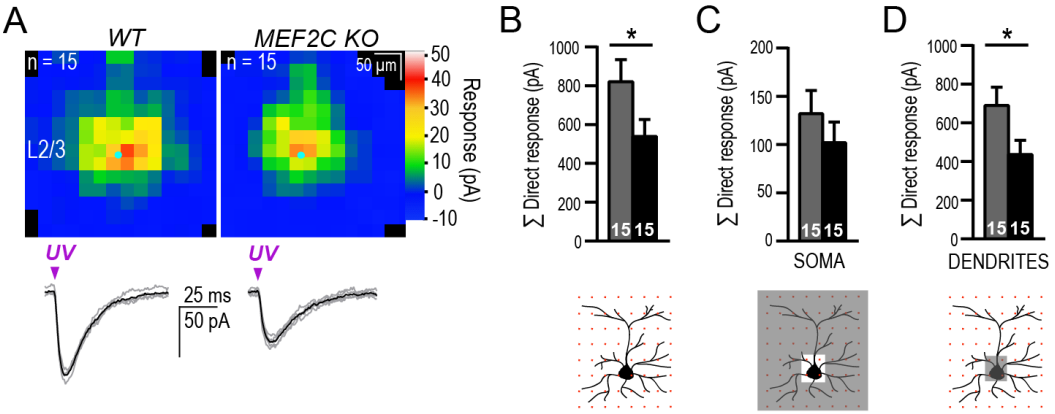

Figure 2.10: Postnatal and postsynaptic *Mef2c* deletion decreases AMPAR-mediated glutamate sensitivity of neocortical L2/3 neurons. (A) Averaged direct response maps to LSPS of WT and MEF2C KO L2/3 neurons. Maps are aligned to soma location (cyan dot). Below: direct LSPS-evoked responses in WT and MEF2C KO neurons. **(B)** Quantification of summed LSPS-evoked responses recorded from WT and MEF2C KO neurons. **(C)** Quantification of summed LSPS-evoked responses within a 25-µm radius of the soma. Shaded region indicates excluded stimulation locations over the dendrites. **(D)** Quantification of summed dendritic LSPS-evoked responses greater than a 25-µm radius of the soma. Shaded region indicates excluded stimulation locations over the soma.

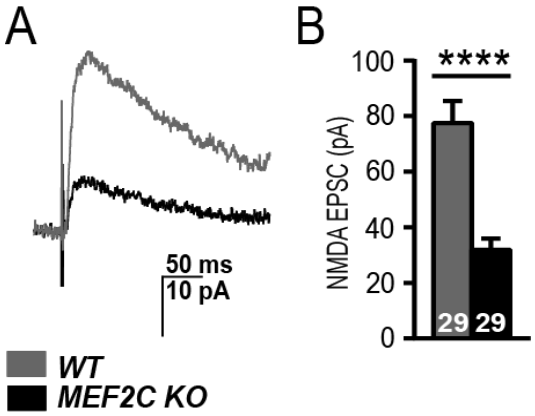

Figure 2.11: Postnatal Mef2c deletion decreases L4 → L2/3 evoked NMDAR-mediated synaptic transmission onto neocortical L2/3 pyramidal neurons. (A) Example NMDA-receptor-mediated EPSCs from WT and MEF2C KO L2/3 neurons in response to L4 electrical stimulation. **(B)** Average NMDA-EPSC amplitude.

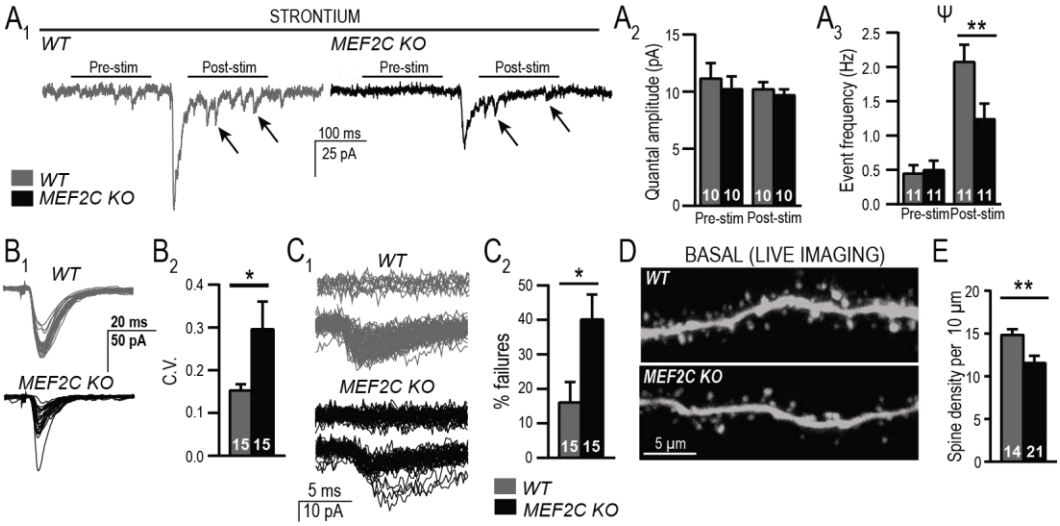

Figure 2.12: Postnatal deletion of *Mef2c* in L2/3 neurons decreases functional and structural excitatory synaptic connectivity from L4. (A_1) Example evoked L4 → L23 EPSCs recorded from WT and MEF2C KO L2/3 neurons in Sr^{+2}. **(A_2)** Quantal event amplitude and **(A_3)** frequency within pre- and post-stimulation analysis windows (black bars in B_1). **(B_1)** Example evoked L4 → L2/3 EPSCs recorded from WT and MEF2C KO neurons. **(B_2)** C.V. of evoked L4 → L2/3 EPSCs in WT and MEF2C KO neurons. **(C_1)** Representative EPSCs recorded from WT and MEF2C KO L2/3 neurons in response to minimal electrical stimulation of L4. **(C_2)** Average synaptic failure rate in WT and MEF2C KO neurons. **(D)** Representative images of spines on secondary basal dendrites of live, Alexa488-filled WT and MEF2C KO L2/3 neurons. **(E)** Average basal dendritic spine density. $p < 0.05$*, $p < 0.01$**, 2-way ANOVA interaction $p < 0.05$ (Ψ).

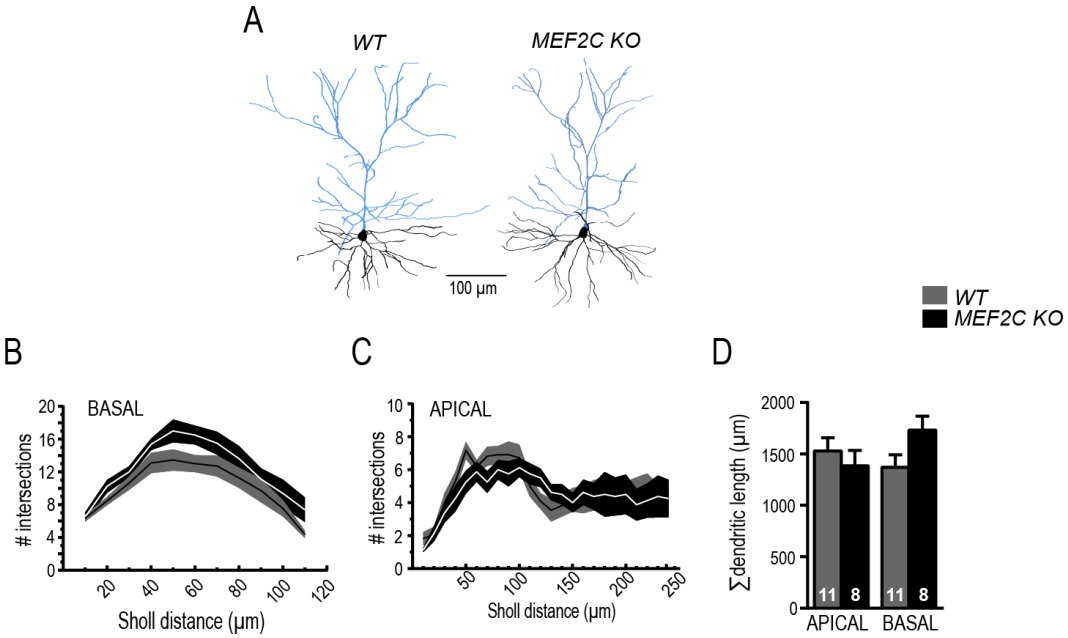

Figure 2.13: Postnatal and postsynaptic *Mef2c* deletion does not affect dendritic arborization. (A) Traced dendritic arbors of WT and MEF2C KO L2/3 neurons. Apical and basal dendritic compartments represented by blue and black, respectively. Sholl analyses for **(B)** basal and **(C)** apical compartments of WT and MEF2C KO L2/3 neurons. **(D)** Summed length of apical and basal dendritic compartments of WT and MEF2C KO L2/3 neurons.

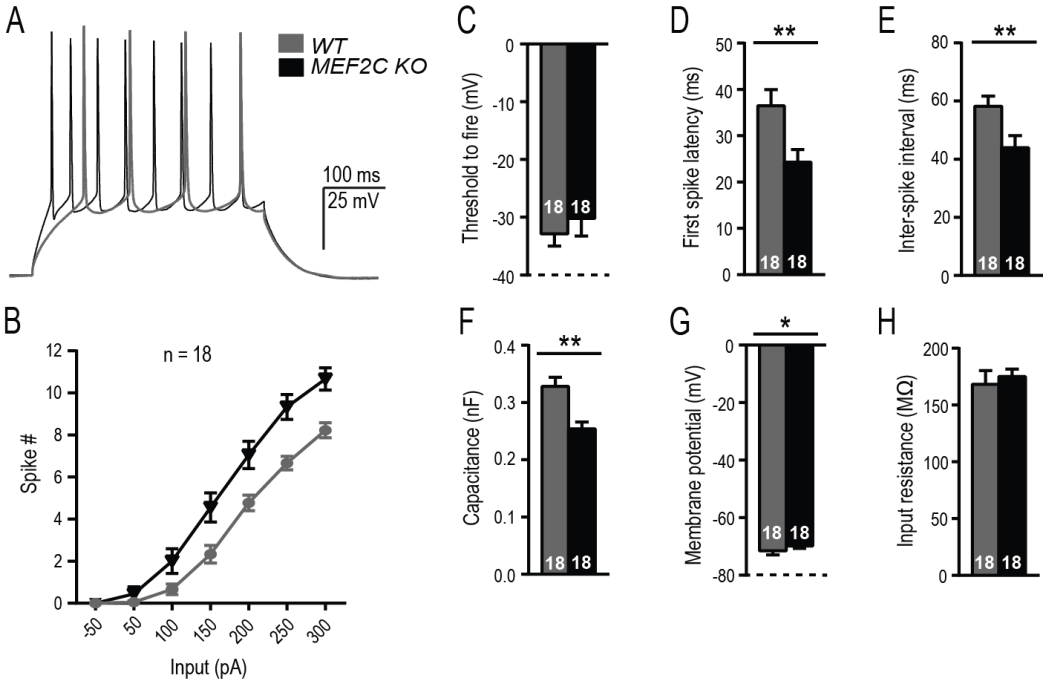

Figure 2.14: L2/3 neurons with *Mef2c* deletion are hyperexcitable. (A) Example traces of burst action potential firing patterns in WT and MEF2C KO L2/3 pyramidal neurons in response to a depolarizing 250-pA current injection. **(B)** Averaged input/output curves of the number of action potentials in response to increasingly depolarizing current injections in 50-pA increments. Averaged firing threshold potentials **(C)**, first-spike latency **(D)**, inter-spike intervals between the second and third action potentials fired to account for firing adaption **(E)**, capacitance **(F)**, resting membrane potential **(G),** and input resistance **(H)** measure from WT and MEF2C KO neurons in response to a depolarizing 250-pA current injection. All graphs represent data simultaneously collected from WT and MEF2C KO L2/3 neuron pairs in 4 mM $CaCl_2$ and 4 mM $MgCl_2$. Statistics: **B**, 2-way ANOVA with repeated measures for both cell genotype and current injection; **C-H**, paired t-test. P < .0.05*, < 0.01**, < 0.001***, < 0.0001****.

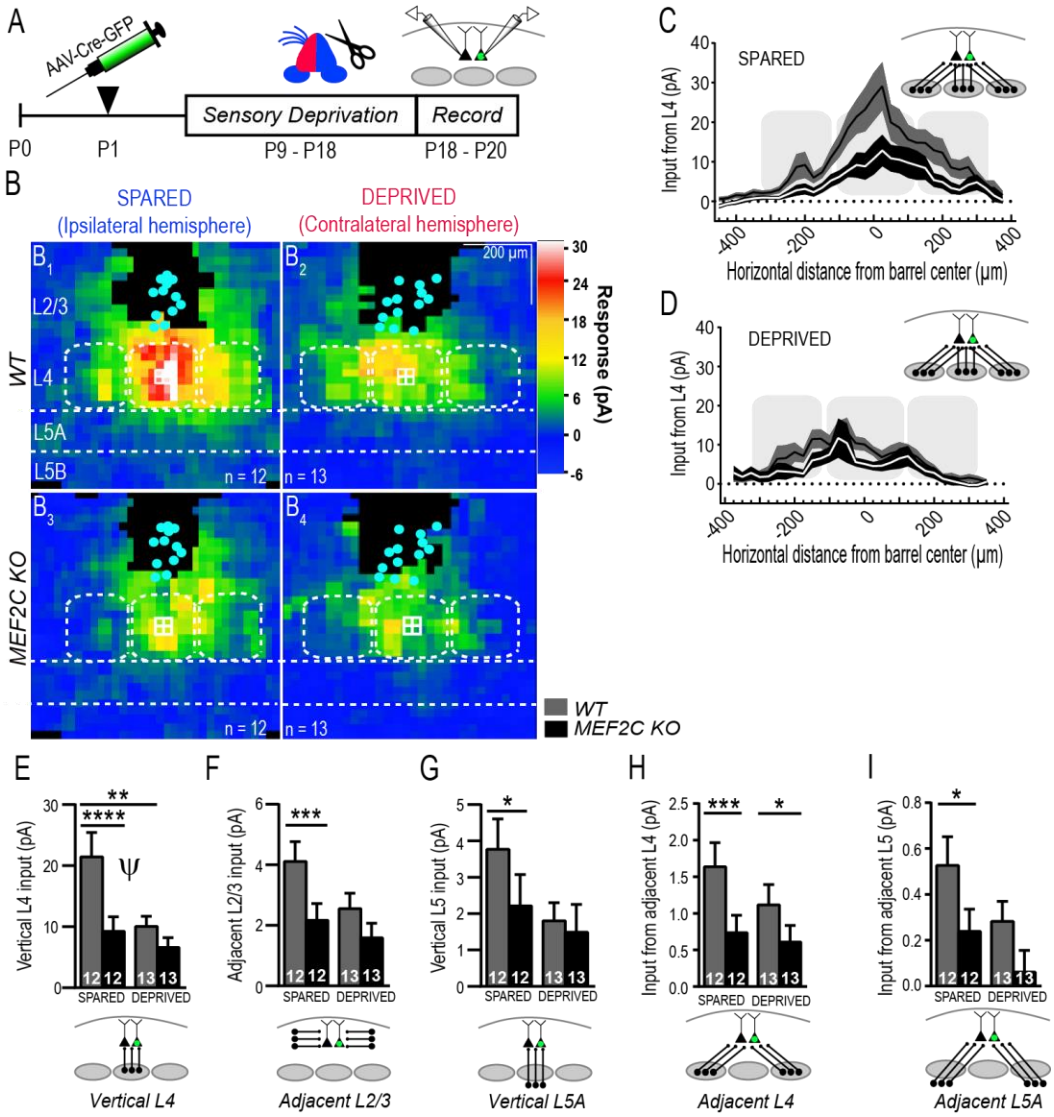

Figure 2.15: *Mef2c* and sensory experience interact to promote excitatory synaptic inputs onto L2/3 neurons at specific local input pathways. (A) Timeline of whisker trimming and recording. **(B)** Averaged LSPS maps of spared WT **(B_1)**, spared MEF2C **KO (B_2)**, deprived WT **(B_3)**, and deprived MEF2C-KO **(B_4)**. Horizontal synaptic profiles of L4 → L2/3 input onto WT and MEF2C KO L2/3 neurons in spared **(C)** and deprived **(D)** hemispheres. Average LSPS-evoked synaptic input onto WT and MEF2C KO L2/3 neurons at vertical L4 → L2/3 **(E)**, horizontal L2/3 → L2/3 **(F)**, vertical L5A → L2/3

(G), adjacent L4 → L2/3 **(H)**, and adjacent L5A → L2/3 **(I) p**athways. $p < 0.05$*, 0.01**, 0.001***, 0.0001****. 2-way ANOVA interaction; $p < 0.05$ (Ψ).

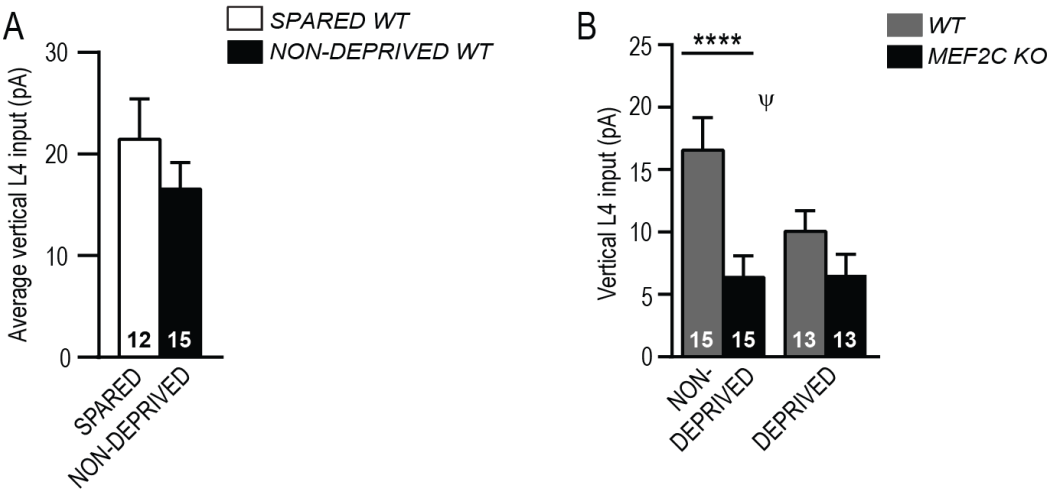

Figure 2.16: Sensory experience and *Mef2c* interact to strengthen L4 → L2/3 synaptic inputs. (A) Averaged LSPS-evoked vertical L4 → L2/3 inputs onto WT neurons in spared and non-deprived barrel cortices is similar. Inputs onto "spared" L2/3 neurons were recorded from barrel cortices ipsilateral to whisker trimming (replotted from Fig. 3E). "Non-deprived" L2/3 neurons were recorded from barrel cortices in non-trimmed mice (replotted from Fig. 1K). **(B)** MEF2C and sensory experience interact in a common cellular pathway to promote vertical L4 input onto L2/3 neurons in non-trimmed and deprived *Mef2c*$^{fl/fl}$ mice. Averaged vertical L4 input onto WT and MEF2C KO L2/3 neuron pairs in deprived barrel cortex (replotted from Fig. 3E) and non-deprived barrel cortex (replotted from Fig. 1K). Deprived barrel cortices are the contralateral (left) barrel cortex of whisker trimming on the right facial pad. Non-deprived barrel cortices refer to barrel cortices within mice not subjected to whisker trimming. $p < 0.05$*, < 0.01**, < 0.001***, < 0.0001****. 2 way ANOVA; interaction, $p < 0.05$ (Ψ).

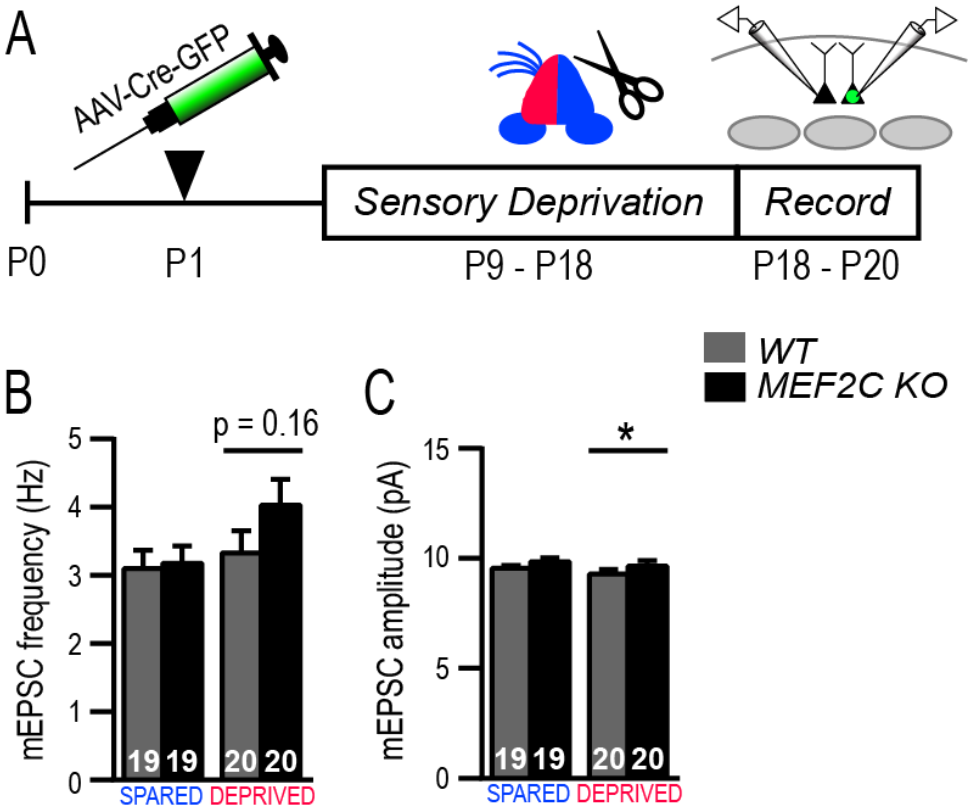

Figure 2.17: *Mef2c* deletion and sensory deprivation do not interact to regulate excitatory spontaneous synaptic transmission onto neocortical L2/3 neurons. (A) Experimental timeline depicting unilateral whisker trimming and recording paradigms. Red hemisphere denotes the deprived barrel cortex contralateral to whisker trimming (scissors). Blue hemisphere represents spared barrel cortex ipsilateral to whisker trimming, which receives input from intact whiskers. Miniature EPSC frequency **(B)** and amplitude **(C)** recorded from WT and MEF2 KO L2/3 neuron pairs in either spared or deprived barrel cortices. Statistics: 2-way ANOVA with repeated measures for genotype only. $p < 0.05$*

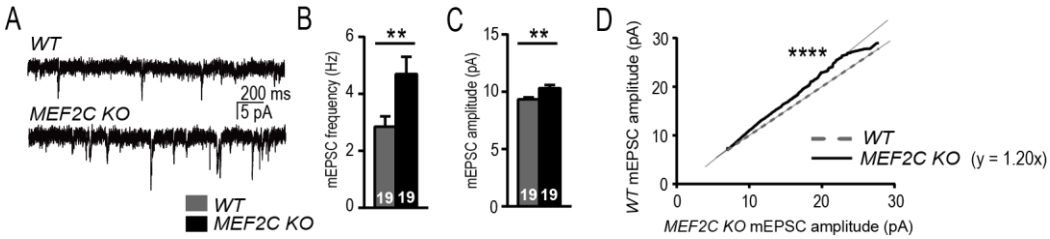

Figure 2.18: Postsynaptic *Mef2c* deletion increases excitatory spontaneous synaptic transmission onto L2/3 neurons. (A) Example mEPSCs recorded simultaneously from WT and MEF2C KO L2/3 neurons. Average mEPSC frequency **(B)** and amplitude **(C). (D)** Rank-order plot of mEPSC amplitudes plotted against WT mEPSC amplitude (slope = 1x, dashed gray line). Inset equation (y = 1.20x, solid line) represents slope increase of event size of MEF2C KO neurons compared to WT. Statistics: **B**, **C**, paired t-test; **D**, Kolmogorov-Smirnov test. $p < 0.05$*, < 0.01**, < 0.001***, < 0.0001****.

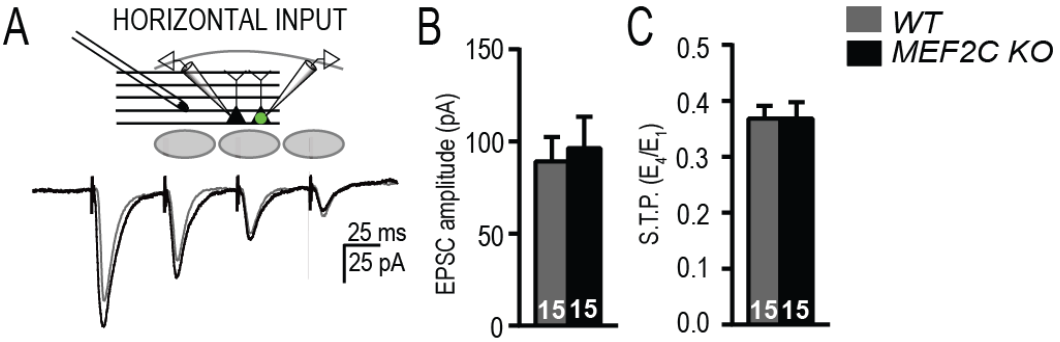

Figure 2.19: Horizontal inputs onto *Mef2c*-deleted L2/3 neurons are normal. (A) Top: Schematic of recording and electrical stimulation configuration of horizontally projecting axon pathways in L2/3. Bottom: Representative EPSCs recorded from WT and MEF2C KO L2/3 neuron pairs in response to stimulation of horizontal L2/3 pathways. Average evoked EPSC amplitude **(B)** and STP **(C)**. Statistics: **B**, **C**, paired t-test. $p < 0.05$*, < 0.01**, < 0.001***, < 0.0001****.

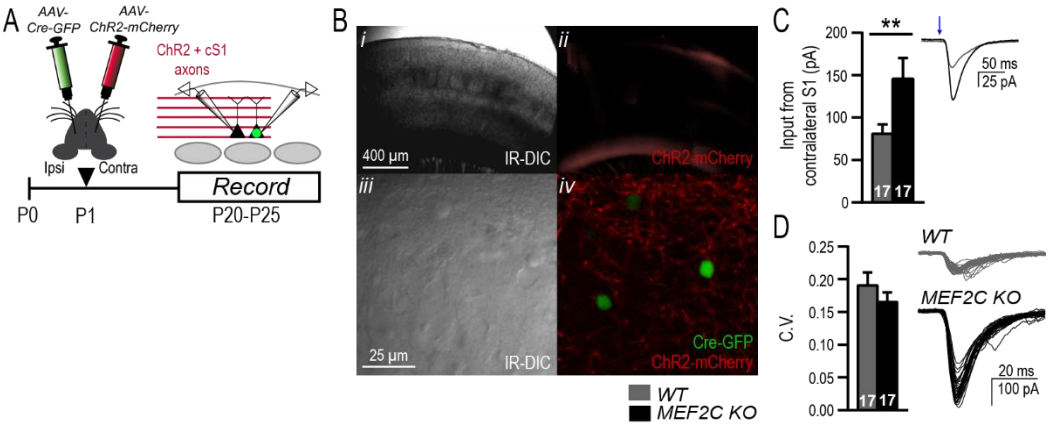

Figure 2.20: Postnatal and postsynaptic *Mef2c* deletion potentiates long-range intercortical inputs from the contralateral barrel cortex onto neocortical L2/3 neurons. (A) Timeline and schematic of ChR2-evoked stimulation of cS1 input. **(B**) Images of IR-DIC (i, iii) and ChR2-mCherry expression (ii, iv) in barrel cortex. **(C)** Average light-evoked EPSC amplitude of cS1 input onto WT and MEF2C KO L2/3 neurons. Inset: Averaged traces of light-evoked EPSCs from WT and MEF2C KO L2/3 neurons. **(D)** C.V. of evoked ChR2-EPSCs of cS1 inputs onto WT and MEF2C KO L2/3 pyramidal neurons. Inset: Example traces of light-evoked ChR2-EPSCs from WT and MEF2C KO L2/3 neurons. Statistics: **C**, **D**, paired t-test. $p < 0.05$*, < 0.01**.

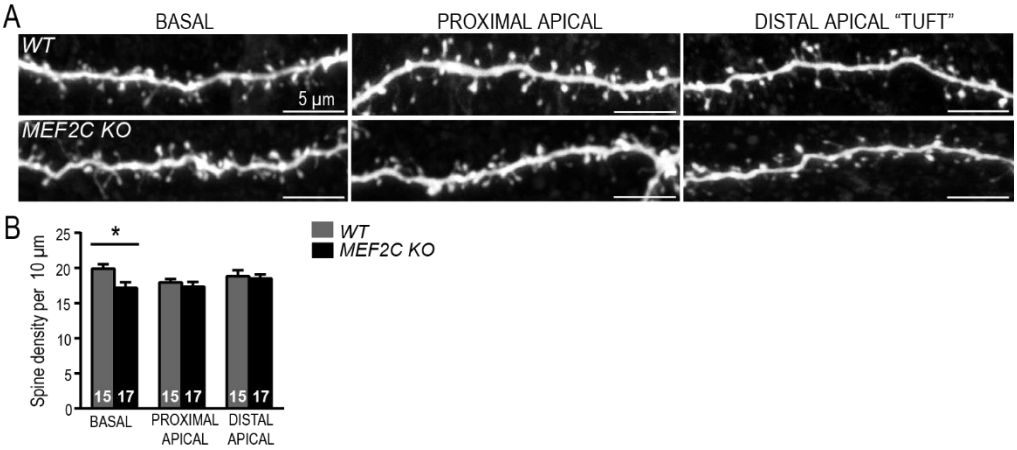

Figure 2.21: Postnatal *Mef2c* deletion decreases structural excitatory synapse number within L2/3 basal but not apical dendritic compartments. (A) Representative images of spines within basal, proximal apical, and distal apical dendritic compartments of WT and MEF2C KO L2/3 neurons. **(B)** Mean spine density in basal, proximal apical, and distal apical compartments. $p < 0.05$*.

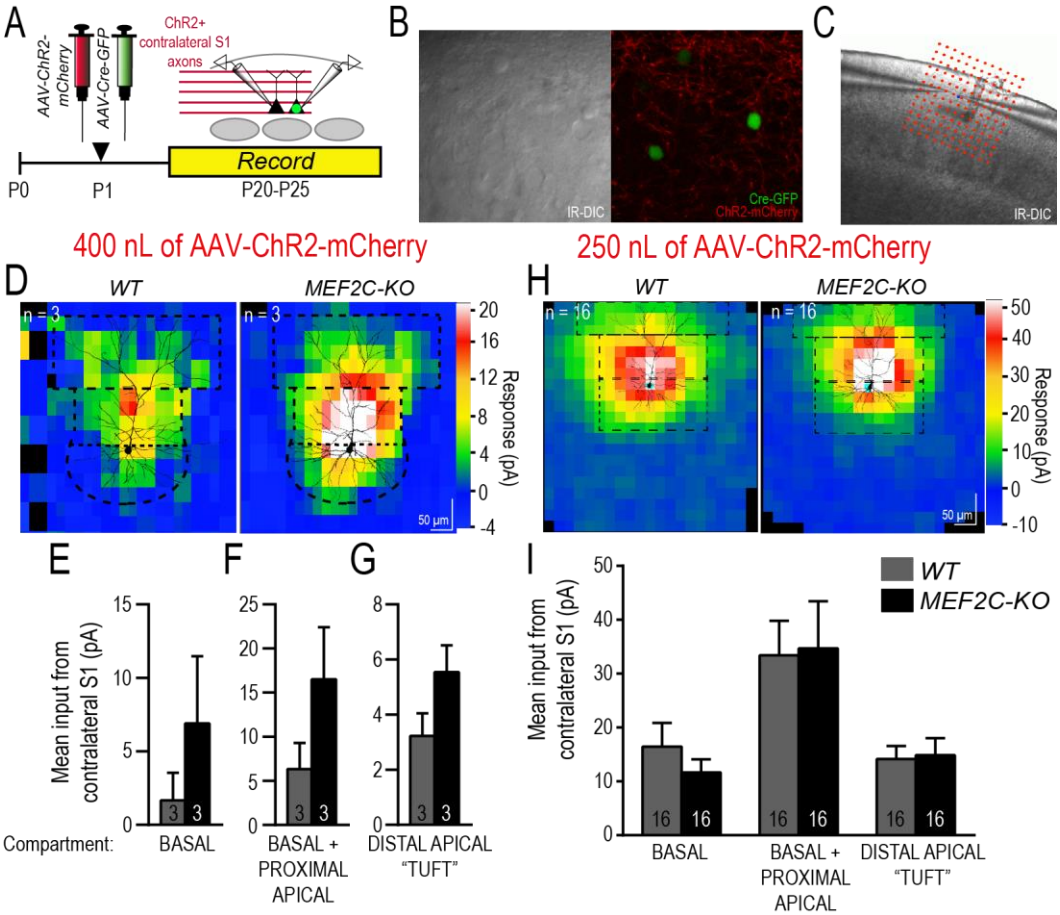

Figure 2.22: Compartment- and/or input-specific regulation of distal cortical inputs onto L2/3 pyramidal neurons remains to be determined. (A) Timeline and schematic of ChR2-evoked stimulation of cS1 input. **(B**) Images of IR-DIC (Left) and ChR2-mCherry expression (Right) in L2/3 of barrel cortex. **(C)** DIC image (4x) of an acutely prepared brain slice during simultaneous sCRACM of WT and MEF2C KO L2/3 neurons with superimposed stimulation grid. **(D)** Average sCRACM maps of ChR2-evoked EPSCs recorded from WT and MEF2C KO neurons within mice that were injected with 400 nL of AAVChR2-mCherry. Dashed lines indicate the analysis regions for basal, proximal apical + basal, and distal apical dendritic compartments. All individual maps comprising the average map were aligned with respect to the soma. Example dendritic arbors were superimposed for crude visualization of dendrites in the maps; no sCRACM maps were ever actually linked to dendritic morphology. Quantification of ChR2-evoked EPSC

amplitude in basal **(E)**, proximal apical + basal **(F)**, and distal apical **(G)** dendritic compartments from sCRACM in **(D)**. **(H)** Average sCRACM maps of ChR2-evoked EPSCs recorded from WT and MEF2C KO neurons within mice that were injected with 250 nL of AAVChR2-mCherry. **(I)** Quantification of ChR2-evoked EPSC amplitude in basal, proximal apical + basal, and distal apical dendritic compartments from sCRACM in **(H)**.

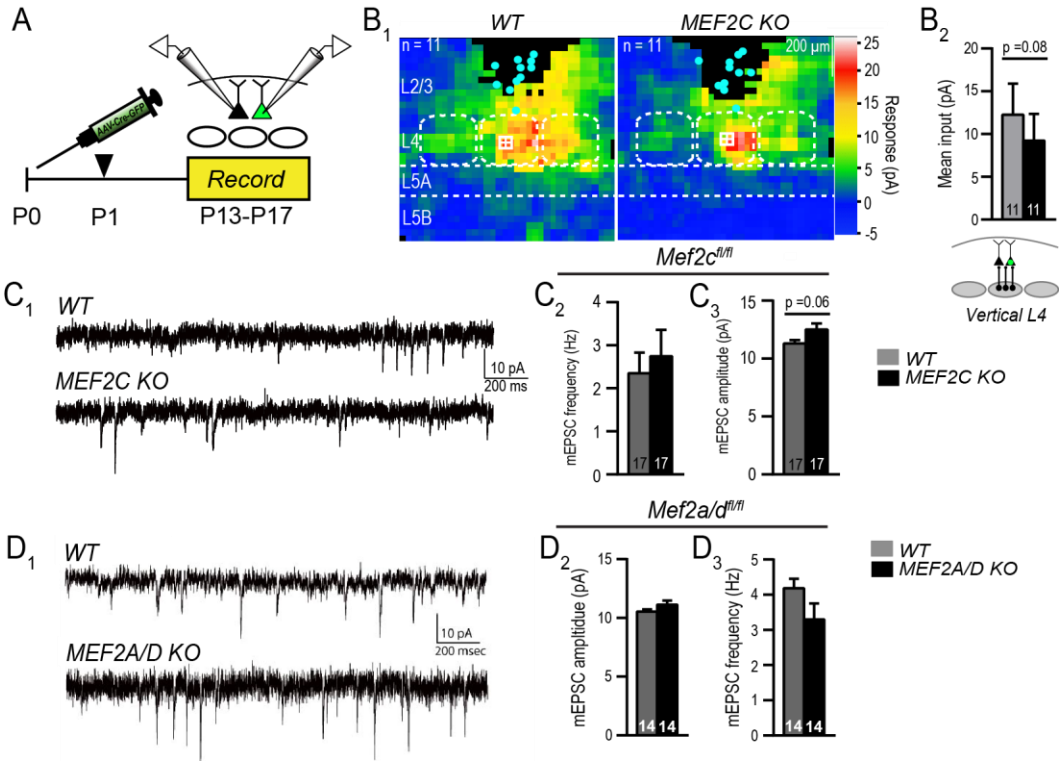

Figure 2.23: Sparse postnatal deletion of MEF2 genes do not affect excitatory synaptic transmission onto neocortical L2/3 pyramidal neurons at 2 weeks of age. **(A)** Experimental timeline and dual whole-cell recording paradigm. **(B_1)** Averaged maps of LSPS-evoked EPSCs onto WT and MEF2C KO L2/3 neurons. Maps are aligned to the "home" barrel center (white crosshair) and averaged. **(B_2)** Mean synaptic input onto WT and MEF2C KO neuron pairs in the vertical L4 → L2/3 input pathway from averaged LSPS responses of neurons shown in (B_1). Inset: Cartoon of L4 → L2/3 pathway within the barrel cortex. **(C_1)** Example traces of mEPSCs recorded simultaneously from WT and MEF2C KO L2/3 neurons. Averaged mEPSC frequency **(C_2)** and amplitude **(C_3)**. **(D_1)** Example traces of mEPSCs recorded simultaneously from WT and MEF2A/D KO L2/3 neurons. Averaged mEPSC amplitude **(D_2)** and frequency **(D_3)**. Statistics: paired t-tests for all panels. $p < 0.05$*.

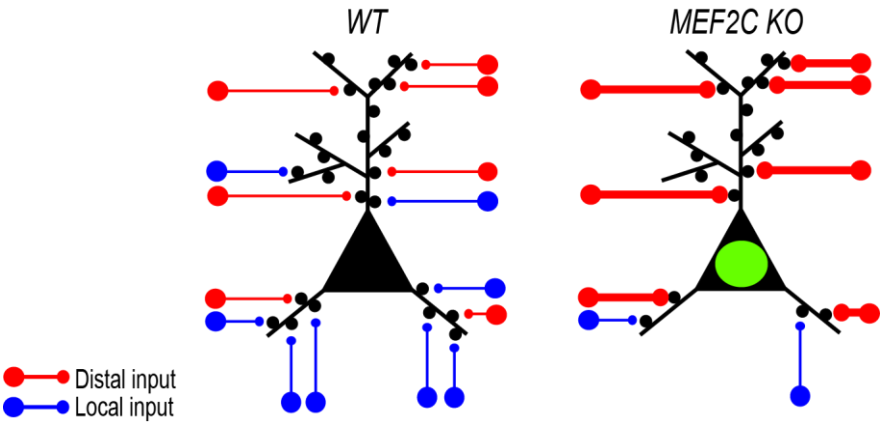

Figure 2.24: Circuit diagram of L2/3 pyramidal neurons summarizing the input pathway-specific consequences of *Mef2c* deletion. Postnatal, cell-autonomous *Mef2c* deletion reduces synaptic connections from local input pathways (blue). In contrast, long-range inputs (red) are potentiated as depicted by larger axon fibers and boutons. Although local inputs are known to synapse on both basal and apical dendritic compartments in L2/3 (Feldmeyer 2012a), only a decrease in dendritic spine density (black dots) on basal compartments was observed. Long-range inputs primarily target the L2/3 apical dendritic compartment.

Table 2.1: Additional Electrophysiological properties of AAV-Cre-GFP-infected and Uninfected L2/3 Neocortical L2/3 Pyramidal Neurons

Neuron genotype	AAV-Cre-GFP	R_{input} (MΩ)	Resting V_m[#] (mV)
Mef2c$^{fl/fl}$	-	180.6 ± 11.43 (24)	-69.06 ± 0.73 (18)
	+	184.7 ± 11.99 (24)	-66.49 ± 0.82* (18)
Mef2c$^{fl/+}$	-	170.2 ± 13.08 (18)	-69.33 ± 1.45 (12)
	+	170.9 ± 11.10 (18)	-71.67 ± 0.74 (12)
Mef2a^{flfl};*Mef2d*$^{fl/fl}$	-	168.7 ± 10.81 (19)	-69.00 ± 0.72 (19)
	+	197.7 ± 30.54 (19)	-67.37 ± 0.85 (19)

[#]not corrected for junction potential; *$p < 0.05$, paired t-test; number of cells indicated in parentheses

CHAPTER THREE

MEF2C REGULATES CORTICAL INHIBITORY SYNAPSES AND BEHAVIORS RELEVANT TO NEURODEVELOPMENTAL DISORDERS

Summary

Numerous genetic variants associated with *MEF2C* are linked to risk for autism, intellectual disability (ID) and schizophrenia (SCZ), and MEF2C is highly expressed in developing and mature cortical neurons. However, its role in cortical development remains unclear. I show here that conditional embryonic deletion of *Mef2c* in excitatory forebrain neurons causes functional synaptic abnormalities involving a differential regulation of inhibitory and excitatory synaptic transmission. This work was performed as a collaborative effort with Adam J. Harrington, Christopher W. Cowan, and others; currently these results are in preparation for publication. Here, the collaborators (A.J.H., C.W.C.) demonstrate that mice lacking *Mef2c* in excitatory neural networks exhibit numerous abnormal behavioral phenotypes with potential relevance to multiple human neurodevelopmental disorders, including autism and SCZ, and that the synaptic deficiencies that I identified may underlie these behavioral abnormalities. These behavioral phenotypes are correlated with a dramatic reduction in cortical network activity *in vivo*, due in part to a dramatic increase in GABAergic synapse density. I show here that MEF2C suppresses inhibitory GABAergic synaptic function to promote excitation of neocortical networks during early cortical development and will discuss the phenotypic differences observed when *Mef2c* is deleted in a sparse neural population versus large neural networks.

Introduction

Imbalance of excitatory and inhibitory synaptic transmission in the brain is an emerging theory of the pathophysiology of multiple neurodevelopmental and neuropsychiatric disorders (Garber 2007, Zoghbi 2003), including autism and SCZ. However, the genes and molecules that regulate the number of excitatory and inhibitory synapses formed and maintained on neurons remain poorly understood.

The MEF2 transcription factor genes are expressed in both excitatory and inhibitory neurons throughout development and adulthood in overlapping, but unique, expression patterns (Lyons et al 2012a, McKinsey et al 2002, Shalizi & Bonni 2005), and they have been shown to regulate excitatory synapse density on multiple neuron types (Barbosa et al 2008, Flavell et al 2006, Li et al 2008, Pulipparacharuvil et al 2008b). For example, MEF2A and MEF2D can regulate activity-dependent elimination of glutamatergic synapses on both hippocampal pyramidal neurons and medium spiny neurons of the striatum in a cell-autonomous manner (Flavell et al 2006, Pulipparacharuvil et al 2008b). Expression of a constitutively-active form of MEF2C (MEF2C-VP16) promotes excitatory synapse elimination in hippocampal pyramidal neurons in a complex process that requires the RNA-binding protein, Fragile X mental retardation protein (FMRP) (Flavell et al 2006, Pfeiffer et al 2010b, Tsai et al 2012, Wilkerson et al 2014).

Brain-wide deletion of *Mef2c* was reported to cause an increase in dendritic spine density on dentate granule neurons of the hippocampal dentate gyrus (Barbosa et al 2008), whereas another group reported that *Mef2c* deletion in embryonic neural stem cells (nestin-cre), caused deficits in cortical neuron migration and excitatory synaptic transmission in a subset of animals (Li et al 2008). Recent genetic studies have linked human *MEF2C* to a syndromic form of intellectual disability with autistic features, and single-nucleotide

polymorphisms (SNPs) near *MEF2C* produce significant risk for SCZ (Cardoso et al 2009, Engels et al 2009, Le Meur et al 2010, Mikhail et al 2011, Novara et al 2010, Paciorkowski et al 2013b). However, the cellular functions of MEF2C that underlie its role in these neurodevelopmental disorders, and the role(s) of MEF2C in cortical synapse development remain unclear. In the central nervous system, MEF2C is highly expressed very early in brain development (~E11.5), and its expression is enriched in differentiated forebrain neurons within the neocortex and dentate gyrus (Leifer et al 1993, Leifer et al 1997, Lyons et al 1995b). Here, I sought to evaluate the role of MEF2C in differentiated cortical excitatory neurons, and to determine whether loss of MEF2C function in expansive excitatory neuronal populations might produce synaptic phenotypes potentially associated with neurodevelopmental disorders.

Materials and methods

Animals:

Mice were group housed (2-5 mice/cage; unless specified) with same-sex littermates on a 12 hour light-dark cycle with access to food and water ad libitum. *Mef2c*$^{fl/fl}$ and *Emx1*$^{Cre/+}$ knock-in mice are described previously (Arnold et al 2007b, Iwasato et al 2008), and were maintained on a mixed SVeV-129/C57BL/6J background strain. Experimental mice (*Mef2c*$^{fl/fl}$*; Emx1*$^{Cre/+}$) were compared to Cre-negative littermates (*Mef2c*$^{fl/fl}$). Experimenters were blind to genotype during data acquisition and analysis. All procedures were conducted in accordance with the Institutional Animal Care and Use Committee (IACUC) and National Institute of Health guidelines.

Brain slice preparation and electrophysiology:

Acute neocortical slices of somatosensory, or "barrel" cortex, were prepared from male or female *Mef2c*$^{fl/fl}$ or *Mef2c*$^{fl/fl}$*; Cre*^{Emx1} littermates from age P20-25 (3 week) and bred on a mixed SVeV-129/C57BL/6J background. Mice were anesthetized with an I.P. injection of Ketamine (125 mg/kg)/Xylazine (25 mg/kg) and the brain removed. Coronal slices, 250-300 μm thick, were prepared in partially frozen dissection buffer consisting of (in mM): 110 choline chloride, 2.5 KCl, 1.25 $Na_2H_2PO_4$, 25 $NaHCO_3$, 25 D-glucose, 3.1 Na pyruvate, 11.6 Na ascorbate, 1 kynurenate, 7 $MgCl_2$, and 0.5 $CaCl_2$, aerated with 95% O_2 and 5% CO_2 prior to and during the slicing procedure. Slices for some experiments were prepared in 4°C dissection buffer consisting of (in mM): 75 sucrose, 87 NaCl, 3 KCl, 1.25 NaH_2PO_4, 7 $MgSO_4$, 26 $NaHCO_3$, 20 dextrose, and 0.5 $CaCl_2$, aerated with 95% O_2 and 5% CO_2. All solutions were pH 7.4. Genotypic differences using these different dissection solutions were the same so the results were pooled. For experiments in animals aged ≥P21, the mice were transcardially perfused with dissection buffer containing 1 mM kynurenic acid. Slices were then transferred to a 300 mOsM artificial cerebrospinal fluid (ACSF) solution containing in mM: 125 NaCl, 2.5 KCl, 1.25 $Na_2H_2PO_4$, 25 $NaHCO_3$, 10 D-glucose, 1 kynurenic acid, 2 $MgCl_2$, and 2 $CaCl_2$, to recover at 35°C for 25 minutes, and then transferred to room temperature (~21° C) for 30 minutes prior to recording. Whole-cell recordings were performed in layer 2/3 neurons (resting V_m < -50mV, input resistance > 80 MΩ) centered above a barrel hollow, and cells were targeted with IR-DIC optics in an Olympus FV300 microscope. Recordings were performed at room temperature. Data were collected with a 10 kHz sampling rate and a 3 KHz Bessel filter.

Miniature excitatory postsynaptic currents (mEPSCs):

Miniature EPSCs were recorded in voltage clamp (at -70mV) in ACSF containing (in mM): 126 NaCl, 3 KCl, 1.25 NaH_2PO_4, 2 $MgSO_4$, 26 $NaHCO_3$, 25 dextrose, and 2 $CaCl_2$ with 1 µM tetrodotoxin (TTX), and 100 µM picrotoxin, to block mIPSCs. ACSF was aerated with 95% O_2 and 5% CO_2 and recycled. The internal solution contained in mM: 120 K-Gluconate, 5 NaCl, 10 HEPES, 1.1 EGTA, 4 MgATP, 0.4 Na_2GTP, 15 phosphocreatine, 2 $MgCl_2$, and 0.1 $CaCl_2$, pH 7.25 and 290 mOsm. The junction potential was ~10 mV and was not corrected.

Miniature inhibitory postsynaptic currents (mIPSCs):

Miniature IPSCs were recorded in voltage clamp (at -70 mV) using a high-chloride internal solution containing in mM: 79 K-gluconate, 44 KCl, 6 NaCl, 10 HEPES, 0.2 EGTA, 4 MgATP, 0.4 Na_2GTP, 15 phosphocreatine, 2 $MgCl_2$, and 0.1 $CaCl_2$, which results in inward mIPSCs. To pharmacologically isolate mIPSCs, the extracellular ACSF contained 1 µM TTX, 5 µM CPP (NMDA-receptor antagonist), and 20 µM DNQX (AMPA-receptor antagonist).

mPSC Analysis:

Miniature EPSCs and mIPSCs were analyzed using Mini Analysis (Synaptosoft) with the following parameters: amplitude threshold = 7 pA, area threshold = 10 pA. Events were automatically detected by the software, and non-events were then manually deleted upon visual inspection.

UP state recordings:

Persistent activity states or "UP" states were measured in acute neocortical slices obtained from P18-24 mice as previously described (Hays et al 2011). Briefly thalamocortical slices (400 µm) were perfused in ACSF containing (in mM) 126 NaCl, 3 KCl, 1.25 NaH_2PO_4, 26 NaHCO3, 2 $MgCl_2$, 2 $CaCl_2$, and 25 D-glucose for 1 hour at 32°C in an interface recording chamber, and then perfused for 45 minutes with the same ACSF supplemented with 5 mM KCl, 1 mM $MgCl_2$ and 1 mM $CaCl_2$, which mimics endogenous ionic concentrations. Spontaneously-generated UP-states were extracellularly recorded from layer 4 (L4) of the primary somatosensory cortex for 10 minutes using 0.5 MΩ tungsten microelectrodes, amplified 10,000-fold, sampled at 2.5 kHz, and filtered between 300 Hz and 5 kHz. All measurements were analyzed using custom Labview software. The beginning of an UP-state was defined as events in which the amplitude remained above threshold for at least 100 msec. The end of the UP-state was determined after the event amplitude decreased below threshold for >600 msec. Two events within 600 msec were defined as a single UP-state. All of the 20 slices prepared from $MEF2C^{fl/fl}$ mice displayed UP states, whereas only 9 of 18 slices from *Mef2c*$^{fl/fl}$*; Cre*^{Emx1} mice displayed UP states during a 10 minute recording session, perhaps reflecting the reduced excitability of the $MEF2C^{fl/fl}$; Cre^{Emx1} circuits. Therefore, UP state duration and amplitude was only measured in the 9 slices that expressed UP states.

Results:

Mef2c mRNA is enriched in the developing cortical plate, mature cortex and dentate gyrus (Leifer et al 1993). Immunostaining of mature brain slices with MEF2C-specific monoclonal antibodies revealed that >99% of the MEF2C-positive cells co-localized with the neuronal marker, NeuN (**Fig. 3.1A**), indicating that MEF2C expression

in the cortex is primarily restricted to neurons. To generate conditional gene disruption of *Mef2c* selectively in differentiated forebrain excitatory neurons, we bred homozygous floxed *Mef2c* mutant mice (Lin et al 1997) with mice heterozygous for Cre recombinase inserted into the endogenous *Emx1* gene (Iwasato et al 2008), which produces Cre in newly differentiated neurons, and in some glia, starting as early as embryonic day 11.5 (E11.5). The *MEF2C cKO* ($Mef2c^{fl/fl};Emx1^{Cre}/^{+}$) show selective and dramatic reduction of MEF2C protein levels throughout the cortex and hippocampus, but no reductions were observed in striatum or thalamus (**Fig. 3.1B**): Emx1-Cre-negative regions that express low levels of MEF2C.

Although *MEF2C cKO* mice did exhibit a slight decrease (~10%) in neocortical thickness compared to controls (**Fig. 3.1C**), A.J.H. and C.W.C. observed normal gross brain morphology and cortical layer organization in young adult *MEF2C cKO* mice, (**Fig. 3.1D**). However, during my electrophysiological recordings in the barrel cortex, I – as the experimenter – could not be blinded to the animal's genotype because *MEF2C cKO* mice did not have visibly distinguishable barrel columns when acute brain slices were visualized with IR-DIC optics, suggesting that *MEF2C cKO* mice do, in fact, have some developmental abnormalities of neocortical laminarization (data not shown). Such anatomical features of the *MEF2C cKO* brain slices could easily be overlooked with immunohistological imaging methods. Hence, *MEF2C cKO* mice likely have decreased neocortical thickness due to deficits in neural migration reported previously (Li et al 2008). Overall, *MEF2C cKO* offspring were viable and healthy, and their body weights, growth trajectories, and Mendelian frequency appear indistinguishable from their Cre-negative littermates (**Fig. 3.1E** and data not shown).

MEF2C regulates both excitatory and inhibitory synapses when deleted in developing excitatory neocortical neural networks

MEF2 transcriptional activity promotes excitatory synapse elimination in the hippocampus (Flavell et al 2006, Pfeiffer et al 2010b, Tsai et al 2012, Zang et al 2013), and *MEF2C cKO* DEGs showed significant enrichment for synapse-linked genes (unpublished data performed by A.J.H.; C.W.C). Therefore, I sought to test whether loss of *Mef2c* in the cortex alters cortical synaptic transmission *in vivo*. UP states are spontaneous, synchronous oscillations of neocortical networks that are driven by recurrent excitatory and inhibitory synaptic circuitry (Gibson et al 2008, Hays et al 2011), and they are employed to assess overall synaptic function and excitability of the neocortical network within the barrel fields of the primary somatosensory cortex (S1BF) in the *MEF2C cKO* mice. Surprisingly, I – along with Dr. Gemma Molinaro, PhD – observed large reductions in the frequency (~90% reduction) of spontaneous UP states in *ex vivo* slices from the S1BF of *MEF2C cKO* mice (**Fig. 3.2A**). In addition, the UP states in the *MEF2C cKO* mice were shorter in duration (~50%) and smaller in amplitude (~50%) (**Fig. 3.2A**). To further explore this decrease in neocortical circuit activity, I performed patch-clamp recordings of L2/3 pyramidal neurons from S1BF slices. In the *MEF2C cKO* slices, I detected small decreases in both the frequency and amplitude of mEPSCs (**Fig. 3.2B**), although the decrease in frequency did not quite reach statistical significance (p=0.07). Additionally, large increases in both the frequency and amplitude of mIPSCs (**Fig. 3.2C**) were observed. A.J.H. and C.W.C. report an increase in GABAergic synapse number and concomitant decrease in dendritic spine density in cultured dissociated neocortical neurons (**Fig. 3.3A-B**). Additionally, dendritic complexity is normal in cultured neocortical *MEF2C cKO* neurons *in vitro* (**Fig. 3.3C**).

Immunostained GABAergic synaptic co-clusters are normally distributed in cultured neocortical MEF2C cKO neurons (**Fig. 3.3D-F**).

To determine the developmental effects of network *Mef2c* deletion on both excitation and inhibition, I recorded mEPSCs and mIPSCs in L2/3 pyramidal neurons during the second postnatal week. Miniature EPSC frequency was unchanged at this developmental age, while mEPSC amplitude was slightly increased (**Fig. 3.4A-B**). Both mIPSC frequency and amplitude was increased (**Fig. 3.4C-D**), suggesting that network *Mef2c* deletion increases inhibitory synaptic transmission prior to decreasing excitatory synapse number. However, the increase in mEPSC amplitude at this age demonstrates that both excitation and inhibition are regulated simultaneously by MEF2C developing cortical synapses.

Together, these findings indicate that the embryonic loss of MEF2C in cortical excitatory neurons results in a small reduction of structural and functional glutamatergic synapse number and a large increase in inhibitory synapse number – the combination of which likely contributes to the dramatic reduction in cortical network activity as detected by spontaneous UP states.

MEF2C cKO mice display behaviors reminiscent of human autism, ID and SCZ

In humans, impairments in communication and social interactions are common symptom domains of autism and SCZ. *MEF2C cKO* mice displayed dramatic abnormalities in a putative form of oral social communication in mice – ultrasonic vocalizations (USVs) produced by a young adult male mouse when placed in the presence of a female in estrous or upon young pup separation from its mother (**Fig. 3.5A-C**) (Ey et al 2013, Hanson &

Hurley 2012). In the presence of a sexually-receptive female, *MEF2C cKO* males generated many fewer USV calls in comparison to WT littermates (~70% reduction, **Fig. 3.5A**). In contrast, *MEF2C cKO* mice produced a ~5-fold increase in unstructured USVs, and a corresponding decrease in complex, but not simple, USVs (**Fig. 3.5B**). Similar to the adults, *MEF2C cKO* mice at postnatal days 4-10 produced significantly fewer USVs upon separation from the mother (distress calls) (**Fig. 3.5C**). Together these data indicate that *MEF2C cKO* mice produce significantly fewer USVs in a species-specific form of putative oral communication.

In a social interaction test, the WT littermates spent significantly more time interacting with an unfamiliar mouse than an empty chamber (**Fig. 3.5D**). The *MEF2C cKO* mice also spend more time interacting with the social animal vs. the empty chamber, but the *MEF2C cKO* mice spent significantly less time interacting with the social animal than the control mice (**Fig. 3.5D**). The reduction in social interaction did not appear to be due to deficits in olfactory recognition of social animals or basic novelty detection, since *MEF2C cKO* mice showed a strong preference to interact with a social-related smell from an unfamiliar mouse (**Fig. 3.5E**). In addition to social interaction deficits, *MEF2C cKO* mice showed significant reductions in another social-related behavior, nest building (Fig. 3.4F) (Deacon 2006a, Etherton et al 2009, Kwon et al 2006).

Deficits in brain reward function have been proposed to contribute to some autistic behaviors, including social interaction (Dichter et al 2012, Insel 2003). Autism is characterized by restricted or repetitive patterns of behavior, interests or activities (American Psychiatric Association 2013). Additionally, intellectual disability is also a common associated symptom of autism (American Psychiatric Association 2013), and

cognitive deficits comprise one of the three major symptom domains in SCZ. A battery of additional behavioral assays were performed to measure MEF2C cKO behaviors associated with hedonic pleasure-seeking, stereotypy, learning and memory, and hyperactivity (unpublished data; A.J.H., C.W.C.).

In humans, *MEF2C* haploinsufficiency appears to be sufficient, at least in reported individuals, to produce this complex and severe neurodevelopmental disorder. Generally consistent with previous reports (Barbosa et al 2008, Li et al 2008), our preliminary studies indicate that loss of one gene copy of *Mef2c* (*Mef2c*$^{fl/+}$*;Emx1*^{Cre}/$^{+}$) in the Emx1-cell lineage produces mice with behaviors indistinguishable from their Cre-negative WT controls (A.J.H. and C.W.C., unpublished observations).

Together these findings suggest that embryonic loss of MEF2C in excitatory forebrain neurons causes significant deficits in learning and memory, multiple social behaviors, socially-motivated ultrasonic vocalizations, and reward-related behavior. *MEF2C cKOs* also show significant increases in repetitive motor behaviors and overall hyperactivity – all symptom domains with potential relevance to human neurodevelopmental disorders such as autism, ID and SCZ.

Discussion:

Here I have identified a role for MEF2C in regulating both excitatory and inhibitory spontaneous synaptic transmission in neocortical L2/3 pyramidal neurons within the mouse barrel cortex when *Mef2c* is deleted in excitatory neocortical neuron populations during embryonic development *in vivo*. My data suggest that MEF2C suppresses inhibitory synaptic transmission while promoting excitatory synaptic transmission, and these findings are supported by those of A.J.H. and C.W.C. where cultured neocortical *MEF2C cKO*

neurons display a ~2-fold increase in GABAergic synapse density and ~50% reduction of dendritic spines: structural correlates of excitatory synapses. These synaptic alterations ultimately decrease network synchrony and excitation as demonstrated by the dramatic reduction in UP states. Furthermore, the decreased excitatory neocortical network activity is associated with behaviors associated with neurodevelopmental disorders such as autism.

In humans, *MEF2C* haploinsufficiency appears to be sufficient, at least in reported individuals, to produce this complex and severe neurodevelopmental disorder. Generally consistent with previous reports (Barbosa et al 2008, Li et al 2008), these preliminary studies indicate that loss of one gene copy of *Mef2c* ($Mef2c^{fl/+};Emx1^{Cre}/^{+}$) in the Emx1-cell lineage produces mice with behaviors indistinguishable from their Cre-negative WT controls (A.J.H. and C.W.C., unpublished observations).

These observations suggest that human *MEF2C* haploinsufficiency symptoms are a result of its loss of function in non-forebrain excitatory cell populations or that, in humans, there are other factors that influence disease penetrance and severity, including unique or sensitized functions for MEF2C through human evolution, human-specific genetic modifiers and/or environmental influences that increase symptom penetrance. Nonetheless, these findings here indicate that MEF2C plays an essential role in early cortical synaptic development, and that reduction in MEF2C function in forebrain excitatory neurons produces animals with numerous behaviors potentially relevant to intellectual and developmental disorders.

Schizophrenia is a debilitating mental illness with neurodevelopmental origins that affects nearly 1% of the world's population, and there is significant overlap in risk genes for ASDs and SCZ. In contrast to ASDs, human postmortem brain analysis of SCZ brains

revealed a thinning of the cortex, a decrease in dendritic spine density, and hypofunction of excitatory synaptic transmission is a leading hypothesis for the pathophysiology of SCZ (Coyle et al 2016). Recently, 108 genomic loci were identified by SNP meta-analysis as conferring significant risk for SCZ, and *MEF2C* was identified as a candidate risk gene (Schizophrenia Working Group of the Psychiatric Genomics 2014). *MEF2C cKO* mice exhibited a thinning of the cortex, a decrease in dendritic spine density of *MEF2C cKO* cortical neurons, and behavioral phenotypes that are reminiscent of cognitive and negative symptoms of SCZ (*e.g*. reduced sociability and poverty of speech). While the potential relevance of *MEF2C cKO* phenotypes to the pathophysiology and symptoms of ASDs, ID and/or SCZ is not clear, these findings reveal an essential role for MEF2C in cortical neuron development and typical animal behaviors (A.J.H. and C.W.C.).

Previous studies have demonstrated an important role for MEF2A and MEF2D in the process of activity-dependent excitatory synapse elimination in hippocampal neurons (Flavell et al 2006, Pfeiffer et al 2010b, Tsai et al 2012). However, similar to a previous report (Li et al 2008), we found that loss of MEF2C produced a *decrease* in cortical excitatory synaptic transmission, suggesting that MEF2C is a positive regulator of excitatory synapses in cortical neurons.

Loss of MEF2C in forebrain neurons produces an *increase* in structural and functional excitatory synapses formed onto hippocampal dentate granule neurons (DG) (Adachi et al 2015, Barbosa et al 2008), suggesting that MEF2C might have cell-type specific functions or that the increase in DG excitatory synaptic transmission is an indirect, homeostatic effect of decreased cortical stimulation of DG neurons. In the future, cell autonomous manipulations of the DG neurons will be important to resolve this question.

Also, postnatal *Mef2c* gene deletion in forebrain excitatory neurons did not alter social or repetitive behaviors in the *Mef2c* mutant mice, despite the increase in DG dendritic spine density (Adachi et al 2015), suggesting a dissociation of hippocampal DG spine density and postnatal MEF2C deletion from several ASD-related behaviors. As such, the role(s) for MEF2C in embryonic and/or early postnatal forebrain development might be more critical for producing the behavioral phenotypes observed in our *MEF2C cKO* mice.

Imbalances in excitatory and inhibitory synaptic transmission are proposed to underlie many neuropsychiatric disorders, including ASDs (Cellot & Cherubini 2014, Rubenstein 2010) and SCZ (Coyle et al 2016). Genetic analyses of patients affected by these disorders revealed mutations in many synapse-related genes (Garber 2007, McCarthy et al 2014). In mice, *increased* excitatory synaptic function has been reported in several mouse ASD models, including mutant mice lacking *Fmr1*, *Pten*, and *Tsc1/2* genes (Bateup et al 2013, Gibson et al 2008, Williams et al 2015). In contrast, only a few prior studies have examined the role of altered inhibitory synapse function in ASD-related behaviors. For example, mice containing a human disease mutation in the *Nlgn3* gene (*Nlgn3 R451C*) displayed an increase in inhibitory synaptic transmission and several autism-associated behaviors (Tabuchi et al 2007), suggesting that altered E/I balance in either direction can produce behavioral phenotypes with potential relevance to neurodevelopmental disorders.

In summary, I show here that *Mef2c* is required for proper synapse development on excitatory forebrain neurons, and that its embryonic loss in excitatory forebrain neuron populations causes a shift in the functional synaptic E/I balance in L2/3 pyramidal neurons of the mouse barrel cortex. My findings are supported by those of A.J.H. and C.W.C. which demonstrate that MEF2C cKO mice exhibit behavior phenotypes reminiscent of

multiple neurodevelopmental disorders, including autism and intellectual disability. Overall, MEF2C plays a critical role in embryonic cortical development, where its loss of function during embryogenesis causes robust and persistent synaptic deficits throughout expansive neural networks.

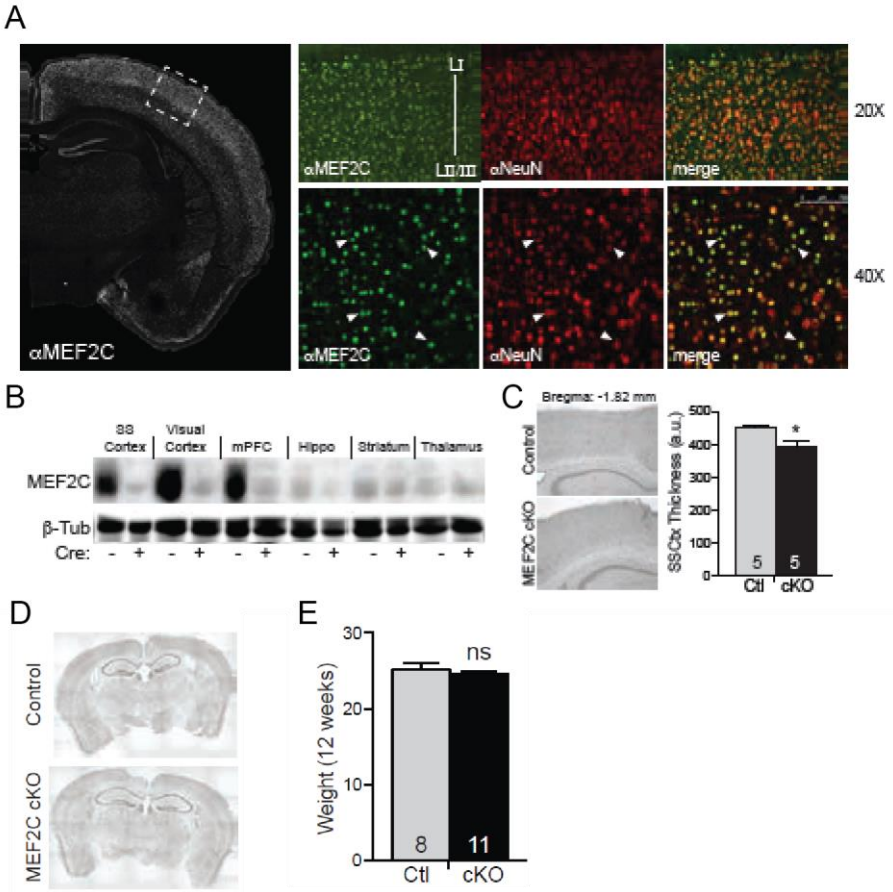

Figure 3.1: Generation of *MEF2C cKO* mice. (A) MEF2C protein (green) is enriched in NeuN-positive cortical neurons (red). **(B)** Western blot of MEF2C in various brain regions. **(C)** Somatosensory cortical thickness was slightly reduced in *MEF2C cKO* brains (~10%) compared to control littermates. Thickness was averaged over 4 slices/brain from 5 brains per genotype. **(D**) Nissl staining of adult control and *MEF2C cKO* brains show no gross morphological changes in the brain. **(E)** There was no difference in body weight between *MEF2C cKO* mice and control littermates during behavioral testing (12 weeks). Data are represented as mean ± SEM. Statistical significance was determined by unpaired t-test. *$p<0.05$, ns=not significant.

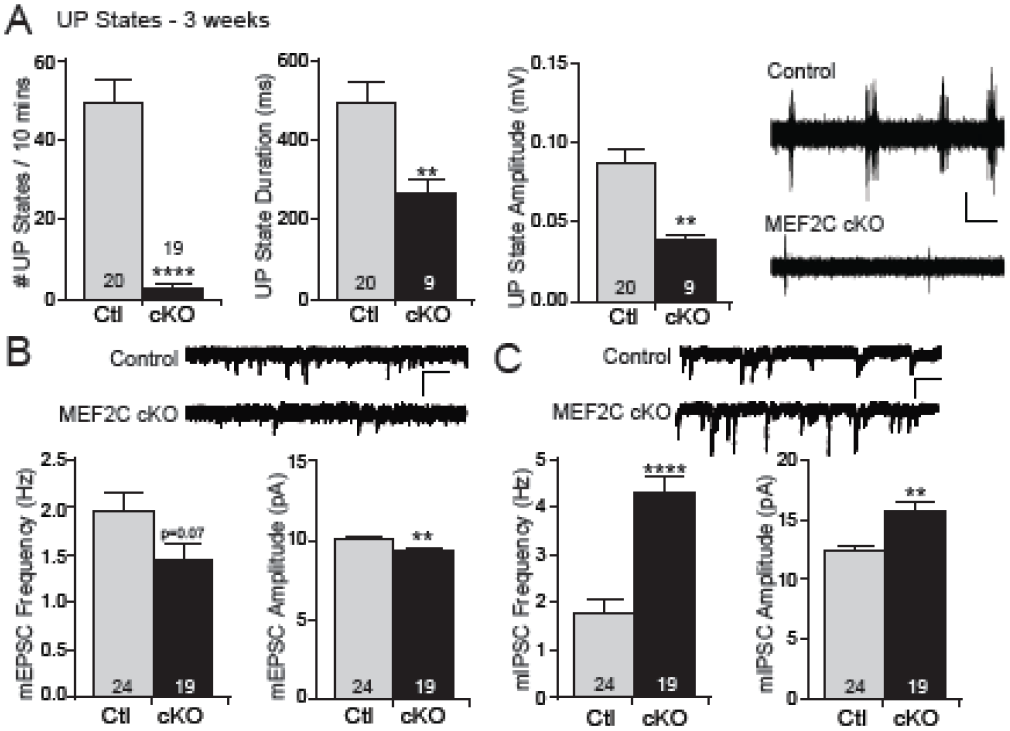

Figure 3.2: Increased cortical inhibition in *MEF2C cKO* mice. (A) UP states in 3-week old *MEF2C cKO* mice. *MEF2C cKO* mice have fewer spontaneous UP states than control mice. Additionally, the duration and amplitude of each spontaneous UP state was significantly reduced in the *MEF2C cKO* mice. Representative recordings from control and *MEF2C cKO* organotypic slices. Scale bar = 50 µV, 1 sec. **(B)** *MEF2C cKO* mice have reduced mEPSC frequency and amplitude in cortical layer 2/3 pyramidal neurons from 3-week old mice. Scale bar = 200 ms, 10 pA. **(C)** *MEF2C cKO* mice have increased mIPSC frequency and amplitude in cortical layer 2/3 pyramidal neurons from 3-week old mice. Scale bar = 200 ms, 10 pA. Data are represented as mean ± SEM. Statistical significance was determined by unpaired t-test using GraphPad Prism. *$p<0.05$, **$p<0.01$, ****$p<0.0001$. Numbers of slices/neurons (n) are reported in each bar for respective experiment.

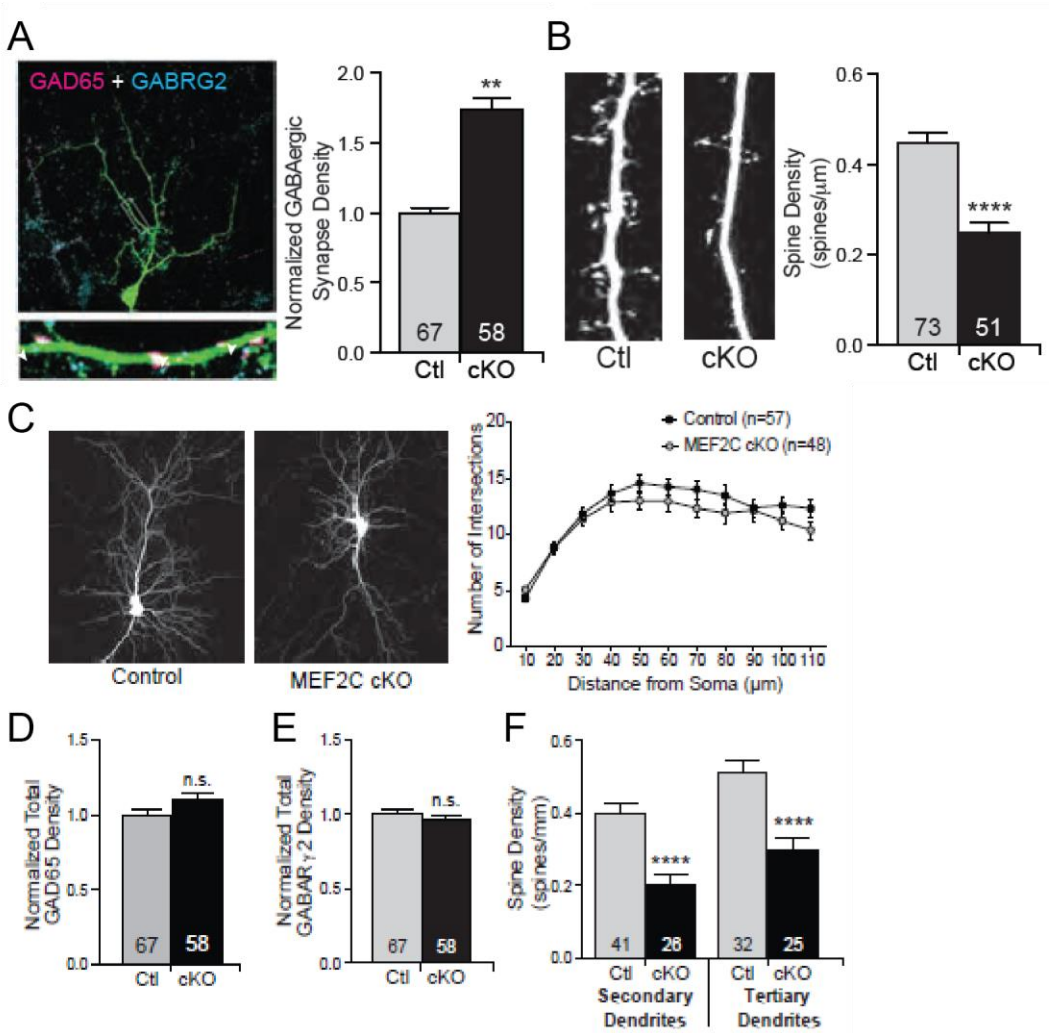

Figure 3.3: MEF2C suppresses inhibitory synapse number while promoting excitatory synapse number in neocortical neurons *in vitro*. (A) Representative image of a GFP expressing mouse cortical neuron immunostained with antibodies against GAD65 (pre-synaptic) and GABRG2 (post-synaptic). Quantification of inhibitory synapse density (see methods) on *MEF2C cKO* neurons showed an increase compared to wildtype control neurons. **(B)** Representative image of spine density across a dendritic stretch. Quantification of spine density on *MEF2C cKO* neurons showed a reduction compared to wildtype control neurons. **(C)** Representative images of GFP-transfected primary cortical neurons at DIV18. Sholl analysis of pyramidal neurons at DIV18 reveals no significant changes in dendritic complexity in *MEF2C cKO* neurons in vitro. n=57 neurons for control and n=48 neurons for *MEF2C cKO*. Immunocytochemical analysis of

inhibitory GAD65-presynaptic **(D)** and GABARγ2-postsynaptic **(E)** puncta in cultured cortical neurons at DIV18. Cortical neurons from *Mef2c cKO* mice show no change in inhibitory presynaptic puncta (GAD65 positive) or postsynaptic puncta (GABARγ2 positive) compared to controls as measured by co-localization of GAD65 (presynaptic) and GFP (neuron mask). **(F)** *MEF2C cKO* neurons have fewer dendritic spines than control neurons. Primary cortical neurons were grown to DIV18, and spines were visualized using myristoylated-GFP. Reduced spine density was observed in both secondary and tertiary dendrites, resulting in an overall reduction in spine density in all dendrites (Fig. 3.3B). Numbers of dendritic stretches (n) are reported in each bar from at least 30 control and 22 *MFE2C cKO* neurons. Data are represented as mean ± SEM. Statistical significance was determined by unpaired t-test. ****$p<0.0001$, ns=not significant.

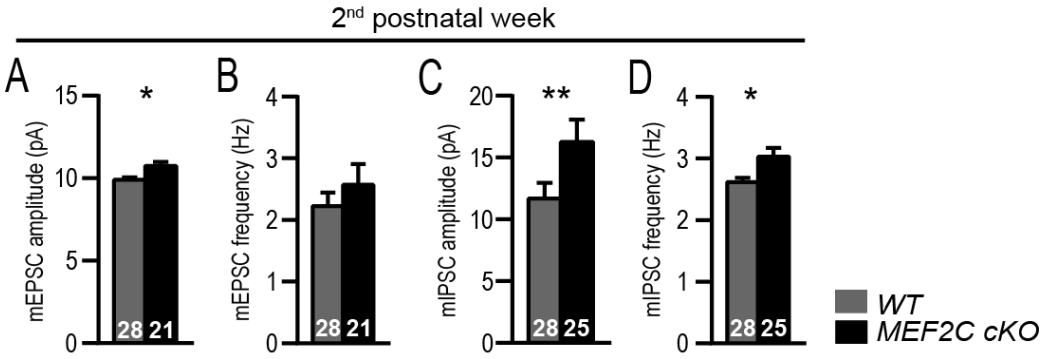

Figure 3.4: MEF2C regulates both excitatory and inhibitory synaptic transmission simultaneously during the second postnatal week of neocortical development. mEPSC amplitude **(A)**, mEPSC frequency **(B)**, mIPSC amplitude **(C)**, and mIPSC frequency **(D)** recorded from L2/3 pryamidal neurons in barrel cortices of WT and *MEF2C cKO* mice.

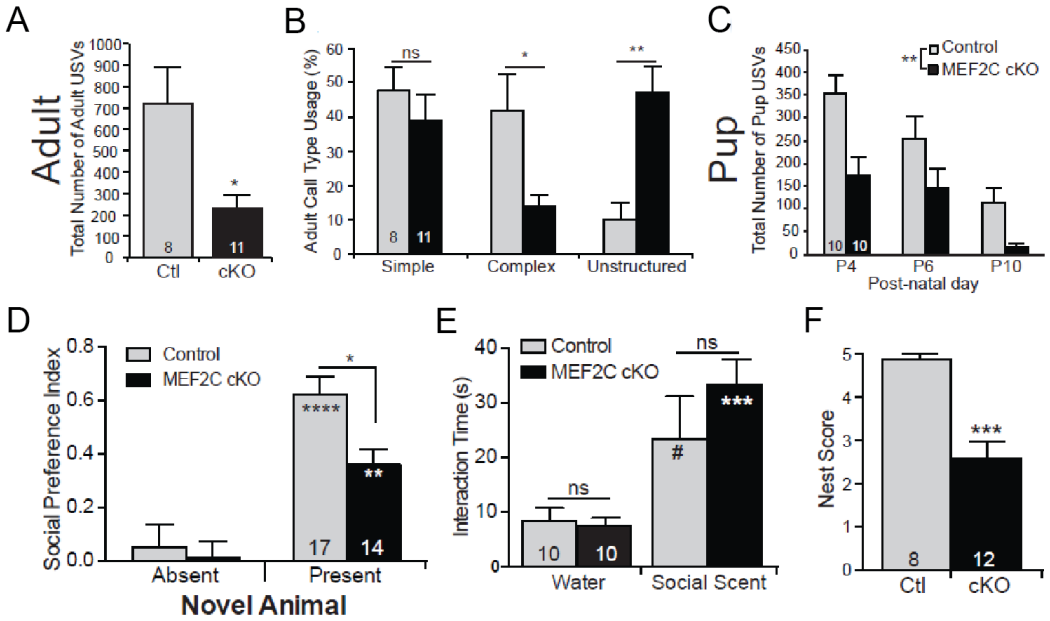

Figure 3.5: Communication deficits in *MEF2C cKO* mice. (A) Adult *MEF2C cKO* male mice emit fewer USVs to an estrous female than control littermates. **(B)** Adult *MEF2C cKO* male mice show different call types than control littermates. *MEF2C cKO* mice have more unstructured USVs (%) and fewer complex USVs than control mice. **(C)** Juvenile *MEF2C cKO* mice (pups) emit fewer USVs during maternal separation than control littermates. USVs were recorded on postnatal days (P) 4, 6, and 10. **(D)** *MEF2C cKO* mice show reduced preference for interacting with a novel social target. **(E)** *MEF2C cKO* mice show normal olfactory response to novel social scent. **(F)** *MEF2C cKO* mice fail to build structured nest when utilizing a nest score system (Deacon 2006b). Data are represented as mean ± SEM. Statistical significance was determined by unpaired t-test using GraphPad Prism. *$p<0.05$, **$p<0.01$, ****$p<0.0001$. Numbers of slices/neurons (n) are reported in each bar for respective experiment.

CHAPTER FOUR

Discussion and Implications

The data presented in this manuscript describe the roles of specific MEF2 genes in cell-autonomous regulation of neocortical synapse development and further detail the circuit consequences when transcriptional activity of select MEF2 proteins is ablated within individual L2/3 pyramidal neurons. I observe that MFE2A and MEF2D mildly affect synaptic function in L2/3 pyramidal neurons, while MEF2C deletion robustly decreases structural and functional excitatory synapse number. Likely through its promotion of synapse number, MEF2C is required for experience-dependent strengthening of local synaptic inputs. Furthermore, MEF2C suppresses the strength of distal synaptic inputs onto L2/3 neurons, suggesting that MEF2C is capable of differentially regulates specific synaptic populations. These findings provide a novel role for MEF2C as a positive regulator of excitatory neural connectivity in the postnatal mammalian neocortex.

I also report that deletion of *Mef2c* in excitatory neural networks decreases cortical function via a decrease in excitation and concomitant increase in inhibitory synaptic transmission; these changes are observed within L2/3 pyramidal neurons and neocortical neuron populations across WT and MEF2C cKO mice. These physiological changes are associated with decreased excitatory and increased inhibitory structural synapses. Lastly, MEF2C cKO mice exhibit behaviors in mice linked with neurodevelopmental disorders including autism and schizophrenia.

These data demonstrate that MEF2 transcription factors non-redundantly regulate neocortical synapse development and provide insight into MEF2-dependent regulation of

developmental and experience-dependent circuit plasticity critical for normal brain function.

Does MEF2C promote synapse formation or stabilization in L2/3 pyramidal neurons?

My data provide multiple evidences implicating MEF2C as a positive regulator of synapse number at local synaptic input pathways. However, my study does not lend insight into the dynamic regulation that MEF2C may have in forming or stabilizing synapses onto L2/3 pyramidal neurons. The basal dendrites of L2/3 pyramidal neurons are within an appropriate cortical depth (~100 – 200 µm) for resolution of two-photon imaging *in vivo*. Using two-phone imaging through a cranial window and expression of AAV-GFP a bicistronic AAV-Cre-GFP virus inducing cytosolic GFP expression in a sparse population of L2/3 pyramidal neurons in separate barrel cortices, dendritic spines on basal dendrites of WT and MEF2C KO neuron can be imaged over the course of days or weeks. If MEF2C mediates stability of dendritic spines, then I would expect to observe a frequent turnover of spines with shorter lifetimes in the MEF2C KO neurons. If MEF2C mediated synapse formation, then I would expect to observe no change in spine turnover but rather an overall, constant decrease in MEF2C KO neurons. This experiment could be performed in acute brain slices over a smaller period of time as well.

Additionally, my data are unable to distinguish between the possibilities of MEF2C in facilitating synapse formation or suppression of synapse elimination. To tease apart these two outcomes, acute expression of a γ-domain-positive MEF2C construct *in vivo* could initiate the primary effect of MEF2C repression on overall synapse number.

Acute expression of MEF2-VP16 could also be used, but however, this experiment would be confounded by the fact that MEF2-VP16 is not MEF2C-specific. It is difficult to definitively state whether or not MEF2C causes synapse formation or represses elimination.

Plasticity mechanisms underlying pathway-specific regulation of L2/3 inputs by MEF2C

The experiments outlined in Chapter 2 suggest that MEF2C decreases local connectivity while increasing the strength of distal cortical inputs. This is characteristic of heterosynaptic plasticity mechanisms, which can occur with sensory experience or deprivation. To my knowledge, a transcription factor for regulating heterosynaptic plasticity of excitation has never been identified. My data suggest that MEF2C may be implicated in such cellular processes. This works provides evidence that MEF2C plays a clear role in experience-dependent plasticity of L2/3 circuitry, and it would be interesting to observe synapse dynamics between WT and MEF2C KO *in vivo* to determine if there are patterns resembling competition among neighboring synapses. Perhaps MEF2C induces an effect on synaptic competition similar to that observed through β-catenin signaling (Bian et al 2015), as β-catenin interacts with MEF2 to stimulate Wnt signaling (Ehyai et al 2015). Interestingly, Wnt signaling is associated with synaptogenesis, axon guidance, calcium-activated gene transcription, and cytoskeletal remodeling (Rosso & Inestrosa 2013).

It is curious how a transcription factor within the nucleus could regulate evoked synaptic transmission at specific synaptic populations. One perspective to consider given

the outcomes of *Mef2c* deletion is that synaptic scaling does not necessarily apply to experience-dependent regulation of neocortical circuits. Synaptic scaling is characterized simply by recording spontaneous synaptic transmission but does not take into account that multiple – but specific – synaptic inputs could account for the increase in amplitude of spontaneous events, especially if these pathways target similar regions of the dendritic arbor. Thus, a "global" regulation of inputs has not been definitively characterized. Specific synaptic populations can undergo "clustered" potentiation at specific dendritic segments in response to experience, whereas another synaptic population can be "scaled" in a non-clustered, evenly distributed manner (Makino & Malinow 2011). This study employs a correlation coefficient to measure the extent to which plasticity occurs among neighboring versus distant spines. It would be interesting to determine if MEF2C is regulating the formation and/or stabilization of synaptic clusters that are associated with different synaptic pathways. This could also shed light on whether or not "global" plasticity mechanisms such as homeostatic scaling do, indeed, exist.

Lastly, determining all inputs – both local and distal - onto WT and MEF2C KO L2/3 neurons *in vivo* would be indispensable for understanding the interplay between cortical inputs. The use of genetic retrograde labeling techniques such as modified rabies viruses could be used to conduct such experiments. Three-dimensional reconstruction of the intact brain would elucidate the origins for all potential long-range cortical inputs onto L2/3 neurons that were potentiated with *Mef2c* deletion.

Potential mechanisms for MEF2C-dependent transcriptional regulation of experience-dependent neocortical synapse development

My data suggest that postnatal MEF2C facilitates experience-dependent circuit plasticity, likely through positive regulation of synapse number in L2/3 pyramidal neurons in the mouse barrel cortex. Several modes of regulation can underlie and/or contribute to MEF2C's ability to promote synapse number.

If MEF2C positively regulates synapse number onto L2/3 neurons facilitating whisker sensation, then it is possible that MEF2C expression is regulated by experience. Whether or not MEF2C expression is directly regulated by experience-dependent neural activity *in vivo* is unknown, although this may be unlikely as no changes in barrel cortical MEF2C expression were detected in previous genome-wide sequencing studies (Vallès et al 2011). Additionally, sensory experience does not induce total expression of MEF2A and MEF2D (Chen et al 2012). My data suggest MEF2C to function downstream of experience, and hence, MEF2C is likely already poised upon DNA prior to experience. However, the effects of salient whisker stimulation could alter MEF2C expression after several hours. Perhaps MEF2C could be rapidly degraded upon whisker stimulation. Another possibility is that MEF2C – similar to MEF2A and MEF2D – is targeted by caspase-mediated degradation to shift the threshold for synaptic plasticity. An experimental consideration is that MEF2C-dependent transcription is chronically halted from early postnatal development; this could mask the involvement of MEF2C in metaplastic cellular processes employing caspase-mediated degradation because MEF2C function is lost during a critical developmental stage for experience-dependent synaptic plasticity.

If no changes in total MEF2C expression are detected, then it is possible that alternative splicing of MEF2C mRNA favors expression of either transcriptional repressive

or activating splice variants of MEF2C. In neocortex, alternative splicing of MEF2C mRNA results in ~50% of MEF2C protein containing the repressive γ-domain (Lyons et al 2012b). Expression levels of γ-domain-containing and γ-domain-lacking MEF2C mRNA and/or protein in barrel cortex should be compared in mice that are subjected to sensory deprivation by whisker trimming or high whisker activity. This would determine whether or not MEF2C regulates sensory experience-dependent circuit plasticity via transcriptional repression or activation. Such experiments have never been conducted in neurons *in vivo*.

Furthermore, MEF2C could be regulating experience-dependent circuit plasticity via mechanisms independent of alternative splicing or changes in total expression levels. Determining key post-translational modifications in altering MEF2C transcriptional activity in response to sensory deprivation and enrichment would shed light into how MEF2C is regulating experience-dependent target gene expression. Although post-translational modification is not entirely independent of alternative splicing products, it can alter the transcriptional repression or activity of MEF2C protein if, for example, a MEF2C protein contains the γ-domain (see Chapter 1). Protein replacement studies could be used to assess the physiological importance for transcriptionally repressive modifications, including γ-domain modifications such as phosphorylation of Ser 391 and sumoylation of Ser 396 of MEF2C in sensory deprived and enriched animals. Additionally, point mutations and/or protein replacement studies could be used to modify phosphorylation of Ser 404 – the calcineurin binding site on MEF2C – in response to sensory deprivation and salient experience to determine how transcriptional activating post-translational modifications of MEF2C affect synaptic physiology of neocortical neurons.

Delineating the cellular and physiological consequences of MEF2C-dependent transcriptional regulation can be difficult as a variety of primary and secondary transcriptional events can result in similar outcomes, and likely crosstalk exists between such pathways with downstream effectors. For example, MEF2C could activate transcription of a target gene encoding a micro-RNA that degrades mRNA of a negative regulator of synapse number, hence preventing synapse elimination and causing an overall increase in synapse number. Another possibility is that MEF2C could repress transcription of a target gene such as an ubiquitin E3 ligase that marks a synapse stabilizing protein for proteosomal degradation. MEF2C could also activate or repress gene expression of other transcription factors, which adds another level of signaling complexity. This is to be expected when an experimental manipulation within the nucleus has measurable consequences at the plasma membrane.

Further examining the uniqueness of MEF2 transcription factors in regulation of neocortical synapses: Screening for target genes

The data presented in this work demonstrates that MEF2 transcription factors non-redundantly regulate synaptic function in the postnatal mammalian neocortex. Virtually nothing is known of the overlapping and potentially distinct functions of the various MEF2 family members, and their activity-dependent regulation, in cortical neuron function and development. Within individual L2/3 pyramidal neurons of the barrel cortex, MEF2A and MEF2D appear to have relatively modest effects on excitatory synaptic transmission, which may be trans-synaptic in nature to cause changes in release probability and vesicular release dynamics. MEF2C has a clear role on postsynaptic regulation of synapse number

in neocortical L2/3 neurons. What underlies the different effects across specific MEF2 transcription factors in neocortex? An obvious initial feat involves identifying target genes selectively regulated by specific MEF2 transcription factors.

Single-cell RNA sequencing with Fluidigm could be used to profile changes in gene expression upon deletion of *Mef2a*, *Mef2c*, or *Mef2d*. These experiments could also be performed in unilaterally whisker-trimmed mice between spared and deprived barrel cortices, as described in Chapter 1. A caveat for such sequencing experiments is that deletion of one MEF2 gene could lead to a compensatory upregulation of the others. This could be controlled for by measuring levels of not only MEF2 target genes but also expression levels of the MEF2 genes directly. To date, only one study has performed transcriptomic analyses in the brain across WT and MEF2A/D KO mice exposed to a novel environment (Flavell et al 2008). Furthermore, there are currently no published reports for genome-wide sequencing of MEF2C in brain tissue. Hence, more work must be done to delineate the role of specific MEF2 genes in brain development with respect to the target genes regulated by each of them, especially within the neocortex. Identification of overlapping and distinct regulation of target genes would specify candidate target genes that mediate the differences among the MEF2 transcription factors. Given the different results obtained between sparse and network *Mef2c* deletion in regulating neocortical L2/3 synaptic function (see Chapters 2 and 3), it would be interesting to compare changes in gene expression between these two experimental systems. Finding overlap between sparse and network deletion likely reflect the direct cell-autonomous changes accompanying *Mef2c* deletion, whereas the non-overlapping changes in target gene expression are likely due to trans-synaptic or non-cell-autonomous mechanisms.

Molecular players contributing to input-pathway-specific regulation of neocortical synapse development by MEF2C

Identifying MEF2C target genes within individual L2/3 pyramidal neurons would provide an initial list of target genes involved in the differential MEF2C-dependent regulation of decreased local input connectivity versus strengthened distal inputs, as discussed in Chapter 2. Because this study is the first to demonstrate in a single-cell model differential regulation of selective synaptic inputs, I speculate on which classes of target genes could be transcriptionally activated or repressed by MEF2C within cortical L2/3 neurons. Furthermore, I relate what is known about other effector proteins involved in hippocampal MEF2-dependent synapse elimination to implicate them in molecular mechanisms underlying MEF2C-dependent regulation of specific synaptic inputs onto L2/3 neurons.

Single-cell RNA sequencing usually involves cell sorting, fluorescence activated cell sorting (FACS), or collection of cytoplasm through a glass electrode. Thus, only RNAs within the vicinity of the soma are analyzed. Because synaptic RNAs are commonly transported and locally translated in the dendrites near synapses, visualization of these dendritic targets within an intact brain slice may elucidate subcellular gradients of target gene expression throughout the dendritic tree. Indeed, recent advancements in the imaging methods used for visualizing mRNA localization have allowed for the resolution of single transcriptions within single cells. Multiplexed error-robust fluorescence in situ hybridization (MERFISH) has allowed for such imaging capability of as many as ~1,000 mRNAs simultaneously within a single cell (Chen et al 2015). Probes designed against

mRNAs of cell adhesion molecules such as PCDH10 and NL-1, guidance cue receptors for netrins and semaphorins, synaptic scaffolding proteins such as Homer and Shank3, and immediate early genes such as Arc and Bdnf could be used to establish a three-dimensional layout of these transcriptions throughout basal and apical dendrites of neurons residing within a brain slice. This could reveal a gradient of potential MEF2 target genes localized to specific populations of synapses within a specific dendritic compartment, for example. Or perhaps the expression of the probe targets is correlated among neighboring synapses, suggestive of input-pathway specificity of small dendritic segments and synaptic clustering. These experiments would provide a basic screen for genes regulated by specific MEF2 transcription factors that are involved in neocortical synapse development.

MEF2-dependent synapse elimination in the hippocampus requires FMRP, mGluR5, and Arc (Pfeiffer et al 2010a, Wilkerson et al 2014). Despite the canonical role for mGluR5, FMRP, and Arc in negatively regulating synaptic function, observations in neocortical L2/3 pyramidal neurons suggest a positive regulation of evoked excitatory synaptic transmission by FMRP and mGluR5 (Bureau et al 2008, Loerwald et al 2015a). Since *Mef2c* deletion in single L2/3 neurons decreased evoked EPSCs at local inputs while increasing mEPSCs, I hypothesize that other molecular players within the MEF2C signaling pathway would phenocopy these results. Indeed, sparse deletion of *mGluR5* in L2/3 pyramidal neurons results in small but significant concomitant decreased EPSCs and increased mEPSCs (Loerwald et al 2015a). Additionally, mGluR5 maintains experience-dependent synaptic strength in the mouse barrel cortex (Kubota et al 2016), potentially further linking mGluR5 signaling to MEF2C for regulating experience-dependent development of neocortical circuits. Inconsistent with my hypothesis is that mGluR5

reportedly causes experience-dependent changes in presynaptic release probability (Kubota et al 2016), highlighting the potentially multifaceted role for mGluR5 in regulating experience-dependent circuit development. Electrophysiological recordings in AAV-Cre-GFP-injected *Fmr1*$^{fl/fl}$ mice would be expected to be increased in the Fmr1 KO neurons if indeed it is binding to MEF2C target genes. If *Fmr1* deletion does not increase mEPSCs, then perhaps FMRP facilitates more specific regulation of synapse populations or is not involved in the potential heterosynaptic plasticity that may be associated with *Mef2c* deletion (see above). Sparse deletion of *Arc* in early postnatal development has never been used as an experimental model for studying neocortical circuit development.

Divergent phenotypes with sparse versus network-wide *Mef2c* deletion

In general, network and sparse *Mef2c* deletion produce corroborative findings regarding MEF2C function within the mammalian neocortex. In both preparations, MEF2C promotes excitatory synapse number onto neocortical neurons without affecting dendritic arbor development. Additionally, heterozygous deletion of *Mef2c* does not affect synaptic function (i.e. physiological and behavioral).

Interestingly, embryonic deletion of *Mef2c* in forebrain excitatory neurons present phenotypic differences that were not observed with sparse *Mef2c* deletion in neocortical neurons. For example, network deletion of *Mef2c* in cortical excitatory networks upregulated spontaneous inhibitory synaptic transmission, whereas sparse *Mef2c* deletion did not affect either evoked or spontaneous inhibitory synaptic transmission within L2/3 neurons of the barrel cortex. Additionally, sparse *Mef2c* deletion caused a robust increase in mEPSCs linked to pathway-specific potentiation of long-range intercortical inputs,

whereas network *Mef2c* deletion reduced mEPSCs. These discrepancies raise question regarding the primary, cell-autonomous role for MEF2C in regulating neocortical circuit development.

An obvious explanation underlying the phenotypic discrepancy between sparse and network *Mef2c* deletion effects includes the developmental time at which *Mef2c* is deleted. Network *Mef2c* deletion occurred within excitatory forebrain neurons at ~E12: a developmental stage coinciding with onset of neural migration from the cortical subplate (Sauvageot & Stiles 2002), whereas postnatal sparse *Mef2c* deletion occurred at ~P5-P7 (see Fig. 2.1) well after completion of cortical migration. In the cortex, GABAergic synapse formation precedes that of glutamatergic synapse formation (Ben-Ari et al 2007, De Felipe et al 1997, Owens et al 1999), and it can strongly affect the subsequent development of glutamatergic synapses and neuronal morphology (Wang & Kriegstein 2008). It is possible that any role for MEF2C in regulating GABAergic synaptic function is overlooked with sparse postnatal *Mef2c* deletion, whereby relevant proteins comprising functional GABAergic synapses were not perturbed earlier in development as with embryonic network *Mef2c* deletion. This is supported by the fact that mIPSCs are increased prior to reduction of mEPSCs during the second week of postnatal development in *MEF2C cKO* mice (see Chapter 3). Alternatively, embryonic network *Mef2c* deletion could increase mIPSCs as a homeostatic mechanism in response to a large decrease in excitatory drive onto excitatory neocortical neurons such that these neurons will adapt to receive synaptic input regardless of the excitatory or inhibition nature of those inputs. Contradicting this hypothesis is that mIPSCs are increased at this age, whereas mEPSCs are unchanged.

The mEPSCs reflect all inputs onto a neuron, and in the case of sparse postnatal *Mef2c* deletion I was able to relate increased mEPSCs with potentiation of specific long-range intercortical input pathways. Network *Mef2c* deletion could perhaps cause decreased excitatory cortical connectivity while connectivity with subcortical and/or midbrain inputs could be increased to offset the overall change in excitatory synapse number; this scenario would explain why mEPSCs are unchanged during the second postnatal week while mIPSCs are upregulated in the MEF2C cKO mice. To further address this possibility, optogenetics could be used to assess upregulation of evoked synaptic transmission of specific subcortical inputs.

Thirdly, I hypothesize that the neocortical compaction in MEF2C cKO mice likely causes gross changes in neocortical circuit arrangement, especially given that these mice do not have visibly distinguishable barrels, indicating that L4 – the primary target of afferent cortical activity – is abnormal in these mice. Thus, changes in mIPSCs and mEPSCs in MEF2C cKO mice could be resultant of unnatural circuit organization resultant of non-synaptic MEF2C-dependent processes involved in neural migration and maturation, as reported previously (Li et al 2008). To further test this hypothesis, initial immunohistological experiments using antibodies against cortical layer-specific markers such as SatB1 and Six3, for example, could be performed to assess laminarization of the barrel cortex. LSPS with glutamate uncaging could also be performed in L2/3 pyramidal neurons to ensure that L4 → L2/3 inputs evoke the largest EPSCs. Additionally, synaptic LSPS mapping could be performed in L4 spiny stellate neurons to confirm that L2/3 → L4 inputs are not observed.

Lastly, I hypothesize that the increased inhibitory synapse number and function reported in the *MEF2C cKO* cortical neurons is a trans-synaptic, non-cell-autonomous effect of synaptic competition due primarily to decreased excitatory connectivity. Trans-synaptic versus cell-autonomous roles of a gene can be identified when comparing phenotypes between network and sparse gene deletion systems. For example, network and sparse deletion of *Neuroligin-1* (NL-1) – a postsynaptic cell adhesion molecule – in neocortical L2/3 pyramidal neuron revealed decreased NMDAR-mediated EPSCs, while decreased excitatory synapse number was observed only with sparse, mosaic NL-1 deletion (Kwon et al 2012). These data suggest that NL-1 cell-autonomously promotes NMDAR function and trans-synaptically promotes excitatory synapse number. Experiments outlined in chapters 2 and 3 suggest that MEF2C cell-autonomously promotes excitatory synapse number onto excitatory neocortical neurons, as both sparse and network *Mef2c* deletion paradigms exhibit this phenotype. The mosaicism of sparse *Mef2c* deletion occurs at both excitatory and inhibitory corticocortical inputs, whereas network *Mef2c* deletion provides mosaicism only at inhibitory-to-excitatory (I → E) inputs. Thus, network *Mef2c* deletion may foster a cellular environment that 1) cell-autonomously decreases excitatory connectivity, while 2) non-cell-autonomously allowing for postsynaptic competition between GABAergic interneurons and pyramidal neurons for excitatory presynaptic inputs. Synaptic competition of excitatory presynaptic inputs between postsynaptic inhibitory and excitatory connectivity has been observed previously onto PV-expressing interneurons and L2/3 pyramidal neurons within the mouse visual cortex (Saiepour et al 2015). This study demonstrated that network deletion of TrkB.T1 receptors in excitatory neurons upregulated E → I connectivity onto PV-expressing interneurons and concomitantly decreased I → E

synapse density onto pyramidal neurons: a phenotype not observed with sparse TrkB deletion. These data suggest that inhibitory connectivity is regulated by trans-synaptic, non-cell-autonomous mechanisms, while excitatory connectivity is mediated by cell-autonomous processes. Interestingly, NL-1 (A.J.H. and C.W.C. unpublished results) and BDNF (Lyons et al 2012b) signaling mechanisms are regulated by MEF2. I conclude that MEF2C cell-autonomously promotes excitatory synapse number onto neocortical neurons, while changes in inhibition are trans-synaptic and homeostatic effects of *Mef2c* deletion.

Implications for MEF2C within excitatory neocortical neurons and neurodevelopmental disorders, 5q14 deletion syndrome

Converging evidence of both sparse and network deletion of *Mef2c* in neocortical pyramidal neurons demonstrates a clear and critical role for MEF2C in promoting the development of neocortical circuits. These results were obtained in experimental preparations employing complete loss-of-function genetic mutation of *Mef2c in vivo*. However, complete loss of *Mef2c* function *de novo* results in embryonic lethality due to developmental effects in cardiac and skeletal muscle tissues (Lin et al 1997). Hence, the genetic manipulations that I have made to completely terminate MEF2C-dependent transcription in select neuron populations – whether sparse or network deletion – would never occur naturally in biology. In humans, *Mef2c* haploinsufficiency is sufficient to cause neurological and behavioral abnormalities in patients, and different types and sizes (i.e. deletion and duplication) of *Mef2c* gene mutations give rise to a spectrum of behavioral, neurological, and somatic symptoms (Cardoso et al 2009, Le Meur et al 2010, Novara et al 2010, Paciorkowski et al 2013b, Zweier et al 2010, Zweier & Rauch 2012).

Interestingly, heterozygous *Mef2c* deletion in sparse or network excitatory neuron populations does not affect behavior or synaptic function of neocortical neurons *in vivo* (**Fig. 2.3** and data not shown from A.J.H. and C.W.C.). These results suggest multiple hypotheses regarding the contribution made by recessive *Mef2c* mutations within excitatory neocortical neurons to cause intellectual disability and expression of abnormal behaviors. For example, it is possible that human *MEF2C* haploinsufficiency symptoms are a result of its loss of function in non-forebrain excitatory cell populations or that, in humans, there are other factors that influence disease penetrance and severity, including unique or sensitized functions for MEF2C through human evolution, human-specific genetic modifiers and/or environmental influences that increase symptom penetrance.

Mef2c mutations may affect function of inhibitory interneuron subtypes (Paciorkowski et al 2013a), which are not manipulated in experiments performed in chapters 2 and 3. Unpublished data obtained by Xavier H. Jaglin and Gord Fishell at New York University have found striking developmental roles for MEF2C in cell survival of GABAergic interneurons within the neocortex (personal communication with X.H.G.). Immunohistological experiements are performed in *Mef2c*$^{fl/fl}$ mice that also express Cre drivers such as Parvalbumin (PV)-Cre and Somatostatin (SST)-Cre to isolate fast-spiking PV+ and SST+ interneuron populations, respectively. *Mef2c*$^{fl/fl}$*; SST-Cre+* mice develop normally, and the densities of SST+ interneurons do not express apoptotic markers including Caspase-3 and Caspase-9. In contrast, *Mef2c*$^{fl/fl}$*;PV-Cre+* mice reliably die at P9 due to severe seizures, while the *PV* promoter is initially driven at P8-P9 in mouse development *in vivo* (Taniguchi et al 2011). Immunohistological experiments in fixed brain slices prepared from P8 *Mef2c*$^{fl/fl}$*;PV-Cre+* reveal a dramatic loss of PV+

interneurons and an increase in caspase-3 and caspase-9 expression, suggesting that PV+ interneurons are undergoing apoptosis (X.H.G., G.F.). These data also demonstrate that MEF2C-dependent transcription (exon 2 expression) is required for survival of PV+ interneurons, while my experiments reveal that *Mef2c* expression is dispensable for survival of neocortical pyramidal neurons (see also Akhtar et al., 2012). Perhaps the clinical phenotypes associated with *Mef2c* haploinsufficiency are due to death of PV+ interneuron networks, which in turn, diminishes somatic inhibition to cause runaway, epileptic "seizure-like" activity of excitatory neocortical networks. If in humans *MEF2C* functions to promote neocortical excitatory synapse number, then it likely does so in interneuron populations as well. In order to understand the underpinnings of synaptic alterations in patients with 5q14.3-5 deletion syndrome, then experiments in mice should be performed to achieve heterozygous *Mef2c* deletion in GABAergic interneurons populations. To circumvent the cell death at P9, one should use AAV-Cre-GFP infection to cause sparse gene deletion in $Mef2c^{fl/+}$ mice. Perhaps these mice could also express a genetic PV reporter to easily identify neighboring WT and MEF2C HET PV neuron pairs to perform electrophysiological recordings within the same brain slice. Additionally, electrophysiological recordings could be performed in L2/3 pyramidal neurons of $Mef2c^{fl/+}$;*PV-Cre*+ mice or $Mef2c^{fl/+}$;*PV-*Cre^{ERtm}+ mice to observe the chronic and acute effects of *Mef2c* deletion within inhibitory interneurons on neocortical excitatory neocortical networks; all data would be compared to Cre-negative littermates. Behavioral assays similar to those outlined in Fig. 3.4 could also be performed in $Mef2c^{fl/+}$;*PV-Cre*+ and $Mef2c^{fl/+}$;*PV-Cre*- littermates.

Another hypothesis addressing the lack of effects on excitatory synaptic transmission and behavior with heterozygous deletion of *Mef2c* in excitatory neocortical neurons involves the type of genetic manipulation (i.e. position of loxP sites) used to delete *Mef2c* as deletion of exon 2 was utilized for all experiments described within chapters 2 and 3. Mutations within the *Mef2c* locus are variable in size and position within the gene (Cardoso et al 2009, Le Meur et al 2010, Zweier et al 2010), and not all reported mutations involved deletion or duplication of exon 2. Therefore, deletion of other exons within the *Mef2c* gene are likely critical for brain function. In my experimental systems, a truncated C-terminal fragment of MEF2C is expressed within Cre-expressing neurons, and it is likely that this protein fragment mediates interactions between MEF2C and other critical cofactors in regulating synapse development and perhaps other non-transcriptional functions. I sparsely infected neocortical neurons at P1 in *Mef2c*$^{fl/fl}$ mice with a custom AAV that expresses a shRNA against *Mef2c* (90% efficiency *in vitro*) and a GFP reporter (AAV-shMef2c-GFP) and attempted to perform whole-cell recordings as described in chapter 2 but was unable to do so because all infected neurons were either dead or unhealthy, as determined by inability to patch the neurons and by the presence of vacuoles within the somas. (See appendix.) Furthermore, infection efficiency was much lower than typically observed with AAV-Cre-GFP expression, likely because most of the infected neurons had died before I prepared acute neocortical slices at P20-P25. This small finding suggests that MEF2C is critical for survival of excitatory neocortical pyramidal neurons through molecular interactions at the C-terminus, which could possibly be independent of transcriptional regulation. Two experiments should be performed to address this possibility. The first experiment would be to infect L2/3 neocortical neurons with a

scrambled shRNA against *Mef2c* to ensure that the observed cell death is not due to chronic expression of the shRNA itself. The second would be to design a conditional knockout mouse in which the entire *Mef2c* gene was floxed. Electrophysiological recordings in neocortical L2/3 pyramidal neurons would then be performed with sparse postnatal AAV-Cre-GFP infection (or an AAV of a scrambled shRNA against *Mef2c*) or with network deletion using the Emx1-Cre driver line. Behavioral experiments could also be performed to determine if a more accurate model of *Mef2c* haploinsufficiency could recapitulate the clinical autism-like behaviors in mice. Such a mouse does not currently exist. Thus far, additional experiments must be performed to gain insight into whether or not *Mef2c* haploinsufficiency is sufficient to affect excitatory synapse development in mice or if this condition is specific to humans.

CONCLUSIONS

These data demonstrate that specific MEF2 transcription factors promote neocortical synaptic function *in vivo*. I have discovered a clear cell-autonomous role for MFE2C in positively regulating synapse number and experience-dependent circuit plasticity in neocortex: a regulation occurring at specific synaptic inputs. Lastly, my data directly reveal physiological differences between sparse and network genetic manipulations within the same neuronal cell type. This work has provided additional insight into the physiological mechanisms dependent upon specific MEF2 transcription factors for sculpting brain circuit development resultant of postnatal experience.

APPENDIX

List of Pharmacological Reagents

Compound	Site of Action	Effect	Concentration Used
MNI-caged-L-glutamate	Glutmate receptor	Ligand, agonist	20 mM or 40 mM
Kynurenic acid	Glutamate receptor	Antagonist	1 mM
CPP	NMDA reeptor	Antagonist	1 μM or 10 μM
4-aminopyridine	K_V1 channel subunits	Antagonist	100 μM
DNQX	AMPA receptor	Antagonist	20 μM
Bicuculline methiodide (BMI)	$GABA_A$ receptor	Antagonist	5 mM
Picrotoxin (PTX)	GABA-A receptor	Antagonist	100 μM
Tetrodotoxin (TTX)	Na^+ channels	Antangonist	1 μM

List of Viral Constructs

Virus Name	Expression/Notes
AAV2.9-Cre-GFP	Adeno-associated virus expressing Cre recombinase fused to green fluorescent protein under the CMV promoter (UPenn Vector Core)
AAV2.9-ChR2-mCherry	Adeno-associated virus expressing Channelrhodopsin-2 fused to mCherry under the CAG promoter (UPenn Vector Core)
AAV-shMef2c-ZsGreen	Adeno-associated virus constructed from the pZaf vector backbone, expressing a shRNA targeting MEF2C under the U6 promoter and ZsGreen (GFP) under the CMV promoter. Custom AAV prepared by cloning (K.E.R.) and packaging (UPenn Vector Core).

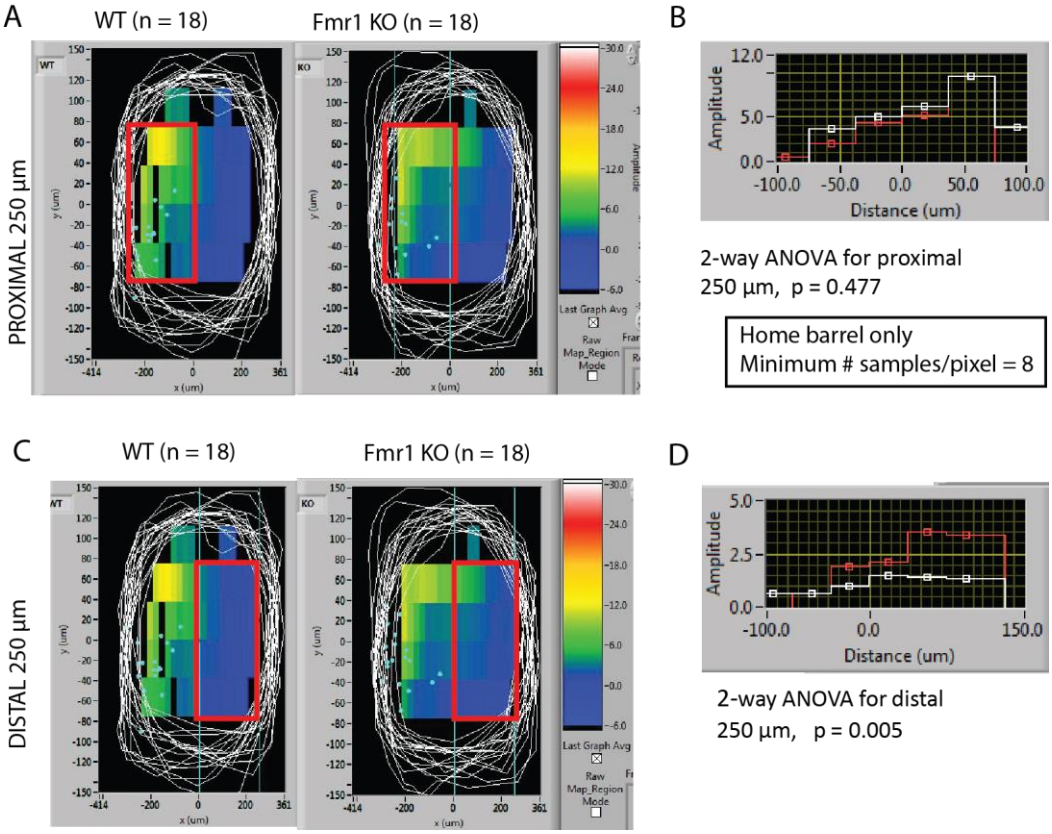

APPENDIX FIGURE 0.1: Initial LSPS mapping of local excitatory inputs onto parvalbumin-expressing interneurons within L4 of WT and Fmr1 KO mice. (A) Average LSPS maps of PV-expressing interneurons in WT and Fmr1 KO mice within the "proximal" 250-µm region of the barrel. Barrel borders are roughly defined by white lines. **(B)** Quantification of the average response amplitude represented as horizontal synaptic profiles in **(A). (C)** Average LSPS maps of PV-expressing interneurons in WT and Fmr1 KO mice within the "proximal" 250-µm region of the barrel. Barrel borders are roughly defined by white lines. **(D**) Quantification of the average response amplitude represented as horizontal synaptic profiles in **(C**). Although PV-expressing interneurons in Fmr1 KO mice received excitatory inputs that are significantly stronger than inputs onto WT PV interneurons, this data cannot be interpreted because input resistance is increased in Fmr1 PV interneurons compared to WT (Gibson et al 2008).

BIBLIOGRAPHY

Adachi M, Lin PY, Pranav H, Monteggia LM. 2015. Postnatal Loss of Mef2c Results in Dissociation of Effects on Synapse Number and Learning and Memory. *Biol Psychiatry*

Adesnik H, Li G, During MJ, Pleasure SJ, Nicoll RA. 2008. NMDA receptors inhibit synapse unsilencing during brain development. *Proc Natl Acad Sci U S A* 105: 5597-602

Adesnik H, Scanziani M. 2010. Lateral competition for cortical space by layer-specific horizontal circuits. *Nature* 464: 1155-60

Akhtar MW, Kim MS, Adachi M, Morris MJ, Qi X, et al. 2012. In Vivo Analysis of MEF2 Transcription Factors in Synapse Regulation and Neuronal Survival. *PLoS One* 7: e34863

American Psychiatric Association. 2013. *Diagnostic and statistical manual of mental disorders : DSM-5*. Washington, D.C.: American Psychiatric Association. xliv, 947 p. pp.

Andrés V, Cervera M, Mahdavi V. 1995. Determination of the consensus binding site for MEF2 expressed in muscle and brain reveals tissue-specific sequence constraints. *Journal of Biological Chemistry* 270: 23246-49

Arnold MA, Kim Y, Czubryt MP, Phan D, McAnally J, et al. 2007a. MEF2C transcription factor controls chondrocyte hypertrophy and bone development. *Developmental cell* 12: 377-89

Arnold MA, Kim Y, Czubryt MP, Phan D, McAnally J, et al. 2007b. MEF2C transcription factor controls chondrocyte hypertrophy and bone development. *Dev Cell* 12: 377-89

Aronoff R, Matyas F, Mateo C, Ciron C, Schneider B, Petersen CC. 2010. Long-range connectivity of mouse primary somatosensory barrel cortex. *European Journal of Neuroscience* 31: 2221-33

Bading H, Ginty DD, Greenberg ME. 1993. Regulation of gene expression in hippocampal neurons by distinct calcium signaling pathways. *Science* 260: 181-86

Barbosa AC, Kim MS, Ertunc M, Adachi M, Nelson ED, et al. 2008. MEF2C, a transcription factor that facilitates learning and memory by negative regulation of synapse numbers and function. *Proc Natl Acad Sci U S A* 105: 9391-6

Bateup HS, Johnson CA, Denefrio CL, Saulnier JL, Kornacker K, Sabatini BL. 2013. Excitatory/inhibitory synaptic imbalance leads to hippocampal hyperexcitability in mouse models of tuberous sclerosis. *Neuron* 78: 510-22

Ben-Ari Y, Gaiarsa JL, Tyzio R, Khazipov R. 2007. GABA: a pioneer transmitter that excites immature neurons and generates primitive oscillations. *Physiological reviews* 87: 1215-84

Ben-Ari Y, Khalilov I, Kahle KT, Cherubini E. 2012. The GABA excitatory/inhibitory shift in brain maturation and neurological disorders. *The Neuroscientist* 18: 467-86

Bender KJ, Allen CB, Bender VA, Feldman DE. 2006a. Synaptic basis for whisker deprivation-induced synaptic depression in rat somatosensory cortex. *The Journal of neuroscience* 26: 4155-65

Bender KJ, Allen CB, Bender VA, Feldman DE. 2006b. Synaptic basis for whisker deprivation-induced synaptic depression in rat somatosensory cortex. *J Neurosci* 26: 4155-65

Bender VA, Bender KJ, Brasier DJ, Feldman DE. 2006c. Two coincidence detectors for spike timing-dependent plasticity in somatosensory cortex. *J Neurosci* 26: 4166-77

Bian WJ, Miao WY, He SJ, Qiu Z, Yu X. 2015. Coordinated Spine Pruning and Maturation Mediated by Inter-Spine Competition for Cadherin/Catenin Complexes. *Cell* 162: 808-22

Bibb JA, Chen J, Taylor JR, Svenningsson P, Nishi A, et al. 2001. Effects of chronic exposure to cocaine are regulated by the neuronal protein Cdk5. *Nature* 410: 376-80

Blaeser F, Ho N, Prywes R, Chatila TA. 2000. Ca2+-dependent gene expression mediated by MEF2 transcription factors. *Journal of Biological Chemistry* 275: 197-209

Bloodgood BL, Sharma N, Browne HA, Trepman AZ, Greenberg ME. 2013a. The activity-dependent transcription factor NPAS4 regulates domain-specific inhibition. *Nature* 503: 121-5

Bloodgood BL, Sharma N, Browne HA, Trepman AZ, Greenberg ME. 2013b. The activity-dependent transcription factor NPAS4 regulates domain-specific inhibition. *Nature* 503: 121-25

Bosman L, Houweling AR, Owens CB, Tanke N, Shevchouk OT, et al. 2011. Anatomical pathways involved in generating and sensing rhythmic whisker movements. *Front Integr Neurosci* 5: 53

Brusco J, Haas K. 2015. Interactions between mitochondria and the transcription factor myocyte enhancer factor 2 (MEF2) regulate neuronal structural and functional plasticity and metaplasticity. *The Journal of physiology* 593: 3471-81

Bureau I, Shepherd GM, Svoboda K. 2008. Circuit and plasticity defects in the developing somatosensory cortex of FMR1 knock-out mice. *The Journal of Neuroscience* 28: 5178-88

Cao H, Dixson L, Meyer-Lindenberg A, Tost H. 2016. Functional connectivity measures as schizophrenia intermediate phenotypes: advances, limitations, and future directions. *Curr Opin Neurobiol* 36: 7-14

Cardoso C, Boys A, Parrini E, Mignon-Ravix C, McMahon JM, et al. 2009. Periventricular heterotopia, mental retardation, and epilepsy associated with 5q14.3-q15 deletion. *Neurology* 72: 784-92

Carrion AM, Link WA, Ledo F, Mellström B, Naranjo JR. 1999. DREAM is a Ca2+-regulated transcriptional repressor. *Nature* 398: 80-84

Celikel T, Szostak VA, Feldman DE. 2004. Modulation of spike timing by sensory deprivation during induction of cortical map plasticity. *Nat Neurosci* 7: 534-41

Cellot G, Cherubini E. 2014. GABAergic signaling as therapeutic target for autism spectrum disorders. *Frontiers in pediatrics* 2: 70

Cheetham CE, Fox K. 2010. Presynaptic development at L4 to l2/3 excitatory synapses follows different time courses in visual and somatosensory cortex. *The Journal of Neuroscience* 30: 12566-71

Cheetham CE, Hammond MS, Edwards CE, Finnerty GT. 2007a. Sensory experience alters cortical connectivity and synaptic function site specifically. *J Neurosci* 27: 3456-65

Cheetham CE, Hammond MS, Edwards CE, Finnerty GT. 2007b. Sensory experience alters cortical connectivity and synaptic function site specifically. *The Journal of neuroscience* 27: 3456-65

Chen C, Regehr WG. 2000. Developmental remodeling of the retinogeniculate synapse. *Neuron* 28: 955-66

Chen KH, Boettiger AN, Moffitt JR, Wang S, Zhuang X. 2015. Spatially resolved, highly multiplexed RNA profiling in single cells. *Science* 348: aaa6090

Chen SX, Cherry A, Tari PK, Podgorski K, Kwong YKK, Haas K. 2012. The transcription factor MEF2 directs developmental visually driven functional and structural metaplasticity. *Cell* 151: 41-55

Chowdhury S, Shepherd JD, Okuno H, Lyford G, Petralia RS, et al. 2006. Arc/Arg3.1 interacts with the endocytic machinery to regulate AMPA receptor trafficking. *Neuron* 52: 445-59

Cohen S, Greenberg ME. 2008. Communication between the synapse and the nucleus in neuronal development, plasticity, and disease. *Annual review of cell and developmental biology* 24: 183

Cole CJ, Mercaldo V, Restivo L, Yiu AP, Sekeres MJ, et al. 2012. MEF2 negatively regulates learning-induced structural plasticity and memory formation. *Nat Neurosci* 15: 1255-64

Colledge M, Snyder EM, Crozier RA, Soderling JA, Jin Y, et al. 2003. Ubiquitination regulates PSD-95 degradation and AMPA receptor surface expression. *Neuron* 40: 595-607

Coyle JT, Balu DT, Puhl MD, Konopaske GT. 2016. History of the Concept of Disconnectivity in Schizophrenia. *Harvard review of psychiatry* 24: 80-6

De Felipe J, Marco P, Fairen A, Jones E. 1997. Inhibitory synaptogenesis in mouse somatosensory cortex. *Cerebral Cortex* 7: 619-34

De Haan M, Johnson MH. 2005. *The cognitive neuroscience of development*. Psychology Press.

Deacon RM. 2006a. Assessing nest building in mice. *Nat Protoc* 1: 1117-9

Deacon RM. 2006b. Digging and marble burying in mice: simple methods for in vivo identification of biological impacts. *Nat Protoc* 1: 122-4

Desai NS, Cudmore RH, Nelson SB, Turrigiano GG. 2002. Critical periods for experience-dependent synaptic scaling in visual cortex. *Nature neuroscience* 5: 783-89

Dichter GS, Richey JA, Rittenberg AM, Sabatino A, Bodfish JW. 2012. Reward circuitry function in autism during face anticipation and outcomes. *Journal of autism and developmental disorders* 42: 147-60

Ehyai S, Dionyssiou MG, Gordon JW, Williams D, Siu KM, McDermott JC. 2015. A p38 MAPK regulated MEF2: β-catenin interaction enhances canonical Wnt signalling. *Molecular and Cellular Biology*: MCB. 00832-15

Elmer BM, Estes ML, Barrow SL, McAllister AK. 2013. MHCI requires MEF2 transcription factors to negatively regulate synapse density during development and in disease. *J Neurosci* 33: 13791-804

Engels H, Wohlleber E, Zink A, Hoyer J, Ludwig KU, et al. 2009. A novel microdeletion syndrome involving 5q14.3-q15: clinical and molecular cytogenetic characterization of three patients. *European journal of human genetics : EJHG* 17: 1592-9

Etherton MR, Blaiss CA, Powell CM, Sudhof TC. 2009. Mouse neurexin-1alpha deletion causes correlated electrophysiological and behavioral changes consistent with cognitive impairments. *Proceedings of the National Academy of Sciences of the United States of America* 106: 17998-8003

Ey E, Torquet N, Le Sourd AM, Leblond CS, Boeckers TM, et al. 2013. The Autism ProSAP1/Shank2 mouse model displays quantitative and structural abnormalities in ultrasonic vocalisations. *Behavioural brain research* 256: 677-89

Faber DS, Korn H. 1991. Applicability of the coefficient of variation method for analyzing synaptic plasticity. *Biophys J* 60: 1288-94

Feldman DE. 2012. The spike-timing dependence of plasticity. *Neuron* 75: 556-71

Feldman DE, Brecht M. 2005. Map plasticity in somatosensory cortex. *Science* 310: 810-5
Feldmeyer D. 2012a. Excitatory neuronal connectivity in the barrel cortex. *Front Neuroanat* 6: 24
Feldmeyer D. 2012b. Excitatory neuronal connectivity in the barrel cortex. *Frontiers in neuroanatomy* 6
Feldmeyer D, Brecht M, Helmchen F, Petersen CC, Poulet JF, et al. 2013. Barrel cortex function. *Progress in neurobiology* 103: 3-27
Feldmeyer D, Egger V, Lübke J, Sakmann B. 1999. Reliable synaptic connections between pairs of excitatory layer 4 neurones within a single 'barrel'of developing rat somatosensory cortex. *The Journal of Physiology* 521: 169-90
Feldmeyer D, Lübke J, Sakmann B. 2006. Efficacy and connectivity of intracolumnar pairs of layer 2/3 pyramidal cells in the barrel cortex of juvenile rats. *The Journal of physiology* 575: 583-602
Feldmeyer D, Lübke J, Silver RA, Sakmann B. 2002. Synaptic connections between layer 4 spiny neurone-layer 2/3 pyramidal cell pairs in juvenile rat barrel cortex: physiology and anatomy of interlaminar signalling within a cortical column. *The Journal of physiology* 538: 803-22
Flavell SW, Cowan CW, Kim TK, Greer PL, Lin Y, et al. 2006. Activity-dependent regulation of MEF2 transcription factors suppresses excitatory synapse number. *Science* 311: 1008-12
Flavell SW, Kim T-K, Gray JM, Harmin DA, Hemberg M, et al. 2008. Genome-wide analysis of MEF2 transcriptional program reveals synaptic target genes and neuronal activity-dependent polyadenylation site selection. *Neuron* 60: 1022-38
Fox K. 1992. A critical period for experience-dependent synaptic plasticity in rat barrel cortex. *The Journal of neuroscience* 12: 1826-38
Fox K. 2002. Anatomical pathways and molecular mechanisms for plasticity in the barrel cortex. *Neuroscience* 111: 799-814
Fu M, Yu X, Lu J, Zuo Y. 2012. Repetitive motor learning induces coordinated formation of clustered dendritic spines in vivo. *Nature* 483: 92-95
Garber K. 2007. Neuroscience. Autism's cause may reside in abnormalities at the synapse. *Science* 317: 190-1
Gau D, Lemberger T, von Gall C, Kretz O, Le Minh N, et al. 2002. Phosphorylation of CREB Ser142 regulates light-induced phase shifts of the circadian clock. *Neuron* 34: 245-53
Gibson JR, Bartley AF, Hays SA, Huber KM. 2008. Imbalance of neocortical excitation and inhibition and altered UP states reflect network hyperexcitability in the mouse model of fragile X syndrome. *J Neurophysiol* 100: 2615-26

Gibson JR, Beierlein M, Connors BW. 1999. Two networks of electrically coupled inhibitory neurons in neocortex. *Nature* 402: 75-79
Globus A, Rosenzweig MR, Bennett EL, Diamond MC. 1973. Effects of differential experience on dendritic spine counts in rat cerebral cortex. *Journal of comparative and physiological psychology* 82: 175
Ha S, Sohn IJ, Kim N, Sim HJ, Cheon KA. 2015. Characteristics of Brains in Autism Spectrum Disorder: Structure, Function and Connectivity across the Lifespan. *Exp Neurobiol* 24: 273-84
Hanson JL, Hurley LM. 2012. Female presence and estrous state influence mouse ultrasonic courtship vocalizations. *PLoS One* 7: e40782
Harris KM, Kater SB. 1994. Dendritic spines: cellular specializations imparting both stability and flexibility to synaptic function. *Annu Rev Neurosci* 17: 341-71
Harvey CD, Svoboda K. 2007. Locally dynamic synaptic learning rules in pyramidal neuron dendrites. *Nature* 450: 1195-200
Hays SA, Huber KM, Gibson JR. 2011. Altered neocortical rhythmic activity states in Fmr1 KO mice are due to enhanced mGluR5 signaling and involve changes in excitatory circuitry. *J Neurosci* 31: 14223-34
Higley MJ. 2014. Localized GABAergic inhibition of dendritic Ca2+ signalling. *Nature Reviews Neuroscience* 15: 567-72
Holtmaat A, Svoboda K. 2009. Experience-dependent structural synaptic plasticity in the mammalian brain. *Nature Reviews Neuroscience* 10: 647-58
Holtmaat AJ, Trachtenberg JT, Wilbrecht L, Shepherd GM, Zhang X, et al. 2005. Transient and persistent dendritic spines in the neocortex in vivo. *Neuron* 45: 279-91
Huttenlocher PR. 1979. Synaptic density in human frontal cortex-developmental changes and effects of aging. *Brain Res* 163: 195-205
Insel TR. 2003. Is social attachment an addictive disorder? *Physiology & Behavior* 79: 351-57
Ivy GO, Akers RM, Killackey HP. 1979. Differential distribution of callosal projection neurons in the neonatal and adult rat. *Brain Research* 173: 532-37
Iwasato T, Inan M, Kanki H, Erzurumlu RS, Itohara S, Crair MC. 2008. Cortical adenylyl cyclase 1 is required for thalamocortical synapse maturation and aspects of layer IV barrel development. *J Neurosci* 28: 5931-43
Janson CG, Chen Y, Li Y, Leifer D. 2001. Functional regulatory regions of human transcription factor MEF2C. *Molecular brain research* 97: 70-82
Kampa BM, Letzkus JJ, Stuart GJ. 2006. Cortical feed-forward networks for binding different streams of sensory information. *Nature neuroscience* 9: 1472-73

Kang J, Gocke CB, Yu H. 2006. Phosphorylation-facilitated sumoylation of MEF2C negatively regulates its transcriptional activity. *BMC biochemistry* 7: 5

Kavalali ET. 2015. The mechanisms and functions of spontaneous neurotransmitter release. *Nat Rev Neurosci* 16: 5-16

Kim Y, Phan D, Van Rooij E, Wang D-Z, McAnally J, et al. 2008. The MEF2D transcription factor mediates stress-dependent cardiac remodeling in mice. *The Journal of clinical investigation* 118: 124-32

Knott GW, Holtmaat A, Wilbrecht L, Welker E, Svoboda K. 2006. Spine growth precedes synapse formation in the adult neocortex in vivo. *Nat Neurosci* 9: 1117-24

Kubota J, Mikami Y, Kanemaru K, Sekiya H, Okubo Y, Iino M. 2016. Whisker experience-dependent mGluR signaling maintains synaptic strength in the mouse adolescent cortex. *European Journal of Neuroscience*

Kwon CH, Luikart BW, Powell CM, Zhou J, Matheny SA, et al. 2006. Pten regulates neuronal arborization and social interaction in mice. *Neuron* 50: 377-88

Kwon H-B, Kozorovitskiy Y, Oh W-J, Peixoto RT, Akhtar N, et al. 2012. Neuroligin-1-dependent competition regulates cortical synaptogenesis and synapse number. *Nature neuroscience* 15: 1667-74

Larkum ME, Nevian T. 2008. Synaptic clustering by dendritic signalling mechanisms. *Current opinion in neurobiology* 18: 321-31

Larkum ME, Waters J, Sakmann B, Helmchen F. 2007. Dendritic spikes in apical dendrites of neocortical layer 2/3 pyramidal neurons. *The Journal of Neuroscience* 27: 8999-9008

Larsen DD, Callaway EM. 2006. Development of layer-specific axonal arborizations in mouse primary somatosensory cortex. *Journal of Comparative Neurology* 494: 398-414

Larsen DD, Wickersham IR, Callaway EM. 2007. Retrograde tracing with recombinant rabies virus reveals correlations between projection targets and dendritic architecture in layer 5 of mouse barrel cortex. *Frontiers in neural circuits* 2: 5

Le Bé J-V, Silberberg G, Wang Y, Markram H. 2007. Morphological, electrophysiological, and synaptic properties of corticocallosal pyramidal cells in the neonatal rat neocortex. *Cerebral Cortex* 17: 2204-13

Le Meur N, Holder-Espinasse M, Jaillard S, Goldenberg A, Joriot S, et al. 2010. MEF2C haploinsufficiency caused by either microdeletion of the 5q14.3 region or mutation is responsible for severe mental retardation with stereotypic movements, epilepsy and/or cerebral malformations. *Journal of medical genetics* 47: 22-9

Lee S, Kruglikov I, Huang ZJ, Fishell G, Rudy B. 2013. A disinhibitory circuit mediates motor integration in the somatosensory cortex. *Nature neuroscience* 16: 1662-70

Lefort S, Tomm C, Sarria J-CF, Petersen CC. 2009. The excitatory neuronal network of the C2 barrel column in mouse primary somatosensory cortex. *Neuron* 61: 301-16

Leifer D, Krainc D, Yu YT, McDermott J, Breitbart RE, et al. 1993. MEF2C, a MADS/MEF2-family transcription factor expressed in a laminar distribution in cerebral cortex. *Proceedings of the National Academy of Sciences of the United States of America* 90: 1546-50

Leifer D, Li YL, Wehr K. 1997. Myocyte-specific enhancer binding factor 2C expression in fetal mouse brain development. *Journal of molecular neuroscience : MN* 8: 131-43

Lendvai B, Stern EA, Chen B, Svoboda K. 2000. Experience-dependent plasticity of dendritic spines in the developing rat barrel cortex in vivo. *Nature* 404: 876-81

Li H, Radford JC, Ragusa MJ, Shea KL, McKercher SR, et al. 2008. Transcription factor MEF2C influences neural stem/progenitor cell differentiation and maturation in vivo. *Proc Natl Acad Sci U S A* 105: 9397-402

Li S, Hang L, Ma Y. 2016. FGF22 protects hearing function from gentamycin ototoxicity by maintaining ribbon synapse number. *Hearing research* 332: 39-45

Lin Q, Schwarz J, Bucana C, Olson EN. 1997. Control of mouse cardiac morphogenesis and myogenesis by transcription factor MEF2C. *Science* 276: 1404-07

Lin Y, Bloodgood BL, Hauser JL, Lapan AD, Koon AC, et al. 2008. Activity-dependent regulation of inhibitory synapse development by Npas4. *Nature* 455: 1198-204

Loerwald KW, Patel AB, Huber KM, Gibson JR. 2015a. Postsynaptic mGluR5 promotes evoked AMPAR-mediated synaptic transmission onto neocortical layer 2/3 pyramidal neurons during development. *Journal of neurophysiology* 113: 786-95

Loerwald KW, Patel AB, Huber KM, Gibson JR. 2015b. Postsynaptic mGluR5 promotes evoked AMPAR-mediated synaptic transmission onto neocortical layer 2/3 pyramidal neurons during development. *J Neurophysiol* 113: 786-95

Lu W, Bushong EA, Shih TP, Ellisman MH, Nicoll RA. 2013. The cell-autonomous role of excitatory synaptic transmission in the regulation of neuronal structure and function. *Neuron* 78: 433-39

Lübke J, Roth A, Feldmeyer D, Sakmann B. 2003. Morphometric analysis of the columnar innervation domain of neurons connecting layer 4 and layer 2/3 of juvenile rat barrel cortex. *Cerebral Cortex* 13: 1051-63

Lynch G, Larson J, Kelso S, Barrionuevo G, Schottler F. 1983. Intracellular injections of EGTA block induction of hippocampal long-term potentiation. *Nature* 305: 719-21

Lyons GE, Micales BK, Schwarz J, Martin J, Olson EN. 1995a. Expression of mef2 genes in the mouse central nervous system suggests a role in neuronal maturation. *The Journal of neuroscience* 15: 5727-38

Lyons GE, Micales BK, Schwarz J, Martin JF, Olson EN. 1995b. Expression of mef2 genes in the mouse central nervous system suggests a role in neuronal maturation. *J Neurosci* 15: 5727-38

Lyons MR, Schwarz CM, West AE. 2012a. Members of the myocyte enhancer factor 2 transcription factor family differentially regulate Bdnf transcription in response to neuronal depolarization. *The Journal of neuroscience : the official journal of the Society for Neuroscience* 32: 12780-5

Lyons MR, Schwarz CM, West AE. 2012b. Members of the myocyte enhancer factor 2 transcription factor family differentially regulate Bdnf transcription in response to neuronal depolarization. *The Journal of Neuroscience* 32: 12780-85

Ma L, Qiao Q, Tsai JW, Yang G, Li W, Gan WB. 2016. Experience-dependent plasticity of dendritic spines of layer 2/3 pyramidal neurons in the mouse cortex. *Dev Neurobiol* 76: 277-86

Madison DV, Malenka RC, Nicoll RA. 1991. Mechanisms underlying long-term potentiation of synaptic transmission. *Annual review of neuroscience* 14: 379-97

Makino H, Malinow R. 2011. Compartmentalized versus global synaptic plasticity on dendrites controlled by experience. *Neuron* 72: 1001-11

Malenka RC, Bear MF. 2004. LTP and LTD: an embarrassment of riches. *Neuron* 44: 5-21

Manabe T, Wyllie D, Perkel DJ, Nicoll RA. 1993. Modulation of synaptic transmission and long-term potentiation: effects on paired pulse facilitation and EPSC variance in the CA1 region of the hippocampus. *Journal of Neurophysiology* 70: 1451-59

Mao T, Kusefoglu D, Hooks BM, Huber D, Petreanu L, Svoboda K. 2011. Long-range neuronal circuits underlying the interaction between sensory and motor cortex. *Neuron* 72: 111-23

Mao Z, Bonni A, Xia F, Nadal-Vicens M, Greenberg ME. 1999. Neuronal activity-dependent cell survival mediated by transcription factor MEF2. *Science* 286: 785-90

Mao Z, Wiedmann M. 1999. Calcineurin enhances MEF2 DNA binding activity in calcium-dependent survival of cerebellar granule neurons. *Journal of Biological Chemistry* 274: 31102-07

Maravall M, Koh IY, Lindquist WB, Svoboda K. 2004. Experience-dependent changes in basal dendritic branching of layer 2/3 pyramidal neurons during a critical period for developmental plasticity in rat barrel cortex. *Cerebral Cortex* 14: 655-64

Marin-Padilla M. 1978. Dual origin of the mammalian neocortex and evolution of the cortical plate. *Anatomy and embryology* 152: 109-26

Markram H, Lubke J, Frotscher M, Roth A, Sakmann B. 1997. Physiology and anatomy of synaptic connections between thick tufted pyramidal neurones in the developing rat neocortex. *J Physiol* 500 (Pt 2): 409-40

McCarthy SE, Gillis J, Kramer M, Lihm J, Yoon S, et al. 2014. De novo mutations in schizophrenia implicate chromatin remodeling and support a genetic overlap with autism and intellectual disability. *Molecular psychiatry* 19: 652-8

McConnell SK, Kaznowski CE. 1991. Cell cycle dependence of laminar determination in developing neocortex. *Science* 254: 282-85

McKinsey TA, Zhang CL, Lu J, Olson EN. 2000a. Signal-dependent nuclear export of a histone deacetylase regulates muscle differentiation. *Nature* 408: 106-11

McKinsey TA, Zhang CL, Olson EN. 2000b. Activation of the myocyte enhancer factor-2 transcription factor by calcium/calmodulin-dependent protein kinase-stimulated binding of 14-3-3 to histone deacetylase 5. *Proceedings of the National Academy of Sciences* 97: 14400-05

McKinsey TA, Zhang CL, Olson EN. 2002. MEF2: a calcium-dependent regulator of cell division, differentiation and death. *Trends in biochemical sciences* 27: 40-7

Mikhail FM, Lose EJ, Robin NH, Descartes MD, Rutledge KD, et al. 2011. Clinically relevant single gene or intragenic deletions encompassing critical neurodevelopmental genes in patients with developmental delay, mental retardation, and/or autism spectrum disorders. *American journal of medical genetics. Part A* 155A: 2386-96

Molkentin JD, Black BL, Martin JF, Olson EN. 1996. Mutational analysis of the DNA binding, dimerization, and transcriptional activation domains of MEF2C. *Molecular and Cellular Biology* 16: 2627-36

Morgan JI, Cohen DR, Hempstead JL, Curran T. 1987. Mapping patterns of c-fos expression in the central nervous system after seizure. *Science* 237: 192-97

Mulkey RM, Malenka RC. 1992. Mechanisms underlying induction of homosynaptic long-term depression in area CA1 of the hippocampus. *Neuron* 9: 967-75

Novara F, Beri S, Giorda R, Ortibus E, Nageshappa S, et al. 2010. Refining the phenotype associated with MEF2C haploinsufficiency. *Clinical genetics* 78: 471-7

Ohi K, Shimada T, Nitta Y, Kihara H, Okubo H, et al. 2016. Specific gene expression patterns of 108 schizophrenia-associated loci in cortex. *Schizophrenia research*

Okamoto S-i, Li Z, Ju C, Schölzke MN, Mathews E, et al. 2002. Dominant-interfering forms of MEF2 generated by caspase cleavage contribute to NMDA-induced neuronal apoptosis. *Proceedings of the National Academy of Sciences* 99: 3974-79

Oliet SH, Malenka RC, Nicoll RA. 1996. Bidirectional control of quantal size by synaptic activity in the hippocampus. *Science* 271: 1294-97

Owens DF, Liu X, Kriegstein AR. 1999. Changing properties of GABAA receptor–mediated signaling during early neocortical development. *Journal of Neurophysiology* 82: 570-83

Paciorkowski AR, Traylor RN, Rosenfeld JA, Hoover JM, Harris CJ, et al. 2013a. MEF2C Haploinsufficiency features consistent hyperkinesis, variable epilepsy, and has a role in dorsal and ventral neuronal developmental pathways. *neurogenetics* 14: 99-111

Paciorkowski AR, Traylor RN, Rosenfeld JA, Hoover JM, Harris CJ, et al. 2013b. MEF2C Haploinsufficiency features consistent hyperkinesis, variable epilepsy, and has a role in dorsal and ventral neuronal developmental pathways. *Neurogenetics* 14: 99-111

Patel AB, Loerwald KW, Huber KM, Gibson JR. 2014. Postsynaptic FMRP promotes the pruning of cell-to-cell connections among pyramidal neurons in the L5A neocortical network. *J Neurosci* 34: 3413-8

Pelvig D, Pakkenberg H, Stark A, Pakkenberg B. 2008. Neocortical glial cell numbers in human brains. *Neurobiology of aging* 29: 1754-62

Perry RL, Yang C, Soora N, Salma J, Marback M, et al. 2009. Direct interaction between myocyte enhancer factor 2 (MEF2) and protein phosphatase 1α represses MEF2-dependent gene expression. *Molecular and cellular biology* 29: 3355-66

Petersen CC. 2007. The functional organization of the barrel cortex. *Neuron* 56: 339-55

Petreanu L, Huber D, Sobczyk A, Svoboda K. 2007a. Channelrhodopsin-2-assisted circuit mapping of long-range callosal projections. *Nat Neurosci* 10: 663-8

Petreanu L, Huber D, Sobczyk A, Svoboda K. 2007b. Channelrhodopsin-2–assisted circuit mapping of long-range callosal projections. *Nature neuroscience* 10: 663-68

Petreanu L, Mao T, Sternson SM, Svoboda K. 2009. The subcellular organization of neocortical excitatory connections. *Nature* 457: 1142-45

Petrus E, Rodriguez G, Patterson R, Connor B, Kanold PO, Lee HK. 2015. Vision loss shifts the balance of feedforward and intracortical circuits in opposite directions in mouse primary auditory and visual cortices. *J Neurosci* 35: 8790-801

Pfeiffer BE, Zang T, Wilkerson JR, Taniguchi M, Maksimova MA, et al. 2010a. Fragile X mental retardation protein is required for synapse elimination by the activity-dependent transcription factor MEF2. *Neuron* 66: 191-97

Pfeiffer BE, Zang T, Wilkerson JR, Taniguchi M, Maksimova MA, et al. 2010b. Fragile X mental retardation protein is required for synapse elimination by the activity-dependent transcription factor MEF2. *Neuron* 66: 191-7

Pignataro A, Borreca A, Ammassari-Teule M, Middei S. 2015. CREB Regulates Experience-Dependent Spine Formation and Enlargement in Mouse Barrel Cortex. *Neural Plasticity* 2015

Potthoff MJ, Olson EN. 2007. MEF2: a central regulator of diverse developmental programs. *Development* 134: 4131-40

Povysheva NV, Gonzalez-Burgos G, Zaitsev AV, Kroner S, Barrionuevo G, et al. 2006. Properties of excitatory synaptic responses in fast-spiking interneurons and pyramidal cells from monkey and rat prefrontal cortex. *Cerebral cortex (New York, N.Y. : 1991)* 16: 541-52

Pulipparacharuvil S, Renthal W, Hale CF, Taniguchi M, Xiao G, et al. 2008a. Cocaine regulates MEF2 to control synaptic and behavioral plasticity. *Neuron* 59: 621-33

Pulipparacharuvil S, Renthal W, Hale CF, Taniguchi M, Xiao G, et al. 2008b. Cocaine regulates MEF2 to control synaptic and behavioral plasticity. *Neuron* 59: 621-33

Rakic P. 1988. Specification of cerebral cortical areas. *Science* 241: 170-76

Rakic P. 2009. Evolution of the neocortex: a perspective from developmental biology. *Nature Reviews Neuroscience* 10: 724-35

Rakic P, Bourgeois JP, Eckenhoff MF, Zecevic N, Goldman-Rakic PS. 1986. Concurrent overproduction of synapses in diverse regions of the primate cerebral cortex. *Science* 232: 232-5

Rash BG, Grove EA. 2006. Area and layer patterning in the developing cerebral cortex. *Current opinion in neurobiology* 16: 25-34

Ripke S, Neale BM, Corvin A, Walters JT, Farh K-H, et al. 2014. Biological insights from 108 schizophrenia-associated genetic loci. *Nature* 511: 421

Rodriguez A, Ehlenberger DB, Dickstein DL, Hof PR, Wearne SL. 2008. Automated three-dimensional detection and shape classification of dendritic spines from fluorescence microscopy images. *PLoS One* 3: e1997

Rodriguez A, Ehlenberger DB, Hof PR, Wearne SL. 2006. Rayburst sampling, an algorithm for automated three-dimensional shape analysis from laser scanning microscopy images. *Nat Protoc* 1: 2152-61

Rosso SB, Inestrosa NC. 2013. WNT signaling in neuronal maturation and synaptogenesis. *Front Cell Neurosci* 7: 103

Rubenstein JL. 2010. Three hypotheses for developmental defects that may underlie some forms of autism spectrum disorder. *Current opinion in neurology* 23: 118-23

Saiepour MH, Chakravarthy S, Min R, Levelt CN. 2015. Competition and Homeostasis of Excitatory and Inhibitory Connectivity in the Adult Mouse Visual Cortex. *Cerebral Cortex* 25: 3713-22

Santiago C, Bashaw GJ. 2014. Transcription factors and effectors that regulate neuronal morphology. *Development* 141: 4667-80

Sauvageot CM, Stiles CD. 2002. Molecular mechanisms controlling cortical gliogenesis. *Current opinion in neurobiology* 12: 244-49

Schizophrenia Working Group of the Psychiatric Genomics C. 2014. Biological insights from 108 schizophrenia-associated genetic loci. *Nature* 511: 421-7

Schubert D, Kötter R, Luhmann H, Staiger J. 2006. Morphology, electrophysiology and functional input connectivity of pyramidal neurons characterizes a genuine layer Va in the primary somatosensory cortex. *Cerebral cortex* 16: 223-36

Schubert D, Kötter R, Staiger JF. 2007. Mapping functional connectivity in barrel-related columns reveals layer-and cell type-specific microcircuits. *Brain Structure and Function* 212: 107-19

Schwartz N, Schohl A, Ruthazer ES. 2009. Neural activity regulates synaptic properties and dendritic structure in vivo through calcineurin/NFAT signaling. *Neuron* 62: 655-69

Shalizi A, Gaudilliere B, Yuan Z, Stegmuller J, Shirogane T, et al. 2006. A calcium-regulated MEF2 sumoylation switch controls postsynaptic differentiation. *Science* 311: 1012-7

Shalizi AK, Bonni A. 2005. brawn for brains: the role of MEF2 proteins in the developing nervous system. *Current topics in developmental biology* 69: 239-66

Shepherd GM, Pologruto TA, Svoboda K. 2003. Circuit analysis of experience-dependent plasticity in the developing rat barrel cortex. *Neuron* 38: 277-89

Silver RA, Lübke J, Sakmann B, Feldmeyer D. 2003. High-probability uniquantal transmission at excitatory synapses in barrel cortex. *Science* 302: 1981-84
Stern EA, Maravall M, Svoboda K. 2001. Rapid development and plasticity of layer 2/3 maps in rat barrel cortex in vivo. *Neuron* 31: 305-15
Tabuchi K, Blundell J, Etherton MR, Hammer RE, Liu X, et al. 2007. A neuroligin-3 mutation implicated in autism increases inhibitory synaptic transmission in mice. *Science* 318: 71-6
Takahashi N, Kitamura K, Matsuo N, Mayford M, Kano M, et al. 2012. Locally synchronized synaptic inputs. *Science* 335: 353-56
Tanaka YR, Tanaka YH, Konno M, Fujiyama F, Sonomura T, et al. 2011. Local connections of excitatory neurons to corticothalamic neurons in the rat barrel cortex. *The Journal of Neuroscience* 31: 18223-36
Tang X, Wang X, Gong X, Tong M, Park D, et al. 2005. Cyclin-dependent kinase 5 mediates neurotoxin-induced degradation of the transcription factor myocyte enhancer factor 2. *J Neurosci* 25: 4823-34
Taniguchi H, He M, Wu P, Kim S, Paik R, et al. 2011. A resource of Cre driver lines for genetic targeting of GABAergic neurons in cerebral cortex. *Neuron* 71: 995-1013
Theyel BB, Llano DA, Sherman SM. 2010. The corticothalamocortical circuit drives higher-order cortex in the mouse. *Nature neuroscience* 13: 84-88
Trachtenberg JT, Chen BE, Knott GW, Feng G, Sanes JR, et al. 2002. Long-term in vivo imaging of experience-dependent synaptic plasticity in adult cortex. *Nature* 420: 788-94
Tsai NP, Wilkerson JR, Guo W, Maksimova MA, DeMartino GN, et al. 2012. Multiple autism-linked genes mediate synapse elimination via proteasomal degradation of a synaptic scaffold PSD-95. *Cell* 151: 1581-94
Tsubota T, Okubo-Suzuki R, Ohashi Y, Tamura K, Ogata K, et al. 2015. Cofilin1 Controls Transcolumnar Plasticity in Dendritic Spines in Adult Barrel Cortex. *PLoS biology* 13: e1002070-e70
Turrigiano G. 2011. Too many cooks? Intrinsic and synaptic homeostatic mechanisms in cortical circuit refinement. *Annual review of neuroscience* 34: 89-103
Turrigiano GG, Leslie KR, Desai NS, Rutherford LC, Nelson SB. 1998. Activity-dependent scaling of quantal amplitude in neocortical neurons. *Nature* 391: 892-96
Vallès A, Boender AJ, Gijsbers S, Haast RA, Martens GJ, de Weerd P. 2011. Genomewide analysis of rat barrel cortex reveals time-and layer-specific mRNA expression changes related to experience-dependent plasticity. *The Journal of Neuroscience* 31: 6140-58
Veinante P, Deschênes M. 2003. Single-cell study of motor cortex projections to the barrel field in rats. *Journal of Comparative Neurology* 464: 98-103

Vetere G, Restivo L, Cole CJ, Ross PJ, Ammassari-Teule M, et al. 2011. Spine growth in the anterior cingulate cortex is necessary for the consolidation of contextual fear memory. *Proceedings of the National Academy of Sciences* 108: 8456-60

Viviani B. 2006. Preparation and coculture of neurons and glial cells. *Curr Protoc Cell Biol* Chapter 2: Unit 2 7

Vong LH, Ragusa MJ, Schwarz JJ. 2005. Generation of conditional Mef2cloxP/loxP mice for temporal-and tissue-specific analyses. *Genesis* 43: 43-48

Wang DD, Kriegstein AR. 2008. GABA regulates excitatory synapse formation in the neocortex via NMDA receptor activation. *The Journal of Neuroscience* 28: 5547-58

Wayman GA, Lee Y-S, Tokumitsu H, Silva A, Soderling TR. 2008. Calmodulin-kinases: modulators of neuronal development and plasticity. *Neuron* 59: 914-31

West AE, Greenberg ME. 2011a. Neuronal activity-regulated gene transcription in synapse development and cognitive function. *Cold Spring Harb Perspect Biol* 3: a005744

West AE, Greenberg ME. 2011b. Neuronal activity–regulated gene transcription in synapse development and cognitive function. *Cold Spring Harbor perspectives in biology* 3: a005744

White EL, DeAmicis RA. 1977. Afferent and efferent projections of the region in mouse SmL cortex which contains the posteromedial barrel subfield. *Journal of Comparative Neurology* 175: 455-81

Wilkerson JR, Tsai NP, Maksimova MA, Wu H, Cabalo NP, et al. 2014. A role for dendritic mGluR5-mediated local translation of Arc/Arg3.1 in MEF2-dependent synapse elimination. *Cell Rep* 7: 1589-600

Williams MR, DeSpenza T, Jr., Li M, Gulledge AT, Luikart BW. 2015. Hyperactivity of newborn Pten knock-out neurons results from increased excitatory synaptic drive. *J Neurosci* 35: 943-59

Wise S, Jones E. 1976. The organization and postnatal development of the commissural projection of the rat somatic sensory cortex. *Journal of Comparative Neurology* 168: 313-43

Yamada T, Yang Y, Huang J, Coppola G, Geschwind DH, Bonni A. 2013. Sumoylated MEF2A coordinately eliminates orphan presynaptic sites and promotes maturation of presynaptic boutons. *The Journal of Neuroscience* 33: 4726-40

Yang X, Seto E. 2007. HATs and HDACs: from structure, function and regulation to novel strategies for therapy and prevention. *Oncogene* 26: 5310-18

Zang T, Maksimova MA, Cowan CW, Bassel-Duby R, Olson EN, Huber KM. 2013. Postsynaptic FMRP bidirectionally regulates excitatory synapses as

a function of developmental age and MEF2 activity. *Mol Cell Neurosci* 56: 39-49

Zhang Z, Cao M, Chang C-W, Wang C, Shi X, et al. 2016. Autism-Associated Chromatin Regulator Brg1/SmarcA4 Is Required for Synapse Development and Myocyte Enhancer Factor 2-Mediated Synapse Remodeling. *Molecular and cellular biology* 36: 70-83

Zhu B, Gulick T. 2004. Phosphorylation and alternative pre-mRNA splicing converge to regulate myocyte enhancer factor 2C activity. *Molecular and cellular biology* 24: 8264-75

Zoghbi HY. 2003. Postnatal neurodevelopmental disorders: meeting at the synapse? *Science* 302: 826-30

Zuo Y, Yang G, Kwon E, Gan W-B. 2005. Long-term sensory deprivation prevents dendritic spine loss in primary somatosensory cortex. *Nature* 436: 261-65

Zweier M, Gregor A, Zweier C, Engels H, Sticht H, et al. 2010. Mutations in MEF2C from the 5q14. 3q15 microdeletion syndrome region are a frequent cause of severe mental retardation and diminish MECP2 and CDKL5 expression. *Human mutation* 31: 722-33

Zweier M, Rauch A. 2012. The MEF2C-related and 5q14. 3q15 microdeletion syndrome. *Molecular syndromology* 2: 164-70

VITAE

Kacey Elise Rajkovich was born in Grand Forks, North Dakota on April 2, 1987. She was raised in Aurora, MN by her parents, Patricia J. Rajkovich and Richard A. Rajkovich. In 2009, she graduated from the University of Minnesota – Twin Cities campus in Minneapolis, MN with Bachelor of Science degrees in both neuroscience and biochemistry, molecular biology, and biophysics. She has been pursuing a doctoral degree at the UT Southwestern Medical Center since 2010.

Permanent Address: 135 Linda Dr.
Aurora, MN 55705